**Multireference Equation of Motion Coupled Cluster Study**
**of**
**Atomic Excitation Spectra**

by

Zhebing Liu

A thesis
presented to the University of Waterloo
in fulfillment of the
thesis requirement for the degree of
Master of Science
in
Chemistry

Waterloo, Ontario, Canada, 2015

**Author's Declaration**

This thesis consists of material all of which I authored or co-authored: see Statement of Contributions included in the thesis. This is a true copy of the thesis, including any required final revisions, as accepted by my examiners.

I understand that my thesis may be made electronically available to the public.

Zhebing Liu

**Statement of Contribution**

I did all the calculations and analyses of the data for this thesis and compared the results to the experimental data. The authors of the two papers worked together with me on manuscripts are listed below.

**Paper in Chapter 3:**

Multireference Equation of Motion Coupled Cluster study of atomic excitation spectra of first-row transition metal atoms Cr, Mn, Fe and Co. Z. Liu, O. Demel and M. Nooijen, J. Mol. Spectro. 311, 54-63 (2015).

Zhebing Liu and Marcel Nooijen, Department of Chemistry, University of Waterloo, Ontario, Canada. Ondřej Demel, J. Heyrovský Institute of Physical Chemistry of AS CR v.v.i., Prague, Czech Republic.

**Paper in Chapter 4:**

Application of Multireference Equation of Motion Coupled Cluster Method including spin-orbit coupling to atomic spectra of Cr, Mn, Fe and Co.

Zhebing Liu, Lee M. J. Huntington and Marcel Nooijen, Department of Chemistry, University of Waterloo, 200 University Avenue West, Waterloo, Ontario, Canada, N2L 3G1.

This is to be submitted.

**Abstract**

Variants of the family of the recently developed Multireference Equation of Motion Coupled Cluster (MR-EOM-CC) approaches are applied to the atomic excitation spectra of the first-row transition metals, for which experimental data are readily available. The first part of my research is to apply MR-EOM-CC approaches to the atomic excitation spectra of the neutral and the +1 and +2 Cr, Mn, Fe and Co atoms using ACESII program. Scalar relativistic effects are considered but spin-orbit coupling is not included. The computational results are compared to J-averaged experimental values and the errors are typically below 0.1 eV. The second part of this project is to combine MR-EOM approach with a simple treatment of spin-orbit coupling and the resulting MR-EOM-CC-SOC approach can be used to the atomic excitation spectra and the splitings in each L-S multiplet of the Cr, Mn, Fe and Co neutral atoms using the ORCA program. The errors of the spin-orbit calculations in the ORCA program are somewhat larger compared to the J-averaged calculations run in ACESII program and this is still under investigation. From both parts of this research, one can easily find that upon introducing additional cluster operators T, S, X, D and U in different variations of MR-EOM, the dimension of the final diagonalization space is greatly reduced, the overall cost of the calculation is significantly reduced, and finally, the accuracy of the calculations is, perhaps surprisingly, *improved*.

**Acknowledgements**

I would firstly like to thank my supervisor Dr. Marcel Nooijen for all his help, guidance and support during my two years graduate studies. Thanks as well to the committee members my supervisor Dr. Marcel Nooijen, Dr. Pierre-Nicholas Roy and Dr. Scott Hopkins for guiding me through the thesis process. This thesis would not have been possible without all your help or your suggestions. I would like to thank Ondřej Demel and Lee M. J. Huntington for their co-work with the two papers presented in this thesis.

Thanks also to my friends, all the friends I met and worked with during my graduate studies.

Finally, I would like to thank my family: my parents. Your support during my graduate studies was deeply appreciated. Thank you for being the loving family that you are.

**Table of Contents**

**List of Figures**

**List of Tables**

**List of Abbreviations**

| | |
|---|---|
| Hartree Fock | HF |
| Self-consistent field procedure | SCF |
| Coupled cluster | CC |
| Coupled cluster singles and doubles | CCSD |
| Coupled cluster singles and doubles with a perturbative triples | CCSD(T) |
| Configuration interaction | CI |
| Configuration interaction singles and doubles | CISD |
| Single reference | SR |
| Multireference | MR |
| Similarity transformed equation-of-motion | STEOM |
| Similarity transformed equation of motion coupled-cluster | STEOM-CC |
| Equation-of-motion coupled cluster | EOM-CC |
| Multireference equation of motion coupled cluster | MR-EOM-CC |
| Multireference configuration interaction | MR-CI |
| Multireference configuration interaction singles and doubles | MR-CISD |
| MR-CI with davidson-type extensivity correction | MRCI+Q |
| Multireference averaged quadratic coupled cluster | MR-AQCC |
| Multireference averaged coupled pair functional | MR-ACPF |
| Multireference coupled cluster | MR-CC |
| Partially Internally contracted MR-CC | pIC-MR-CC |
| Complete active space | CAS |
| Configuration state function | CSF |
| Complete active space self-consistent field | CASSCF |
| National Institute of Standards and Technology | NIST |
| Complete active space configuration interaction | CASCI |
| Kutzelnigg-Mukherjee normal order | KM normal-ordered |

| | |
|---|---|
| Equation-of-motion coupled cluster singles and doubles | EOM-CCSD |
| Multireference equation of motion spin-orbit coupling | MR-EOM-SOC |
| Domain based localized pair natural orbitals | DLPNOs |
| Symmetry adapted cluster configuration interaction | SAC-CI |
| Coupled cluster linear response theory | CC-LRT |
| Fock-space coupled cluster | FS-CC |
| Quasi-degenerate perturbation Theory | QDPT |
| Spin-orbit mean-field | SOMF |
| Spin-orbit coupling | SOC |

# Chapter 1

# Introduction

The electronic structure problem is one of the most fundamental and important problems in quantum chemistry and many methodologies have been developed to address this problem. Single reference (SR) is a straightforward and easy treatment for solving quantum chemistry problems.[1-7] Single reference can solve many molecular problems when molecules are close to their equilibrium geometry and the wavefunction is dominated by only one Slater determinant.[8] As the starting point of a SR calculation, the Hartree Fock (HF) method is widely used in quantum chemistry. It typically yields over 99% of the total electronic energy. However, the remaining error is relatively large for purposes in chemistry. The inclusion of electron correlation involving many (millions of) small contributions to the wavefunction increases the accuracy beyond the HF approximation. There are two kinds of electron correlations basically. One is the long-

range electron correlation, which can affect forming quasi-degeneracy of several electronic configurations; the other one is short-range dynamical electron correlation, which is the dominant factor such that it can affect the accuracy of calculations directly. Coupled cluster (CC)[1, 2, 3, 4, 9] theory is one of the most accurate and systematic approaches to solve the electronic structure problem, and as such it is widely used in the accurate calculations of energies of small and medium sized molecules. [1, 2, 3, 4, 9] Coupled cluster singles and doubles method (CCSD) is a widely used methodology in chemistry. If a perturbation triples correction is included, the CCSD(T)[10] method often yields chemical accuracy (~ 1 kcal $mol^{-1}$ errors for energy differences) when used with large basis sets and it is considered as the method of choice for ground state chemistry. However, CCSD(T) is only applicable when the single determinant HF wavefunction is a good starting point. Upon increasing the bond length or breaking the chemical bond, the accuracy of traditional CC will decrease fast.[1]

When dealing with bond breaking situations, low lying excited states, magnetic or spin systems, biradicals, polyradicals and transition metal systems, more than one determinant is needed to describe the wavefunction qualitatively, and a large number of determinants are often involved that are important. Traditional methods such as Hartree Fock and coupled cluster theory often break down in such cases. Since an appropriate single determinant cannot be selected as a reasonable approximation for the construction of the wavefunction, the methods mentioned previously have various kinds of problems that cannot be solved efficiently. Multireference (MR)[11] approach appears to be a better choice for solving these problems. There is a branch of

implementations with MR characters that are developed for solving electronic structure problems efficiently, such as Multireference Configuration Interaction (MR-CI)[12, 13], MR-CI with Davidson-type Extensivity Correction (MRCI+ Q)[14], Multireference Averaged Quadratic Coupled Cluster (MR-AQCC)[15], Multireference Averaged Coupled Pair Functional (MR-ACPF)[16], Multireference Coupled Cluster (MR-CC)[11], and Partially Internally Contracted MR-CC (pIC-MR-CC) approach[17].

There are also some approaches that are rooted in multireference theory, but which in practice are applicable as single reference methods. One example is the Similarity Transformed Equation of Motion Coupled-Cluster (STEOM-CC) method.[18, 19] STEOM can be viewed as a transform and diagonalize approach.[18, 19, 20] The zeroth order approximation is CI singles. In STEOM one defines a similarity transform of the Hamiltonian such that all second quantized operators that excite out of the zeroth order CI space are transformed to zero. The STEOM approach is closely related to the method that will be considered in this thesis.

In most multireference approaches, the starting point is a so-called CASSCF calculation.[21, 22] Qualitatively, the states of interest can be described by a limited number of determinants that differ only in the occupation of a small number (~ 10) of active orbitals. If one includes all determinants in the active orbital space, this called a complete active space (CAS).[21, 22] In a CASCI calculation, one performs a diagonalization over the CAS determinants. In CASSCF both the orbitals and the CI coefficients of selected wave functions are optimized. Like single reference Hartree Fock calculations, CASSCF calculations may be qualitatively correct, but they are not accurate enough for

most purposes in chemistry: dynamical correlation is still missing. This can be corrected by MR-CISD calculations in which the Hamiltonian is diagonalized over configurations that include all CAS and all single and double excitations out of the CAS. This approach is very expensive however, and the approach suffers from a lack of size-extensivity.[23]

In Dr. Nooijen's group, an alternative to MR-CI has been developed, that is called Multireference Equation of Motion Coupled Cluster (MR-EOM-CC).[17, 24, 25, 26] The MR-EOM-CC approaches can solve for large numbers of electronic states. The first step of a MR-EOM calculation is to identify reference states of interest that lie in a compact CAS space. Next, a set of transformations is performed to the bare Hamiltonian so that the matrix elements of the second quantized transformed Hamiltonian, which couple determinants in the CAS to other excited determinants, vanish. The compact CAS space in general is not fully decoupled from the excited determinants out of CAS. In MR-EOM, one performs a diagonalization of the transformed Hamiltonian, as in MR-CISD. However, the number of states included in MR-EOM in the final diagonalization is much smaller than in MR-CISD (e.g. 10,000 rather than 10,000,000 configurations). Several benchmark applications of the MR-EOM-CC approaches have been done before. In our work, we used both the ACESII program[27] and ORCA program[28] to benchmark MR-EOM-CC approaches for the excitation energies of transition metal atoms Cr, Mn, Fe, and Co. The calculations are also combined with the atomic mean field approach to spin-orbit coupling as used in the MR-CI implementation in the ORCA program so that we obtain the spin-orbit splittings in each L-S multiplet. We do such kinds of benchmarks of transition metal atoms in order to make a critical and reliable assessment of the MR-

EOM-CC approaches and we also want to demonstrate the efficiency of MR-EOM approaches.

The thesis is organized as follows. In chapter 2, we will discuss the theory underlying MR-EOM, and briefly discuss some special features of MR-EOM. In chapter 3, the published paper “Multireference Equation of Motion Coupled Cluster study of atomic excitation spectra of first-row transition metal atoms Cr, Mn, Fe and Co” co-written by Marcel Nooijen and Ondřej Demel is presented. In chapter 4, the paper that is going to be submitted “Application of Multireference Equation of Motion Coupled Cluster Method including spin-orbit coupling to atomic spectra of Cr, Mn, Fe and Co” is presented. Chapter 5 contains concluding remarks.

# Chapter 2

# Brief introduction to MR-EOM

The Multireference Equation of Motion Coupled-Cluster (MR-EOM-CC) approach[24, 25, 26] has been introduced to solve electronic structure problems by following the transform and diagonalize strategy, which is analogous to the ideas underlying STEOM.[18, 19, 20] If one wants to operate "large-scale" transition metal calculations, it would be reasonable to describe multiple surfaces using MR-EOM approaches. The philosophy underlying MR-EOM is to optimize CASSCF[21, 22] orbitals such that the $\mathrm{E_{CAS}}$ is minimal. As is mentioned before, $|\mathrm{CAS}\rangle$ is a linear combination of determinants of $\mathrm{c_\lambda}|\phi_\lambda^{\mathrm{CAS}}\rangle$ as shown in Eq. (2.1). In the CASSCF, we optimize the energy of the wave functions, which means optimize the orbitals in these spaces and also the coefficients $c_\lambda$ such that the energy is minimized.[21]

$$|\mathrm{CAS}\rangle = \sum_\lambda \mathrm{c_\lambda}|\phi_\lambda^{\mathrm{CAS}}\rangle \qquad (2.1)$$

As is shown in Figure 2.1, the “holes” are all double occupied and “particles” are used as empty orbitals. The so-called $|\mathrm{CAS}\rangle$ only differs by occupation in the “active” space. Figure 2.1 only shows one particular case for the active space. In the following explanations, “hole” (or “h ”) will refer to the inactive orbitals, while “p ” (particle’) refers to virtual orbitals. Many different examples of excitations are listed and are shown in Figure 2.3 further.

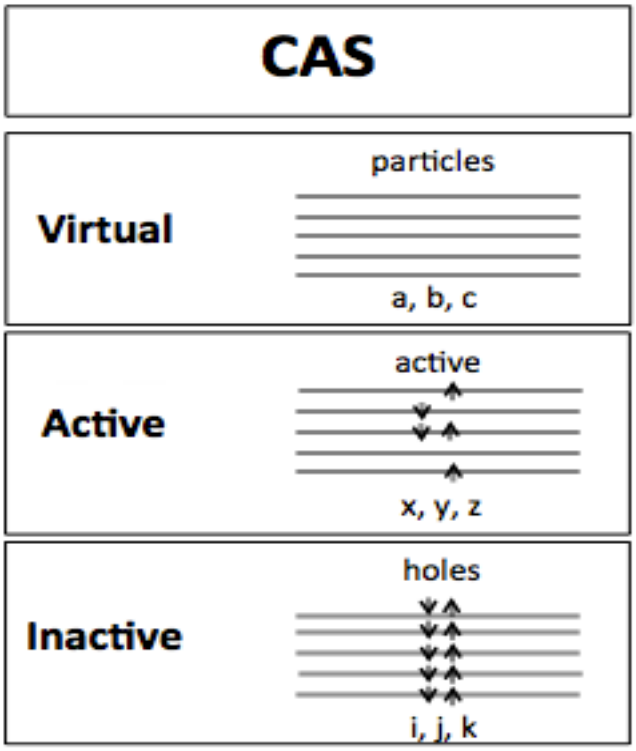


**Figure 2.1.** *One particular case for the CAS space*

(1) 1h excitations: An inactive electron is promoted to the active space, additional active-active excitations can occur.

(2) 1p excitations: An active electron is promoted to the virtual space, additional active-active excitations can occur.

(3) 2h excitations: Two inactive electrons are promoted to the active space.

(4) 1h1p excitations: An inactive electron is promoted to the virtual space; an inactive electron is promoted to the virtual space, additional active-active excitations can occur; an inactive electron is promoted to the active space, an active electron is promoted to the virtual space.

(5) 2h1p excitations: Two holes in the inactive space, and a particle in the virtual space.

(6) 2p excitations: Two active electrons are promoted to the virtual space.

(7) 1h2p excitations: One inactive electron is promoted to the virtual space; another active electron is promoted to the virtual space.

(8) 2h2p excitations: Two inactive electrons are promoted to the virtual space.

The total number of electrons remains constant. Here “h” is electrons are promoted from inactive orbitals and “p” is electrons are promoted to virtual orbitals.

Shown as an example in Figure 2.2, the 1h excitation is interpreted in detail. An electron from the inactive space is promoted to the active space, which leads to creating a hole in the inactive space. The excited electron is colored as red in Figure 2.2. Moreover, the process is combined with internal excitations within the active space without creating any holes.

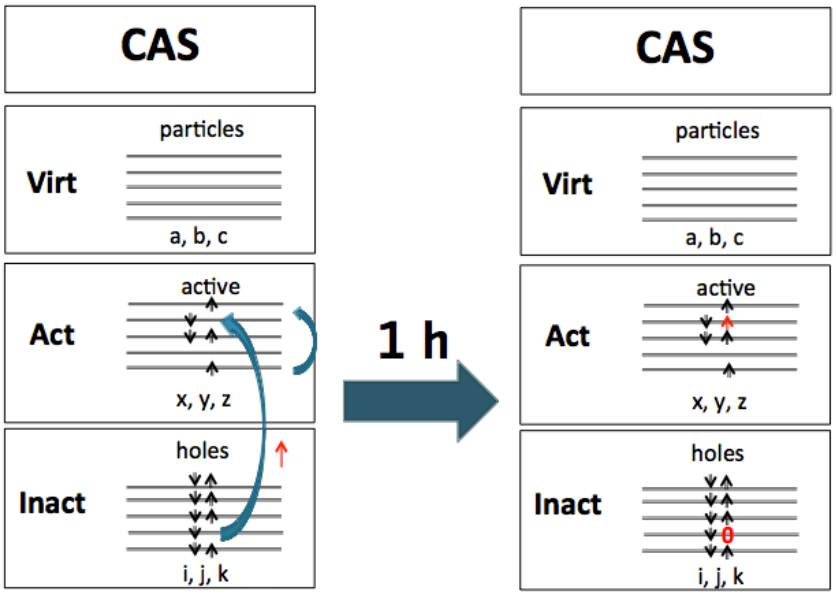


**Figure 2.2.** *1h excitation scheme*

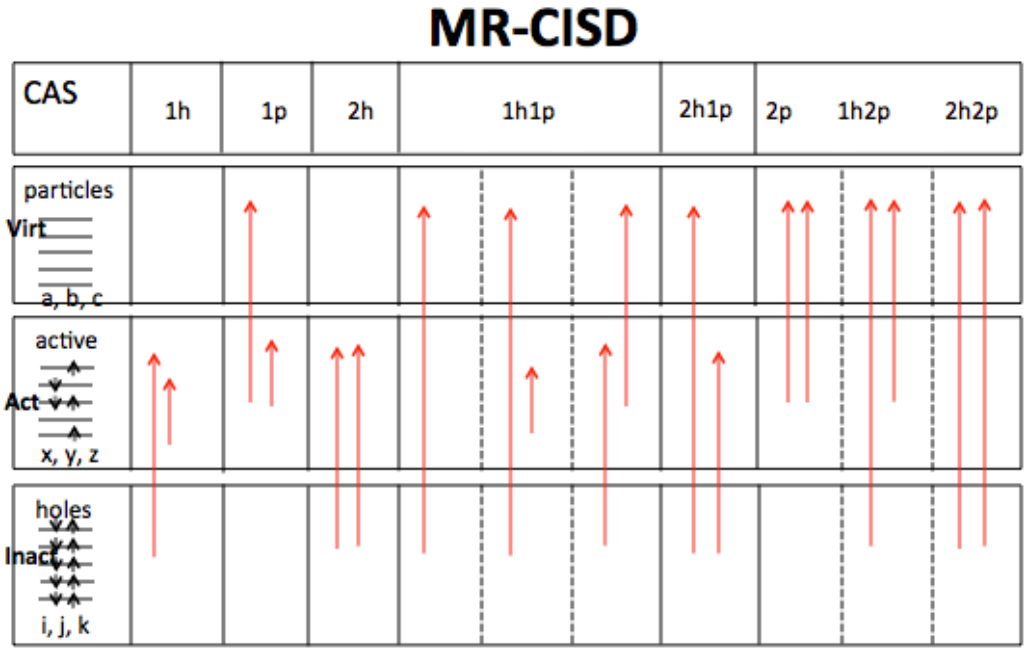


**Figure 2.3.** *All excitations in CAS*

For all the possible excitations in CAS that are shown in Figure 2.3, we can act with a Hamiltonian operator on CAS wave functions so that all these different kinds of determinants are populated Eq. (2.2).

$$|\psi^{MR-CISD}\rangle = |CAS\rangle + \sum_{\lambda} c_{\mu}|x_{\mu}\rangle \,. \tag{2.2}$$

If we do the MR-CI singles and doubles excitations, one optimises the coefficients of determinants $|x_{\mu}\rangle$. The bottom line of the $|\psi^{MR-CISD}\rangle$ wave function calculation is to minimise the energy expression so that all of the optimised coefficients can be determined by minimising the total energy. The most unsatisfying part of a MR-CI calculation is that it is a very expensive problem that needs to optimise coefficients for perhaps almost 10 million configurations even for a very small molecule. The number of determinants can be indicated like:

Number of determinants = Number of excitations * Number of (CAS) determinants. We do not want to explore the huge number; a more satisfactory calculation should therefore be investigated.

The goal of MR-EOM theory is to greatly reduce the size of the diagonalization space compared to MR-CISD. MR-EOM uses a transform and diagonalize strategy. Let us first consider this essential conceptual framework.

Since MR-EOM approach is a transform and diagonalise process, we can divide the process in two parts. The first step of the whole process is the transform process. In MR-EOM we employ a sequence of experimental similarity transformations, "$U = e^{T}$" that aim to decouple the CAS configurations from excited determinants, as in Figure 2.4. Below, the method will be explained in detail.

Eq. (2.3) is the original Schrödinger equation

$$H|\Psi_\lambda\rangle = |\Psi_\lambda\rangle \mathrm{E}_\lambda \tag{2.3}$$

We transform it to get the transformed Hamiltonian $\bar{H}$,

$$\bar{H} = U^{-1}HU \tag{2.4}$$

Then,

$$\bar{H}|\Phi_\lambda\rangle = (U^{-1}HU)(\,U^{-1}|\Psi_\lambda\rangle) = U^{-1}H|\Psi_\lambda\rangle = U^{-1}|\Psi_\lambda\rangle \mathrm{E}_\lambda = |\Phi_\lambda\rangle \mathrm{E}_\lambda$$

Therefore,

$$\bar{H}|\Phi_\lambda\rangle = |\Phi_\lambda\rangle \mathrm{E}_\lambda \tag{2.5}$$

It is seen that the original Hamiltonian and the transformed Hamiltonian have the same eigenvalues, but different eigenstates $|\Phi_\lambda\rangle = U^{-1}|\Psi_\lambda\rangle$. Any operator U can be used to transform the bare Hamiltonian and the eigenvalues will never change. In this way, we can make any transformed Hamiltonian without changing the calculation results. This is the bottom line underlying the MR-EOM approach.

The diagonalization process comes after the transform. Diagonalize the transformed Hamiltonian over the remaining configurations left in the calculation space.

| $\bar{H}$ | CAS | X |
|---|---|---|
| CAS | A | B |
| X | 0 | D |

**Figure 2.4.** *Diagonalization configuration space. CAS here is the excitations remaining in the CAS space and X is the excitations out of CAS*

Act with the transformed Hamiltonian $\overline{H}$ on every crossed block section CAS-CAS, CAS-X, X-CAS and X-X,

$$\langle \phi_{CAS} | \overline{H} | \phi_{CAS} \rangle = A \,,$$

$$\langle \phi_{CAS} | \overline{H} | \phi_{X} \rangle = B \,,$$

$$\langle \phi_{X} | \overline{H} | \phi_{CAS} \rangle = 0 \,,$$

$$\langle \phi_{X} | \overline{H} | \phi_{X} \rangle = D \,. \tag{2.6}$$

The elements of each block are calculated. Now, multiply the matrix block by a simple matrix $\binom{C}{0}$, a much simplified block matrix is addressed.

$$\begin{pmatrix} A & B \\ 0 & D \end{pmatrix} \begin{pmatrix} C \\ 0 \end{pmatrix} = \begin{pmatrix} A \cdot C + B \cdot 0 \\ 0 \cdot C + D \cdot 0 \end{pmatrix} = \begin{pmatrix} A \cdot C \\ 0 \end{pmatrix} \tag{2.7}$$

If, $AC_\lambda = C_\lambda E_\lambda$, $C_\lambda$ is the eigenstate and $E_\lambda$ is eigenvalue.

By following the transform and diagonalize strategy, the calculation become very compact and the eigenvalue remain unchanged. Through the whole process above, MR-EOM approach generates a compact CI space and the diagonalization is much more efficient compared to the bare Hamiltonian calculation, but the results are accurate.

There are a number of variations of the general MR-EOM approach. The different operators that are used in different variants are listed in Table 2.1.

| Acronym | Operator | Operator components | Excitation type |
|---|---|---|---|
| T | $\mathbf{T_1}$ | $t_a^x E_x^a + t_a^i E_i^a$ | 1p, 1h1p |
| | $\mathbf{T_2}$ | $t_{ab}^{xy} E_{xy}^{ab} + t_{ab}^{ix} E_{ix}^{ab} + t_{ab}^{ij} E_{ij}^{ab}$ | 2p, 2p1h, 2p2h |
| S | $\mathbf{S_1}$ | $s_a^x E_i^a + s_a^i E_i^a$ | 1p, 1h1p |
| | $\mathbf{S_2}$ | $s_{ax}^{ij} E_{ij}^{ax}$ | 2h1p |
| X | $\mathbf{X_2}$ | $x_{ay}^{xj} E_{xj}^{ay}$ | 1h1p |
| D | $\mathbf{D_2}$ | $d_{ay}^{ix} E_{ix}^{ay}$ | 1h1p |
| U | $\mathbf{U_2}$ | $u_{xy}^{ij} E_{ij}^{xy}$ | 2h |

**Table 2.1**. *Operators included in various many body similarity transformations. i, j indicate inactive orbitals or hole labels. a, b refer to virtual orbitals or particle. x and y are active labels referring to orbitals with variable occupation in reference configurations. Repeated indices are summed*

The "E" in Table 2.1 are the excitation operators and the "t" coefficients are the amplitudes that need to be solved in the calculation. These are all the excitation types that we have explored so far. We can make different combinations depending on what operators we intend to include in the coupled cluster calculations. For example, we can only use $T_1$ and $T_2$ and it is called MR-EOM-T. If $T_1$, $T_2$, $S_1$, $S_2$, $X_2$ and $D_2$ are included, it is the MR-EOM-T|SXD method. If all cluster operators in Table 2.1 are included, it will be the MR-EOM-T|SXD|U method.

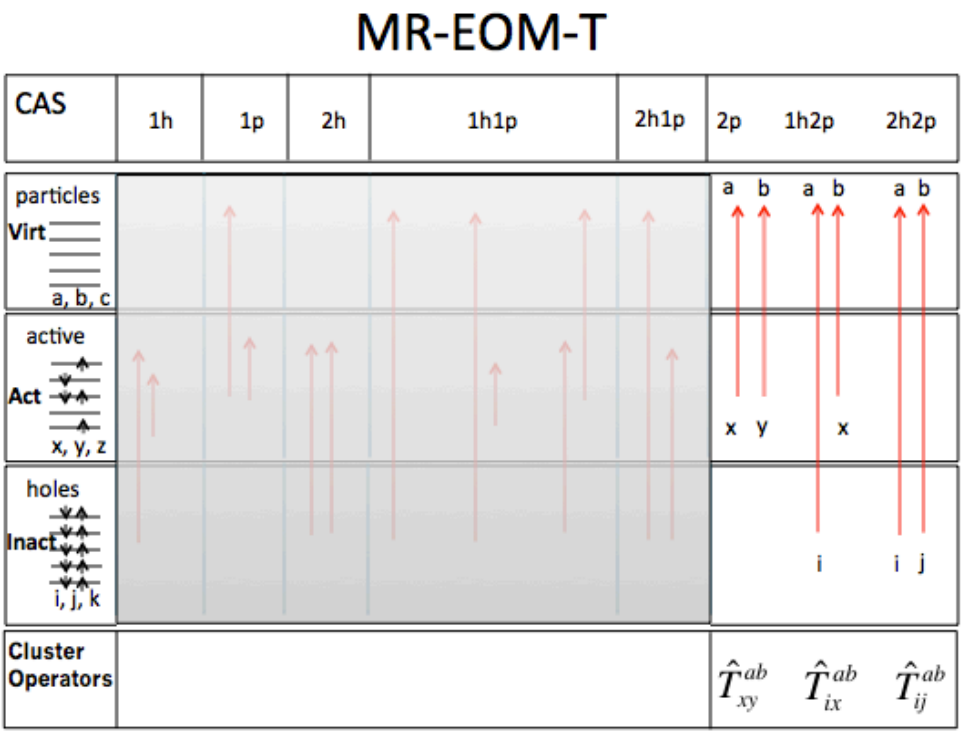


**Figure 2.5.** *Operator T in MR-EOM*

The meaning of each operator will be discussed in detail next. When we optimise the coefficients in the excitation operators, this is called the MR-EOM-T method shown in Figure 2.5, the T operator here is the $T_2$ operator. As a result there is no need to include 2p, 1h2h and 2h2p excitation configurations in the diagonalization space of the CI calculation. The number of $T_2$-amplitudes is just the number of double excitations, not the number of excitations multiplied by the number of determinants (CAS). This is why the method is efficient.

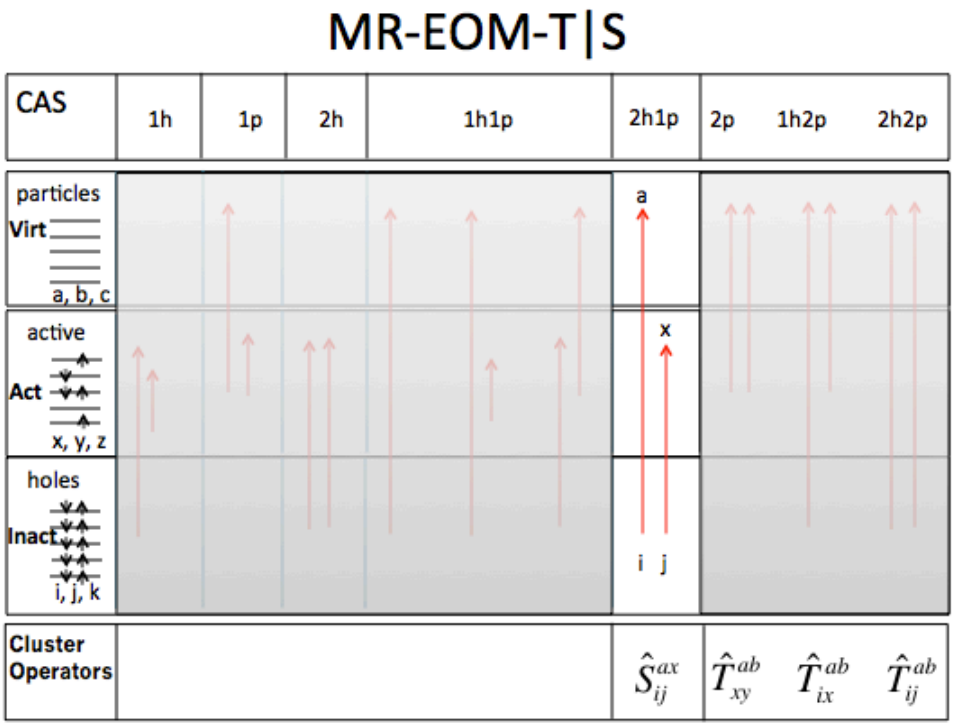


**Figure 2.6.** *Operator S in MR-EOM*

Next, we follow the same strategy to exclude the 2h1p excitation and name the operator as S. We solve for the amplitude of the operator and this process is called MR-EOM-T|S method in Figure 2.6 because both the T and S operators are included. By introducing the T and S operators, the diagonalization space is reduced significantly.

The operators shown in Figure 2.7 are operator T (that is $T_1$), D and X. If these operators are used, we can get rid of the corresponding 1h1p excitations from the CI diagonalization manifold. By introducing the four operators, the diagonalization space is again reduced significantly and the MR-EOM-T|SXD approach is generated.

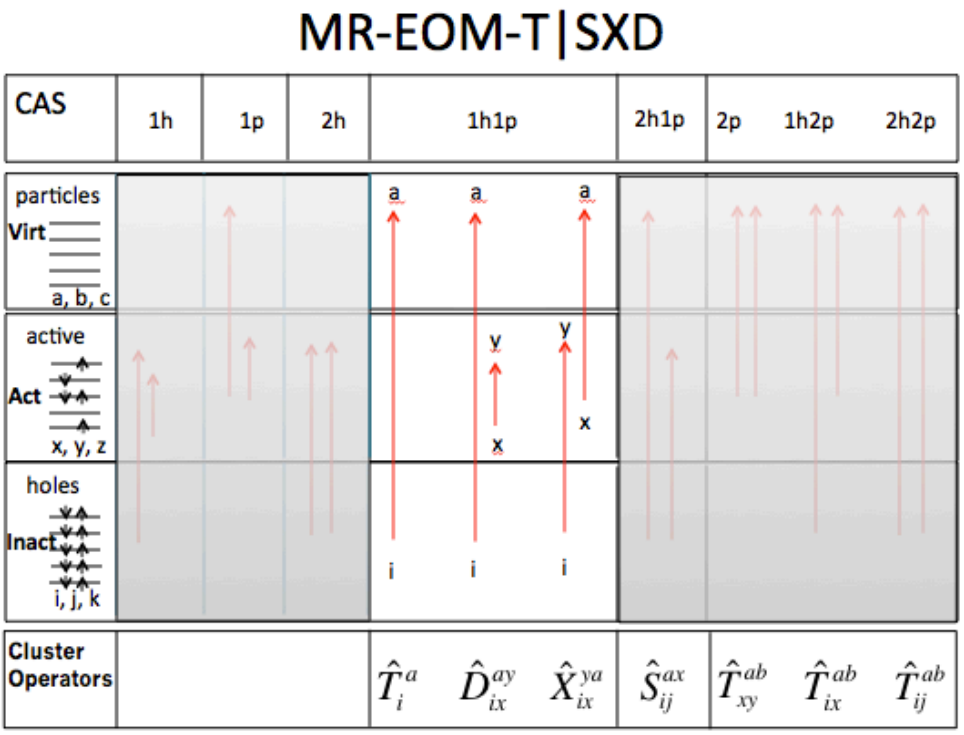


**Figure 2.7.** *Operator T, D and X in MR-EOM*

Finally, U operator indicates double excitations from inactive space to active space and yields the MR-EOM-T|SXD|U method in Figure 2.8. This is the most efficient method we have explored so far. We do not introduce operators for the 1h and 1p excitations at this stage and we have to include them in the CI diagonalization manifold. Therefore, the diagonalization space of the transformed Hamiltonian is reduced a lot and the most compact diagonalization space CAS + 1h + 1p is realized.

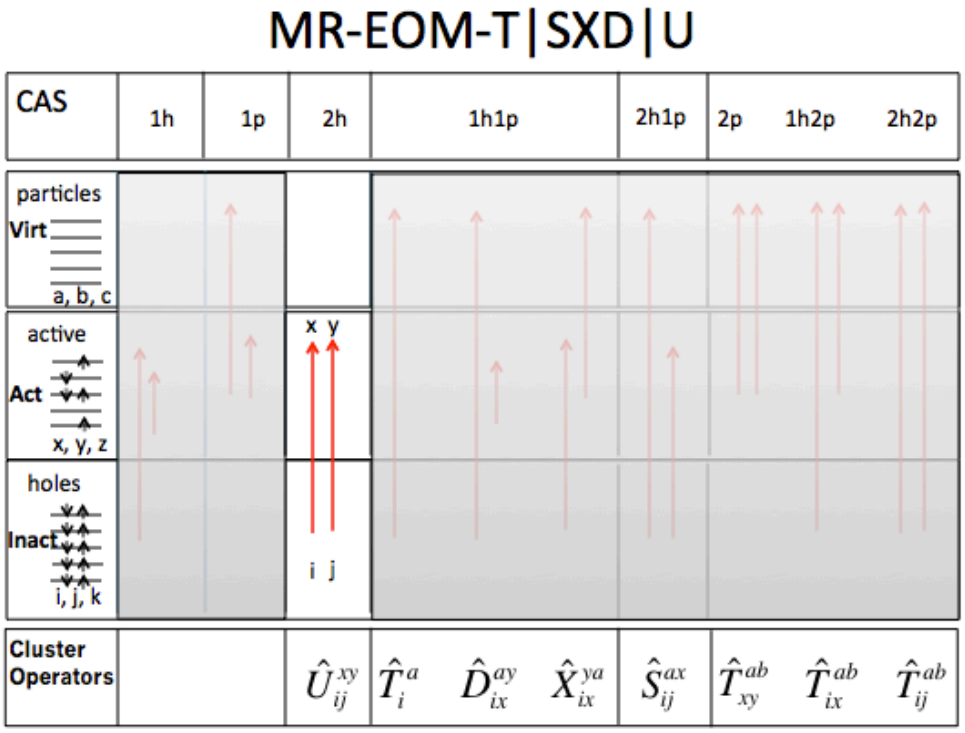


**Figure 2.8.** *Operator U in MR-EOM*

Let us discuss in more detail about the basics of the scheme, and explain the process of generating a similarity transformation from an operator. We can define operator $\hat{T}$ as:

$$\hat{T} = \hat{T}_1 + \hat{T}_2 = \sum_{i,a} \hat{T}_i^a + \sum_{a,b,x,y} \hat{T}_{xy}^{ab} + \sum_{a,b,i,x} \hat{T}_{ix}^{ab} + \sum_{a,b,i,j} \hat{T}_{ij}^{ab} \ . \qquad (2.8)$$

For the T operator, we have $T_1$ and $T_2$. One can determine the operators by making a transformed Hamiltonian $\overline{\mathrm{H}}$ like in Eq. (2.9) and just as in single reference theory, one can work all these computations out. Then, the transformed 0, 1 and 2 particle matrix elements are solved.

$$\overline{\mathrm{H}} = \mathrm{e}^{-\hat{\mathrm{T}}}\mathrm{H}\mathrm{e}^{\hat{\mathrm{T}}} = \bar{\mathrm{h}}_0 + \bar{\mathrm{h}}_{\mathrm{p}}^{\mathrm{q}}\{E_q^p\} + \bar{\mathrm{h}}_{\mathrm{rs}}^{\mathrm{pq}}\{E_{rs}^{pq}\} + \cdots \quad . \qquad (2.9)$$

The t-amplitudes are determined as iterative solutions of a mixed set of amplitude equations. The singles residual equation is a projected residual equation[17]

$$\sum_k \omega_k \left\langle R_k \middle| E_a^{i/x} \overline{H} \middle| R_k \right\rangle = 0. \quad (2.10)$$

Here $\omega_k$ and $|R_k\rangle$ refer to the weights used and states obtained from the CAS CI (or CASSCF), while i and x denote an inactive or active orbital. The doubles residual equation is obtained by setting the elements $\bar{h}_{ij}^{ab}$, $\bar{h}_{ix}^{ab}$, $\bar{h}_{xy}^{ab}$ of the similarity transformed Hamiltonian of Eq. (2.9) to zero,

We can solve for T just by setting the elements $\bar{\mathrm{h}}_{\mathrm{ij}}^{\mathrm{ab}}$, $\bar{\mathrm{h}}_{\mathrm{ix}}^{\mathrm{ab}}$ and $\bar{\mathrm{h}}_{\mathrm{xy}}^{\mathrm{ab}}$ of Eq. (2.9) to zero,

$$\bar{\mathrm{h}}_{\mathrm{ij}}^{\mathrm{ab}} = \bar{\mathrm{h}}_{\mathrm{ix}}^{\mathrm{ab}} = \bar{\mathrm{h}}_{\mathrm{xy}}^{\mathrm{ab}} = 0\ . \quad (2.11)$$

We solve for operators S, X, and D following the same strategy as operator T.

A subsequent transformation is given by

$$G = \{e^{S+X+D}\}^{-1} \overline{\mathrm{H}}_2 \{e^{S+X+D}\} \quad (2.12)$$

Here $\overline{\mathrm{H}}_2$ denotes $\overline{\mathrm{H}}$ truncated to 2-body operators in KM normal-order.[29, 30, 31] The preferred type of amplitude equation is the many-body type in which elements of the transformed Hamiltonian are equated to zero. The S, X, D-amplitudes are solved from

$$g_{ax}^{ij} = g_{ay}^{ix} = g_{ya}^{ix} = 0 \quad (2.13)$$

With these amplitudes, one can diagonalize the transformed G operator over the remaining CAS + 1h +1p + 2h diagonalization configurations.

Finally, we can include the U operator and the transformed Hamiltonian F is calculated.

$$\hat{F} = \{e^U\}^{-1} \hat{G} \{e^U\} \quad (2.14)$$

$$f_{ij}^{xy} = 0 \quad (2.15)$$

The diagonalization space is reduced again with including the operator U and this is the corresponding MR-EOM-T|SXD|U method.

| Method | Operators | Diagonalization space |
|---|---|---|
| BareH | None | CAS, 1h, 1p, 2h, 1h1p, 2h1p |
| T | T=T1+T2 | CAS, 1h, 1p, 2h, 1h1p, 2h1p |
| T\|S | T; S=S1+S2 | CAS, 1h, 1p, 2h, 1h1p |
| T\|SXD | T; S+X+D | CAS, 1h, 1p, 2h, 1h1p |
| T\|SXD-nph | T; S+X+D | CAS, 1h, 1p, 2h |
| T\|SXD\|U | T; S+X+D; U | CAS, 1h, 1p, 2h, 1h1p |
| T\|SXD\|U-min | T; S+X+D; U | CAS, 1h, 1p |

**Table 2.2**. *Variants of Multireference Equation-of-Motion Coupled Cluster theory*

The various members of the MR-EOM family, including the definition of the final diagonalization manifolds are listed in Table 2.2. The MR-EOM-T|SXD-nph method means “no particle hole” in the diagonalization space of a MR-CI calculation. Both the MR-EOM-T|SXD-nph and MR-EOM-T|SXD methods use the same transformation. Here the excitation CI space is still quite large for the MR-EOM-T|SXD method, but it’s smaller for the MR-EOM-T|SXD-nph method. It is expected to yield similar results, but the MR-EOM-T|SXD-nph calculation is much more efficient. Likewise, the MR-EOM-T|SXD|U-min approach uses the minimum CAS + 1h + 1p diagonalization space. To investigate the effectiveness of the transformation, we also consider the 2h and 1p1h excitation in MR-EOM-T|SXD|U. The results of these approaches should be very close if the methodology works well. Even though we include the X, D and U operators, we still need to include the 1h and 1p excitations in the excitation manifold.

Up to three similarity transformations of the second quantized Hamiltonian are executed. Similarity transformations preserve connectedness and symmetries of the Hamiltonian. The final "MR-CI " diagonalization step includes the indicated configurations in an uncontracted fashion. Finally, the most compact diagonalization space is shown in Figure 2.9.

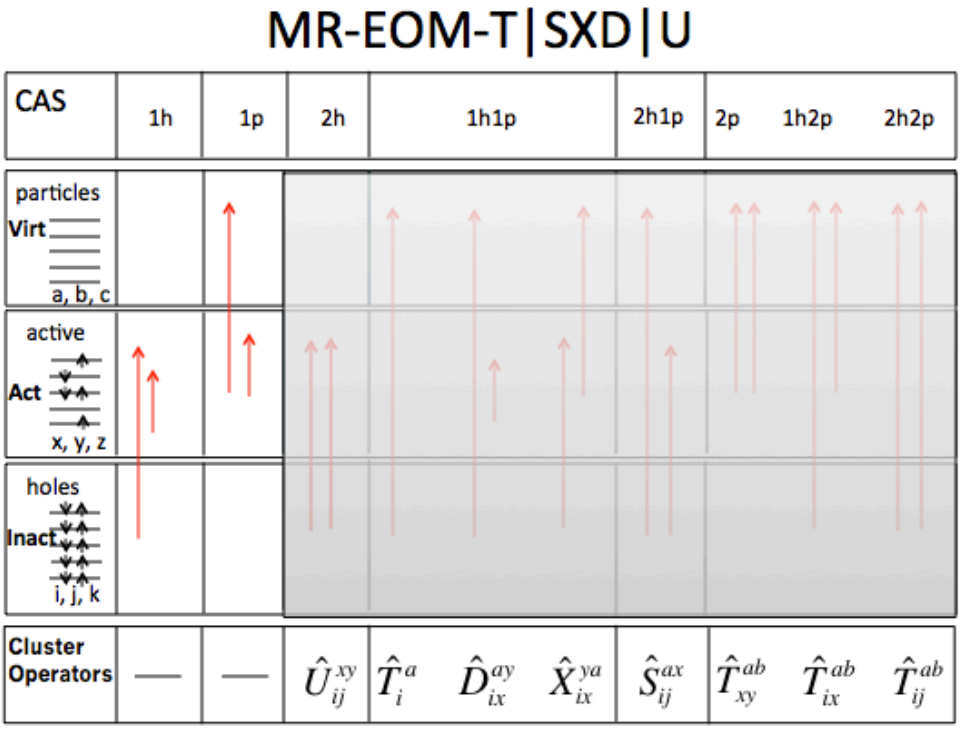


**Figure 2.9.** *All operators in MR-EOM*

To summarize, we have all of these different methods listed in Table 2.1. The reasons why we want to include these operators basically come from two views. First, the calculations that include additional cluster operators have much smaller errors. The accuracy of the results is significantly increased as more operators are included. The primary reason MR-EOM is accurate is that the extensivity errors are very small. The extensivity error (see e.g. Ref. 23) is only affected by the size of the external space in the

final diagonalization (beyond the CAS) which is 1h and 1p in the most compact method.[8] The more operators that are introduced, the more amplitudes are included in the transformation, the fewer configurations are needed in the final diagonalization. Therefore, the extensivity error will be smaller. Second, since the CI dimension of the final diagonalization is much smaller compared to the one without using operators, the cost of a calculation is significantly reduced by using more operators. The lowest cost method, MR-EOM-T|SXD|U-min, processes the final diagonalization step on the CAS + 1h + 1p excitations out of the CAS and this defines a quite compact final diagonalization space. The remaining 1h and 1p cannot be replaced by operators at this stage; we have to include them in the diagonalization of the similarity transformed Hamiltonian. MR-EOM-CC approaches are obtained from a single state-averaged CASSCF calculation. We can get a large number of excited states from a very compact diagonalization of the transformed Hamiltonian after solving a single set of cluster amplitudes. Hence, we can really get a lot of impressive and satisfactory benefits from the MR-EOM-CC calculations: improved efficiency, improved extensivity and improved accuracy.

In this thesis, we investigate different methods generated by different combinations of cluster operator to see the trends. Also, we apply MR-EOM to a selection of transition metal atoms Cr, Mn, Fe and Co and demonstrate the benefit of the MR-EOM-CC method.

# Chapter 3

**Multireference Equation of Motion Coupled Cluster study of atomic excitation spectra of first-row transition metal atoms Cr, Mn, Fe and Co.**

Zhebing Liu and Marcel Nooijen
Department of Chemistry, University of Waterloo, Ontario, Canada
Ondřej Demel
J. Heyrovský Institute of Physical Chemistry of AS CR v.v.i., Prague, Czech Republic

**Abstract**

Variants of the family of the recently developed Multireference Equation of Motion Coupled Cluster (MR-EOM-CC) approaches are applied to the atomic excitation spectra of the neutral and the +1 and +2 charged first-row transition metal atoms Cr, Mn, Fe and Co. Scalar relativistic effects are considered, but spin-orbit coupling is not included. Using a single set of state-averaged CASSCF orbitals and a single set of cluster amplitudes, a large number of excited state is obtained from the diagonalization of a

compact transformed Hamiltonian. Hundreds of excited states (10's of L-S multiplets) are obtained for each atomic species with RMS errors compared to J-averaged experimental values that typically fall below 0.1 eV. All electronic states in MR-EOM are properly spin- and symmetry adapted. The cluster operators included in the variations of MR-EOM are denoted T, S, X, D and U. The inclusion of additional cluster operators is shown to yield a threefold benefit: 1) By inclusion of additional cluster amplitudes the size-extensivity error in MR-EOM-CC is reduced. 2) The accuracy of the results is significantly increased as operators T, S, X and D are included. 3) The overall cost of the calculations is significantly *reduced* with increasing inclusion of cluster amplitudes as the dimension of the final diagonalization step can be greatly reduced. In the most compact MR-EOM-T|SXD|U-min approach the final diagonalization step is over a Hilbert space containing the active space CI determinants (CASCI), and 1-hole and 1-particle excitations out of the CAS.

**3.1 Introduction**

The recently developed Multireference Equation of Motion Coupled Cluster method allows for the convenient calculation of a large number of electronic states that (nearly) all require a multi-determinantal description even at a qualitative level.[24, 25, 32] The MR-EOM approach (or family of approaches) is designed to work well for a selection of electronic states that (qualitatively) have significant partial occupations in a relatively small number of orbitals that comprise an active space. Such situations often arise

naturally in transition metal systems with a partial occupation of 4s and 3d orbitals.[33, 34] Also magnetic systems that can be characterized by a large number of states of various spin-multiplicities having a limited number of open-shell orbitals are suitable systems to be considered in MR-EOM. Moreover, at nuclear geometries in which chemical bonds can be considered broken, multiple low-lying excited states are usually present and MR-EOM is a suitable approach. However, global potential energy surfaces may be harder to classify by a single active space and MR-EOM is to be used with care for such systems.[25]

A great virtue of the MR-EOM family of methods is that they are not very sensitive to the precise definition of the active orbital space. Hence one can use a single state-averaged CASSCF calculation to optimize orbitals and configuration coefficients for a small set of low-lying reference states. Subsequently, a sequence of cluster amplitudes, denoted T, S, X, D, U are solved for.[24, 25, 32] The computational expense of solving for the cluster amplitudes is comparable to solving closed shell CCSD equations (for review see Ref. 2, 4). In practice the equations are about a factor of 3-5 more expensive to solve. The amplitudes define a sequence of similarity transformations of the second quantized Hamiltonian. This transformed Hamiltonian is written in the so-called Kutzelnigg-Mukherjee normal order,[29, 30] and the amplitude equations are defined such that second quantized matrix elements of the KM normal-ordered Hamiltonian vanish. [24, 25, 32] An important feature of the MR-EOM amplitude equations is that these equations are non-singular, in contrast with other internally contracted approaches that use a projection manifold. As a result of the transformations, the first-order interacting subspace out of

the CAS, associated with the transformed Hamiltonian, is much reduced in size. In the most elaborate version of MR-EOM, configurations in the CAS only couple directly to the 1-hole and 1-particle excitations out of the CAS, and this defines a quite compact final diagonalization space. In the present MR-EOM scheme only states that are dominated by CAS configurations are obtained accurately (e.g. 95% of the transformed wave function should live in the CAS space). Various variations of the MR-EOM scheme are tested here that differ in the types of amplitudes included in the transformation, and in the final diagonalization space considered. The MR-EOM approach is a very recent development and the purpose of this study is to benchmark the approach for systems that are well characterized experimentally (i.e. atoms). The present MR-EOM calculations do not include spin-orbit coupling and therefore we compare to J-averaged experimental excitation energies for each particular L-S multiplet. Both positively charged (+1, +2) and neutral systems are considered.

The paper is organized as follows. In section 3.2 we summarize the theoretical underpinnings of the MR-EOM approach and the variations employed in this work. Section 3.3 contains computational details and discusses the reference manifolds and the weights of states in the CASSCF calculations. Section 3.4 presents the results. We explicitly report results for the Co neutral atom and the $Fe^{1+}$ atom to illustrate various aspects of the results. In addition we provide a statistical assessment of the quality of the results for all atom species considered. Detailed computational results are provided as supplementary electronic information (SI). Concluding remarks follow in section 3.5.

**3.2 Theory.**

The Multireference Equation-of-Motion Coupled Cluster method can provide convenient access to many electronic excited states (possibly hundreds) using a convenient transform and diagonalize strategy. [24, 25, 32] All of the accessible electronic states are described predominantly by linear combinations of electronic configurations that differ in the occupation of a relatively small number of so-called active orbitals, comprising a complete active space (CAS). The key consideration in the MR-EOM approach is a sequence of similarity transformations of the second quantized Hamiltonian, such that most of the Hamiltonian matrix elements that couple determinants in the CAS to other classes of determinants (e.g. 1p1h, 2p1h excitations) vanish. Here h (hole) indicates removal of an electron from a doubly occupied orbital in CAS determinants, while p (particle) refers to the population of a virtual or unoccupied orbital.

In the second stage of an MR-EOM calculation the transformed Hamiltonian is diagonalized over a compact subspace that essentially consists of the new first-order interacting subspace out of the CAS. While the basic idea underlying MR-EOM is similar to single reference EOM-CC[2, 35] and similarity transformed EOM-CC,[18, 19] the details of the MR-EOM approaches are more cumbersome. The use of a multiconfigurational form of normal ordering introduced by Mukherjee and Kutzelnigg[29, 30] is crucial (KM normal-order). This normal ordering is defined in terms of the one- and two-body cumulants of, in general, a weighted ensemble of states described by the CAS concept (obtained from

a state-averaged CASSCF calculation). In an abstract way the many body transformations are defined as follows:[32, 36]

$$
\begin{aligned}
&G = \{e^{Y}\}^{-1} H \{e^{Y}\} \rightarrow \{e^{Y}\} G = H \{e^{Y}\} \rightarrow \\
&G = (H\{e^{Y}\})_{Connected} - (\{e^{Y} - 1\} G)_{Connected} = \cdots \\
&\quad = g_0 + g_r^p \{p^+ r\} + \tfrac{1}{4} g_{rs}^{pq} \{p^+ r q^+ s\} + \cdots
\end{aligned}
\tag{3.1}
$$

If the operators in the transformation do not commute, the transformations are expressed in terms of KM normal-ordered exponentials, as indicated by braces. The transformation results in modified or dressed Hamiltonian matrix elements using second quantization. Both the details of the equations and the computer implementation of the MR-EOM method are generated in an automated fashion,[17, 26] as they contain many terms. The computational complexity is substantially larger than in single reference EOM-CC. Regarding computational effort, however, as in the closed shell CCSD approach,[27] there is only one term in these equations that scales as $o^2v^4$, there are around 10 terms that scale as $o^3v^3$, while the great majority of terms scale as $o^4v^2$ or less, where *o* denotes the number of occupied orbitals (active + inactive), while *v* refers to the number of virtual orbitals (related to the size of the one-electron basis set). In Table 3.1 the explicit forms of the operators that are used in the various transformations are listed, using spin-summed generators of the unitary group denoted $\mathrm{E}_{\mathrm{q}}^{\mathrm{p}}$, $\mathrm{E}_{\mathrm{rs}}^{\mathrm{pq}}$. The excitation type generated when such operators act on determinants in the CAS model space are shown in the last column of this table.

| Acronym | Operator | Operator components | Excitation type |
|---|---|---|---|
| T | $\mathbf{T_1}$ | $t_a^x E_x^a + t_a^i E_i^a$ | 1p, 1h1p |
| | $\mathbf{T_2}$ | $t_{ab}^{xy} E_{xy}^{ab} + t_{ab}^{ix} E_{ix}^{ab} + t_{ab}^{ij} E_{ij}^{ab}$ | 2p, 2p1h, 2p2h |
| S | $\mathbf{S_1}$ | $s_a^x E_i^a + s_a^i E_i^a$ | 1p, 1h1p |
| | $\mathbf{S_2}$ | $s_{ax}^{ij} E_{ij}^{ax}$ | 2h1p |
| X | $\mathbf{X_2}$ | $x_{ay}^{xj} E_{xj}^{ay}$ | 1h1p |
| D | $\mathbf{D_2}$ | $d_{ay}^{ix} E_{ix}^{ay}$ | 1h1p |
| U | $\mathbf{U_2}$ | $u_{xy}^{ij} E_{ij}^{xy}$ | 2h |

**Table 3.1**. *Operators included in various many-body similarity transformations. Indices I, j indicate inactive orbitals or hole labels (doubly occupied in each reference configuration), indices a, b refer to virtual orbitals or particle labels (not occupied in any reference configuration), while indices x, y, z are active labels referring to orbitals with variable occupation in reference configurations. Repeated indices are summed.*

In this work we will consider the use of operators T, S, X, D, and U. The most elaborate sequence of transformations used in this paper then takes the following form (see Ref. 25, 32):

$$\overline{\mathrm{H}} = e^{-T} H e^{T}$$

$$= \bar{h}_0 + \bar{h}_p^q \{E_q^p\} + \bar{h}_{pq}^{rs} \{E_{rs}^{pq}\} + \bar{h}_{pqr}^{stu} \{E_{stu}^{pqr}\} + \ldots \tag{3.2}$$

$$\sum_k \omega_k \left\langle R_k \middle| E_a^{i/x} \bar{H} \middle| R_k \right\rangle = 0 \tag{3.3}$$

$$\bar{h}_{ij}^{ab} = \bar{h}_{ix}^{ab} = \bar{h}_{xy}^{ab} = 0 \tag{3.4}$$

Here $\omega_k$and $|R_k\rangle$ refer to the weights used and states obtained from the CAS CI (or CASSCF), while i/x denotes either an inactive or active orbital. A subsequent transformation is given by

$$F = \{e^{S+X+D}\}^{-1} \overline{\mathrm{H}}_2 \{e^{S+X+D}\} \tag{3.5}$$

Here $\overline{\mathrm{H}}_2$ denotes $\bar{H}$ truncated to 2-body operators in KM normal-order. The S, X, D-amplitudes are solved from

$$\sum_k \omega_k \left\langle R_k \middle| E_a^{i/x} F \middle| R_k \right\rangle = 0 \tag{3.6}$$

$$f_{ax}^{ij} = f_{ay}^{ix} = f_{ya}^{ix} = 0 \tag{3.7}$$

Finally the operator U is solved from

$$G = \{e^U\}^{-1} \mathrm{F}_2 \{e^U\}$$

$$g_{xy}^{ij} = 0 \tag{3.8}$$

In all equations only terms up to quadratic in the transformation amplitudes are included, and the transformed Hamiltonian in KM normal-order is truncated to two-body terms. The preferred type of amplitude equation is the many-body type in which elements of the transformed Hamiltonian are equated to zero. For a small number of amplitude types $t_a^{i/x}$, $s_a^{i/x}$ this does not work well (see Ref. 17 for a rationale), and we invoke projected equations instead. The advantage of the many-body equations is that they are much simpler than the projected equations (see Ref. 17), while in addition the many-body amplitude equations are always non-singular, and tend to lead to fairly small amplitudes. In addition the many-body equations tend to only depend very minorly on the 2-body cumulants.[25] This is not true for the projected equations. In the above approach the first order interacting space is reduced to the 1p and 1h configurations out of the CAS. All other matrix-elements coupling a CAS determinant to a determinant in the external space vanish. In the MR-EOM-T|SXD|U-min approach we employ exactly this minimal diagonalization space. In the MR-EOM-T|SXD|U approach we also include 2h and 1p1h configurations in order to investigate potential couplings from the 1h and 1p configurations into the 2h/ 1p1h subspaces. The results including the U

transformation are presented here for the first time. In the MR-EOM-T|SXD-nph approach, the U operator is not included in the similarity transformation, and instead the CI space contains the 2h excitation operators. In the MR-EOM-T|SXD approach, we investigate potential couplings from the 1h/1p/2h space into the 1p1h space, and the latter is now included in the diagonalization space. This significantly increases the size of the diagonalization space. The various members of the MR-EOM family used in this paper, including the definition of the final diagonalization manifolds, are listed in Table 3.2. Many (hundreds of) excited states can be obtained accurately, while the transformed Hamiltonian is calculated only once and only a few states are included in the state-averaged CAS calculation, which determine the reference cumulants used in the amplitude equations. The final transformed Hamiltonian is not Hermitian, and is truncated to up to 2-body operators (in KM normal-order). This 2-body operator can be easily rewritten in bare vacuum form, and this is used as input in the MR-CI module of our local ACESII program.[27]

| Method | Operators | Diagonalization space |
|---|---|---|
| BareH | None | CAS, 1h, 1p, 2h, 1h1p, 2h1p |
| T | T=T1+T2 | CAS, 1h, 1p, 2h, 1h1p, 2h1p |
| T\|S | T; S=S1+S2 | CAS, 1h, 1p, 2h, 1h1p |
| T\|SXD | T; S+X+D | CAS, 1h, 1p, 2h, 1h1p |
| T\|SXD-nph | T; S+X+D | CAS, 1h, 1p, 2h |
| T\|SXD\|U | T; S+X+D; U | CAS, 1h, 1p, 2h, 1h1p |
| T\|SXD\|U-min | T; S+X+D; U | CAS, 1h, 1p |

**Table 3.2**. *Variants of multireference equation-of-motion coupled cluster theory. Up to three similarity transformations of the second quantized Hamiltonian are executed. Similarity transformations preserve connectedness and symmetries of the Hamiltonian, but not hermiticity. The sequence of transformed Hamiltonians is truncated to up to 2-body rank in the Mukherjee-Kutzelnigg normal order at each stage. The final "MR-CI "diagonalization step includes the indicated configurations in an uncontracted fashion*

There are good reasons for performing similarity transformations. One aspect is their cost-effectiveness. The number of excitation amplitudes is similar as in closed shell CCSD calculations and is much smaller than in the uncontracted MR-CI (which multiplies this number essentially by the number of determinants or configuration state functions in the CAS).[30] Moreover, one solves for the transformation amplitudes once, while the diagonalization step scales with the number of roots of interest. For this reason the approach is also more cost-effective than internally contracted MR-CI approaches. Let us emphasize also that the efficiency aspect is different from single reference EOM-CC.[2, 35] In both CISD and EOM-CCSD one diagonalizes a Hamiltonian matrix over the size of singles and doubles. MR-EOM is closer in spirit to STEOM in this respect.[18, 19] Dynamical correlation is included almost exclusively through the use of cluster amplitudes, and the final diagonalization is primarily over the dominant configurations (and 1h and 1p excitations which are not decoupled). A second reason is that the similarity

transformations preserve the connectivity of the Hamiltonian and the remaining extensivity error (see e.g. Ref. 23) directly relates to the size of the external space (beyond the CAS) required in the diagonalization.[32] The more amplitudes that are included in the transformation, the fewer that are needed in the explicit diagonalization, and the smaller are the issues with extensivity. We think the reduction in the size-extensivity error is the primary reason for the improvement in accuracy that is observed in the MR-EOM-T|SXD calculations reported earlier. Hence, one really gets a three-fold benefit from the many-body transformations: improved efficiency, improved extensivity and improved accuracy. This triple benefit is a very promising aspect of the MR-EOM technology.

For the similarity transform approach to work well, the amplitudes should be small (typically 0.1 or less). If they become large, three- and higher-body terms in the transformed Hamiltonian (which are neglected) become important and the accuracy of the approach suffers. The reader may wonder why the remaining 1h and 1p excitations are not also transformed away. Part of the reason is that the corresponding amplitudes tend to become somewhat big, and may be hard to converge. Another reason is that such operators would lead to 3-body operators with exclusively active labels. We would prefer to include these operators in the final diagonalization step, but this will require a significant coding effort. Therefore, at present, the 1h and 1p excitations are treated through diagonalization.

### 3.3 Computational Details

The power and accuracy of the MR-EOM approach is illustrated by calculations of atomic excitation spectra (valence states only). We consider the first row transition metal atoms Cr, Mn, Fe and Co using a Def2-TZVPPD basis, including diffuse basis functions.[29, 38] Both positive cations of charge +1, +2 and neutral systems are investigated. Scalar relativistic effects are included by using the kinetic energy operator,

$$\hat{T} = \sqrt{p^2c^2 + m^2c^4} - mc^2 = \frac{p^2}{m+\sqrt{p^2/c^2+m^2}} \quad (3.9)$$

where $c \approx 137$, m= 1 in a.u.

The critical step in an MR-EOM calculation is the selection of the set of CASSCF configurations. The atomic valence electronic states for the transition metal atoms of interest can be characterized as having $4s^0 3d^n$, $4s^1 3d^{n-1}$ or $4s^2 3d^{n-2}$ character. The character of these states tends to be very pure, and typically only one or two of these types of states are present among the valence-excited states of a particular charged atom.

Our preferred strategy for the reference space is to select a small number of low-lying reference states (complete multiplets) that have the 4s occupations of interest. If possible, we like to perform a single state-averaged CASSCF to obtain a set of orbitals, in line with the general MR-EOM philosophy. In general it is not very hard in MR-EOM to get a balanced description of various atomic states that all have the same 4s configuration. However, it can be harder to achieve a proper balance of the two different types of states, e.g. the $4s^1 3d^{n-1}$ and $4s^2 3d^{n-2}$ states for neutral atoms. In order

not to bias the calculation towards one or the other type of 4s configuration we found it useful to define the weights of the CASSCF reference states such that the 4s occupation is the average of the two types of states. For example, in the above case for neutral atoms this means we define the reference weights such that the average 4s occupation is 1.5. In addition, we choose the weight of *each state* of a particular 4s-type included in the state-averaged CASSCF calculation to be equal. Hence, this protocol yields a unique set of weights once the decision is made as to which multiplets are to be included in the reference manifold. (A very sensible alternative would be to choose the total weight of *each multiplet* (rather than state) of a particular 4s type to be equal. We have not explored this possibility systematically, but think MR-EOM results are not very sensitive as long as the balance between different 4s configurations is achieved). In Table 3.3 the reference configurations and their weights are indicated. For the neutral atoms one always finds a mixture of $4s^1 3d^{n-1}$ and $4s^2 3d^{n-2}$ states, and the weighting is chosen such that the average 4s occupation is 1.5, as noted before. For the atoms of charge +2 one finds only $4s^0 3d^n$ configurations and only such states are included in the reference. For the $Fe^{2+}$ and $Co^{2+}$ atoms the references consist of a single multiplet, while for $Cr^{2+}$ and $Mn^{2+}$, we performed two sets of calculations denoted A or B, where set A has a small set of reference states, while calculation B uses a larger set of state-averaged CASSCF states as a reference manifold. In these di-cation cases the choice of reference space seems to play a more critical role.

For atoms of charge +1, the situation is more complex in general. Both $4s^0 3d^n$ and $4s^1 3d^{n-1}$ states occur. However we found it impossible to define a reasonable CASSCF to

include both. Hence in this case separate calculations on the $4s^0 3d^n$ and $4s^1 3d^{n-1}$ manifolds are performed. If only $4s^0 3d^n$ states or only $4s^2 3d^{n-2}$ states are considered, the active space consists of only the five 3d orbitals. If $4s^1 3d^{n-1}$ states occur, the active space comprises the 3d and 4s orbitals. For the +1 charged atoms we are forced to do separate calculation on the $4s^0 3d^n$ and $4s^1 3d^{n-1}$ manifolds. For the neutral systems we have a choice: We can perform a single calculation, or, we can do two separate calculations. The latter calculation of separate manifolds appears perhaps most natural. In the results section we compare both approaches.

In Table 3.3 all different reference manifolds are listed. In the CAS part of the calculation all spatial components (e.g. 9 components for $^5G$) are included, while the spin averaging is easily carried out analytically and only the states with highest $M_s$ value are included explicitly (see e.g. Ref. 25). It is crucial that the ensemble reduced density matrices are spherically symmetric in both real space and spin space. This leads to properly spin- and symmetry adapted transformation amplitudes and preserves the symmetry properties of the final transformed Hamiltonian in KM normal ordering. In the final MR-CI calculation, in principle we need to calculate only one state of a particular multiplet, as all states are rigorously degenerate. In practice we calculate a few states of various symmetry employing the $D_2$ subgroup, which then allows us to assign the symmetry of the states.

| Atom | Weighted CAS ensembles for calculations | Average 4s occupation |
|---|---|---|
| **Cr ($4s^1 3d^5 + 4s^2 3d^4$)** | 5x ($^7S+^5S$) [$4s^1 3d^5$] + 2x ($^5D$) [$4s^2 3d^4$] | 1.5 |
| **Cr ($4s^1 3d^5$)** | 1x ($^7S+^5S$) [$4s^1 3d^5$]] | 1 |
| **Cr ($4s^2 3d^4$)** | 1x ($^5D$) [$4s^2 3d^4$] | 2 |
| **$Cr^{1+}$ (4s0)** | 1x ($^6S$) [$4s^0 3d^5$] | 0 |
| **$Cr^{1+}$ (4s1)** | 1x ($^6D$) [$4s^1 3d^4$] | 1 |
| **$Cr^{2+}$/ A** | 1x ($^5D$) [$4s^0 3d^4$] | 0 |
| **$Cr^{2+}$/ B** | 1x ($^5D+11^3H+3^3P+7^3F+9^3G$) [$4s^0 3d^4$] | 0 |
| **Mn ($4s^1 3d^6 + 4s^2 3d^5$)** | 1x ($^6D$) [$4s^1 3d^6$] + 5x ($^6S$) [$4s^2 3d^5$] | 1.5 |
| **Mn ($4s^1 3d^6$)** | 1x ($^6D$) [$4s^1 3d^6$] | 1 |
| **Mn ($4s^2 3d^5$)** | 1x ($^6S$) [$4s^2 3d^5$] | 2 |
| **$Mn^{1+}$ (4s0)** | 1x ($^5D$) [$4s^0 3d^6$] | 0 |
| **$Mn^{1+}$ (4s1)** | 1x ($^7S+^5S$) [$4s^1 3d^5$] | 1 |
| **$Mn^{2+}$/ A** | 1x ($^6S+5^4D$) [$4s^0 3d^5$] | 0 |
| **$Mn^{2+}$/ B** | 1x ($^6S+9^4G+3^4P+5^4D$) [$4s^0 3d^5$] | 0 |
| **Fe ($4s^1 3d^7 + 4s^2 3d^6$)** | 5x ($^7F$) [$4s^1 3d^7$] + 7x ($^5D$) [$4s^2 3d^6$] | 1.5 |
| **Fe ($4s^1 3d^7$)** | 1x ($^7F$) [$4s^1 3d^7$] | 1 |
| **Fe ($4s^2 3d^6$)** | 1x ($^5D$) [$4s^2 3d^6$] | 2 |
| **$Fe^{1+}$/ A** | 1x ($^6D$) [$4s^1 3d^6$] | 1 |
| **$Fe^{1+}$/ B (4s0)** | 1x ($^4F$) [$4s^0 3d^7$] | 0 |
| **$Fe^{1+}$/ B (4s1)** | 1x ($^6D$) [$4s^1 3d^6$] | 1 |
| **$Fe^{2+}$** | 1x ($^5D$) [$4s^0 3d^6$] | 0 |
| **Co ($4s^1 3d^8 + 4s^2 3d^7$)** | 1x ($^4F$) [$4s^1 3d^8$] + 1x ($^4F$) [$4s^2 3d^7$] | 1.5 |
| **Co ($4s^1 3d^8$)** | 1x ($^4F$) [$4s^1 3d^8$] | 1 |
| **Co ($4s^2 3d^7$)** | 1x ($^4F$) [$4s^2 3d^7$] | 2 |
| **$Co^{1+}$(4s0)** | 1x ($^3F$) [$4s^0 3d^8$] | 0 |
| **$Co^{1+}$(4s1)** | 1x ($^5F$) [$4s^1 3d^7$] | 1 |
| **$Co^{2+}$** | 1x ($^4F$) [$4s^0 3d^7$] | 0 |

**Table 3.3.** *Weighted CAS ensembles for all calculations on transition metal atoms*

### 3.4 Results and discussion.

To compare the results of the MR-EOM calculations to the experimental values, we average the energies over the J levels in a particular L-S multiplet.

$$E_{LS} = \frac{\sum_{J \in LS} E_J \cdot (2J+1)}{\sum_{J \in LS} (2J+1)} \tag{3.10}$$

Spin-orbit coupling is not included in the current MR-EOM calculations and it seems most reasonable to compare against J-averaged values. The experimental data are taken from atomic tables from National Institute of Standards and Technology (NIST) website (ref. 41). The J-averaged experimental values are naturally arranged as excitation energies, setting the ground state energy to 0. Likewise in the MR-EOM-X calculations one can calculate excitation energies with respect to the ground state. However in such comparison one would assume the ground state is the suitable state to align with experiment (at 0 ev). It is more reasonable to take the average energy of the reference manifold to be aligned with the corresponding average of the experimental excitation energies[40] as collected conveniently on the NIST website[41] The difference between the NIST and MR-EOM-X weighted reference energies defines an energy shift that is applied to all MR-EOM-X excitation energies. This implies that our ground state energies are equal to – E-Shift, and are different from 0 in general.

Let us discuss the generic nature of results, taking the Co neutral atom as a representative example. The reference space consist of $^4$F ($4s^1 3d^8$) and $^4$F ($4s^2 3d^7$) having an average 4s occupation of 1.5. We wish to collect meaningful statistics to gauge the accuracy and trends among the variety of MR-EOM-X methods. When comparing to the NIST J-averaged values, the MR-EOM-X multiplets fall in various categories (See Table 3.4).

| | Total number of L-S multiplets | Low %Active/ states not in reference (Type a) | Number of extra multiplets (Type b) | Bad data (Type c) | Total number of multiplets used in statistics |
|---|---|---|---|---|---|
| **Cr** | 28 | | 3 | 3 | 22 |
| **$Cr^{1+}$ ($4s^0$)** | 16 | | 2 | | 14 |
| **$Cr^{1+}$ ($4s^1$)** | 19 | | 1 | 1 | 17 |
| **$Cr^{2+}$ A Small Reference** | 15 | | | | 15 |
| **$Cr^{2+}$ B Large Reference** | 16 | | 1 | | 15 |
| **Mn** | 26 | | 11 | | 15 |
| **$Mn^{1+}$ ($4s^0$)** | 16 | | 3 | | 13 |
| **$Mn^{1+}$ ($4s^1$)** | 25 | | 2 | | 23 |
| **$Mn^{2+}$ A Small Reference** | 10 | | | | 10 |
| **$Mn^{2+}$ B Large Reference** | 16 | | | | 16 |
| **Fe** | 26 | | 8 | | 18 |
| **$Fe^{1+}$ ($4s^0$)** | 7 | | | 1 | 6 |
| **$Fe^{1+}$ ($4s^1$)** | 24 | | 1 | | 23 |
| **$Fe^{2+}$** | 16 | | 2 | | 14 |
| **Co** | 16 | 2 | 3 | | 11 |
| **$Co^{1+}$ ($4s^0$)** | 13 | | | | 13 |
| **$Co^{1+}$ ($4s^1$)** | 5 | | | | 5 |
| **$Co^{2+}$** | 7 | | 1 | | 6 |

**Table 3.4.** *Details of calculations: numbers of L-S multiplets obtained in MR-EOM-X calculations; numbers of discussed states of type a, b, and c (see text); final number of retained L-S multiplets for statistics*

(a) The % Active character in the MR-EOM state is quite low (< 95% ). This often means that the state has a 4s character that is not included in the reference space. Examples in Table 3.5 are the $^2$D state at 2.78 ev (% Active 83%), and another $^2$D state at 3.46 ev (% Active 94.7%) which has predominantly $4s^0$ character, which is not included in the reference. We do not expect to calculate such states accurately, and this can be diagnosed from the calculation. Such states are excluded from the final statistics, therefore. The % active value refers to the results in a MR-EOM-T|SXD calculation.

(b) It is possible that in MR-EOM-X we calculate additional states that are not listed among the experimental data. Such additional MR-EOM-X states are usually high in energy. It is possible that these states would mix with other configurations (e.g. containing 4p character). There are usually only a small number of additional states. Exceptions are the Fe and Mn neutral systems for which we calculate additional 8 and 11 multiplets, respectively. Of course such states are not included in statistics. This feature is of some concern.

(c) Our algorithm in the CI code converges each multiplet separately, by monitoring the overlap with the zeroth order (CAS-CI) solution. This sometimes gives rise to the locating of the same multiplets twice, if the final state is very different from the starting guess. In such case we miss a state. Often this only occurs for certain variants of MR-EOM. Their occurrences are listed under " bad data". The number of states in the statistics is adjusted accordingly.

(d) For the great majority of our results we can directly compare to NIST J-averaged values. Such multiplets are included in the statistics.

In Table 3.4 we report on the states of various categories. The MR-EOM-X approaches typically behave similarly and we reported the worst-case scenarios.

| Co Neutral Shifted Energies | 2S+1 | L | % Active | Char. Of state | NIST | BareH | MR-EOM | | | | | |
|---|---|---|---|---|---|---|---|---|---|---|---|---|
| | | | | | | | T | T\|S | T\|SXD | T\|SXD-nph | T\|SXD\|U | T\|SXD\|U-min |
| | 4 | F | 97.70% | $4s^2$ | 0.10 | -0.86 | -0.10 | -0.10 | 0.12 | 0.12 | 0.14 | 0.15 |
| | 4 | F | 96.60% | $4s^1$ | 0.52 | 1.48 | 0.71 | 0.71 | 0.50 | 0.49 | 0.47 | 0.46 |
| | 2 | F | 95.60% | $4s^1$ | 0.98 | 1.99 | 1.16 | 1.16 | 0.94 | 0.94 | 0.91 | 0.91 |
| | 4 | P | 97.00% | $4s^2$ | 1.73 | 1.07 | 1.64 | 1.64 | 1.84 | 1.82 | 1.83 | 1.86 |
| | 2 | D | 94.90% | $4s^1$ | 2.07 | 2.22 | 2.18 | 2.18 | 1.94 | 1.91 | 1.90 | 1.88 |
| | 4 | P | 94.80% | $4s^1$ | 1.93 | 3.14 | 2.21 | 2.19 | 1.95 | 1.92 | 1.92 | 1.92 |
| | 2 | G | 98.20% | $4s^2$ | 2.08 | 1.38 | 1.99 | 2.00 | 2.16 | 2.18 | 2.19 | 2.19 |
| | 2 | P | 94.80% | $4s^1$ | 2.30 | 1.80 | 2.25 | 2.27 | 2.27 | 2.25 | 2.24 | 2.25 |
| %Active too low | 2 | D | 83.00% | $4s^2$ | 2.78 | 3.21 | 2.62 | 2.62 | 2.50 | 2.33 | 2.46 | 2.29 |
| | 2 | P | 96.80% | $4s^2$ | 2.57 | 3.66 | 2.69 | 2.67 | 2.62 | 2.64 | 2.60 | 2.63 |
| | 2 | H | 98.20% | $4s^2$ | 2.74 | 2.08 | 2.72 | 2.71 | 2.84 | 2.87 | 2.88 | 2.89 |
| | 2 | G | 95.80% | $4s^1$ | 2.88 | 4.08 | 3.15 | 3.13 | 2.84 | 2.84 | 2.82 | 2.82 |
| $4s^0$ not in reference | 2 | D | 94.70% | $4s^0$ | 3.46 | 4.85 | 3.19 | 3.09 | 3.00 | 2.96 | 2.99 | 2.98 |
| No Nist, excluded | 2 | F | 97.60% | | | 3.98 | 4.37 | 4.38 | 4.52 | 4.53 | 4.51 | 4.54 |
| No Nist, excluded | 2 | S | 93.10% | | | 7.56 | 5.95 | 5.94 | 5.64 | 5.60 | 5.62 | 5.63 |
| No Nist, excluded | 2 | D | 97.20% | | | 7.03 | 6.88 | 6.92 | 7.06 | 7.04 | 7.04 | 7.06 |

**Table 3.5.** *Shifted energies (in eV) of all MR-EOM methods for Co neutral atom*

| Statistical Errors | BareH | MR-EOM | | | | | |
|---|---|---|---|---|---|---|---|
| | | T | T\|S | T\|SXD | T\|SXD-nph | T\|SXD\|U | T\|SXD\|U-min |
| **AVG** | 0.196 | 0.066 | 0.061 | 0.011 | 0.008 | 0.003 | 0.007 |
| **ABSAVG** | 0.830 | 0.147 | 0.139 | 0.056 | 0.063 | 0.073 | 0.083 |
| **STDEV** | 0.864 | 0.155 | 0.148 | 0.066 | 0.077 | 0.086 | 0.097 |
| **RMS** | 0.886 | 0.169 | 0.160 | 0.067 | 0.078 | 0.086 | 0.097 |
| **MIN** | -0.963 | -0.197 | -0.196 | -0.126 | -0.157 | -0.161 | -0.186 |
| **Max** | 1.213 | 0.284 | 0.261 | 0.103 | 0.126 | 0.140 | 0.149 |
| **Max CI dimension** | 35429 | 35429 | 19673 | 19673 | 4593 | 19673 | 4559 |
| **CPU time (s)** | 1849 | 1772 | 833 | 938 | 330 | 907 | 306 |

**Table 3.6.** *Statistical analysis of MR-EOM-X data compared to NIST J-averaged values (in eV) for the Co neutral atom. Max CI dimension indicates the dimension of the final transformed Hamiltonian that is diagonalized. The CPU time (in s) indicates the time for the complete BareH or MR-EOM-X calculation, including the calculation and processing of the reference states (14 states), the solution of the cluster amplitudes (T, SXD, U), and the final diagonalization. In total 18 electronic states are calculated explicitly in the final diagonalization step. This suffices to assign 220 electronic states comprising 16 multiplets (shown in Table 3.5)*

In Table 3.6 the statistical data are shown for the Co neutral atom results, comparing NIST results with the variants of MR-EOM approaches including the BareH approach in which the original Hamiltonian is diagonalized over the same configurations as in MR-EOM-T (up to 2h1p configurations). These results sketch a very consistent picture:

The RMS error in BareH is 0.89 eV. This error drops to 0.17 eV in MR-EOM-T. The accuracy of MR-EOM-T|S is comparable (0.16 eV RMS), but the CI diagonalization space is significantly reduced (from 35,429 to 19,673). The RMS error is again significantly reduced when the $\widehat{\mathrm{X}}$ and $\widehat{\mathrm{D}}$ operators are included (to below 0.1 eV). There are only slight variations between T|SXD, T|SXD|-nph, T|SXD|U and T|SXD|U-min. However, the size of the diagonalization space is significantly reduced if the ph excitations are removed from the diagonalization manifold (to ~ 4600 determinants). The final diagonalization is the dominating cost of the calculations, and we see a corresponding reduction of cpu time with a reduction of CI dimension. The cpu times reported in Table 3.6 include the complete computational time it takes after the integral transformation, using the orbitals from a prior converged state-averaged CASSCF calculation. If 2h1p excitations are included in the final diagonalization, the cost of the calculation is about 1800 s. This reduces to about 900 s when up to 1h1p excitations are included. If only 2h, 1p and 1h excitations are included the time reduces further to about 300s. The solution of the T, SXD and U amplitudes now takes up a significant fraction of the time. It is clear from the results for the Co atom that accuracy increases, as more operators are included in the many-body transformation. This is true in particular for the $\widehat{\mathrm{X}}$ and $\widehat{\mathrm{D}}$

operators. The operator $\hat{S}$ seems to be less important for accuracy, but greatly reduces the cost of the calculations. The benefit of the inclusion of $\hat{U}$ is not entirely clear. It only marginally reduces the size of the CI manifold, and accuracy for the Co neutral atom actually decreases.

There is another reason to include the cluster operators: they reduce the size-extensivity errors of results. As shown in a previous paper [32] the operators $\hat{T}$, $\hat{S}$, $\hat{X}$ and $\hat{D}$ all have major effects, but also the operator $\hat{U}$ is important in reducing the size-extensivity errors. Let us also note that the difference in accuracy between T|SXD and T|SXD|-nph is minor, as is the difference between T|SXD|U and T|SXD|U-min. In the –nph and –min approaches the ph excitations are no longer included in the CI diagonalization. The reduction in computational cost is great, but we anticipate also a slightly smaller extensivity error, for the –nph and –min approaches. We hence find a triple benefit from the inclusion of additional cluster operators in the transformation: Their inclusion reduces extensivity errors, while the accuracy of the calculations is (presumably relatedly) significantly improved. Moreover, since the final diagonalization can be chosen to be more compact, the cost of the calculations decreases as more cluster operators are included in the transformation. The statistical results for the Co atom are shown in Figure 3.1 for all variations of MR-EOM.

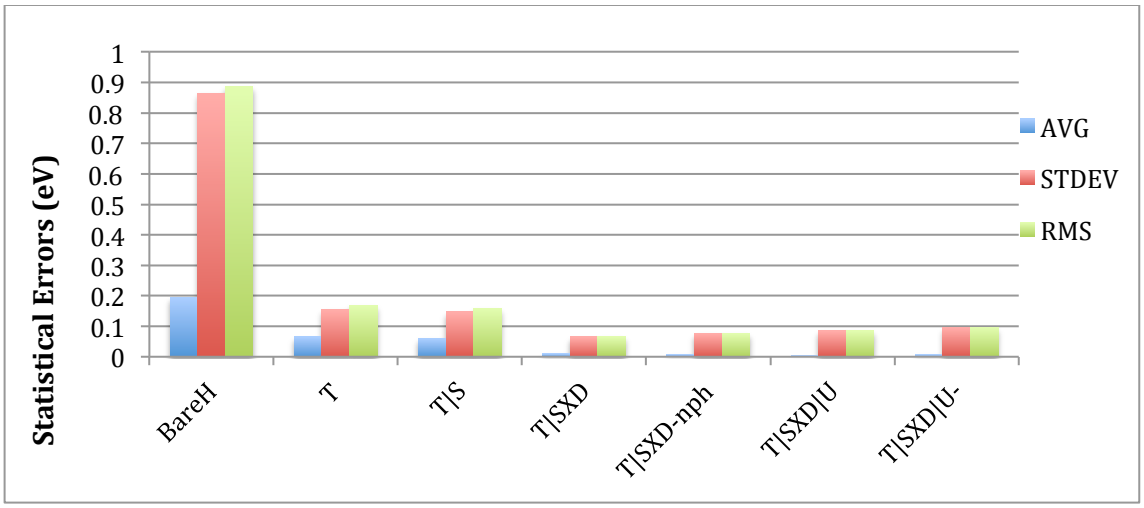


**Figure 3.1.** *Statistical errors of MR-EOM excitation energies (in eV) of valence states compared to J-averaged experimental results compiled by NIST for Co atom*

Our next explicit example is the $Fe^{+1}$ atom. Here we performed two separate calculations for the $4s^0 3d^7$, $4s^1 3d^6$ configurations. The results are listed in Table 3.7 and Table 3.8. In Figure 3.2 and Figure 3.3 we collected the statistics. The trends are very similar to the results for the Co neutral system. The MR-EOM approach that includes at least T|SXD in the transformation all show RMS errors that are below 0.1 eV, and are similar overall.

| $Fe^{1+}$ Shifted Energies | 2S+1 | L | % Active | Char. of state | NIST | BareH | MR-EOM | | | | | |
|---|---|---|---|---|---|---|---|---|---|---|---|---|
| | | | | | | | T | T\|S | T\|SXD | T\|SXD-nph | T\|SXD\|U | T\|SXD\|U-min |
| | 4 | F | 99.20% | $4s^0$ | 0.300 | 0.300 | 0.300 | 0.300 | 0.300 | 0.300 | 0.300 | 0.300 |
| | 4 | P | 97.90% | $4s^0$ | 1.688 | 1.942 | 1.771 | 1.756 | 1.723 | 1.705 | 1.712 | 1.726 |
| | 2 | G | 99.60% | $4s^0$ | 1.993 | 2.216 | 2.060 | 2.063 | 2.009 | 2.018 | 2.007 | 2.005 |
| | 2 | H | 99.40% | $4s^0$ | 2.548 | 2.804 | 2.676 | 2.668 | 2.577 | 2.597 | 2.584 | 2.583 |
| Bad data | 2 | D | 99.10% | $4s^0$ | 2.583 | 2.990 | 2.622 | 2.625 | 2.580 | 2.571 | 2.577 | ***** |
| | 2 | F | 98.40% | $4s^0$ | 3.957 | 4.429 | 4.084 | 4.070 | 3.972 | 3.975 | 3.957 | 3.972 |
| | 2 | D | 97.30% | $4s^0$ | 5.938 | 6.891 | 6.131 | 6.124 | 5.998 | 5.987 | 5.978 | 6.007 |

**Table 3.7.** *Shifted energies (in eV) of all methods for $Fe^{1+}$ $3d^7 4s^0$ configuration. Bad data arises for T|SXD|U-min method (see text)*

| $Fe^{1+}$ Shifted Energies | 2S+1 | L | % Active | Char. Of state | NIST | BareH | MR-EOM | | | | | |
|---|---|---|---|---|---|---|---|---|---|---|---|---|
| | | | | | | | T | T\|S | T\|SXD | T\|SXD -nph | T\|SXD \|U | T\|SXD\| U-min |
| $4s^0$ not in reference | 4 | F | 92.70% | $4s^0$ | 0.30 | 1.48 | 0.24 | 0.23 | -0.04 | -0.15 | -0.11 | -0.26 |
| | 6 | D | 99.20% | $4s^1$ | 0.05 | 0.05 | 0.05 | 0.05 | 0.05 | 0.05 | 0.05 | 0.05 |
| | 4 | D | 98.60% | $4s^1$ | 1.03 | 1.20 | 1.02 | 1.01 | 1.01 | 1.01 | 1.01 | 1.01 |
| $4s^0$ not in reference | 4 | P | 90.70% | $4s^0$ | 1.69 | 2.89 | 1.66 | 1.62 | 1.32 | 1.20 | 1.24 | 1.12 |
| $4s^0$ not in reference | 2 | G | 92.50% | $4s^0$ | 1.99 | 3.35 | 1.98 | 1.97 | 1.65 | 1.54 | 1.57 | 1.42 |
| | 4 | P | 98.90% | $4s^1$ | 2.66 | 3.22 | 2.71 | 2.72 | 2.69 | 2.70 | 2.68 | 2.67 |
| | 4 | H | 99.50% | $4s^1$ | 2.66 | 2.95 | 2.84 | 2.84 | 2.73 | 2.76 | 2.74 | 2.73 |
| | 4 | F | 99.10% | $4s^1$ | 2.83 | 3.25 | 2.94 | 2.95 | 2.88 | 2.90 | 2.88 | 2.87 |
| | 6 | S | 95.80% | $4s^2$ | 2.89 | 1.37 | 2.71 | 2.70 | 2.91 | 2.83 | 2.92 | 2.86 |
| | 2 | P | 98.60% | $4s^1$ | 3.25 | 3.62 | 3.28 | 3.29 | 3.25 | 3.27 | 3.25 | 3.25 |
| | 4 | G | 99.20% | $4s^1$ | 3.19 | 3.57 | 3.35 | 3.35 | 3.26 | 3.28 | 3.25 | 3.25 |
| | 2 | H | 99.10% | $4s^1$ | 3.26 | 3.61 | 3.41 | 3.41 | 3.30 | 3.34 | 3.31 | 3.30 |
| | 2 | F | 96.20% | $4s^1$ | 3.40 | 3.91 | 3.49 | 3.50 | 3.38 | 3.58 | 3.34 | 3.52 |
| | 2 | G | 98.90% | $4s^1$ | 3.79 | 4.26 | 3.92 | 3.92 | 3.83 | 3.86 | 3.83 | 3.83 |
| | 4 | D | 98.70% | $4s^1$ | 3.90 | 4.40 | 4.03 | 4.03 | 3.96 | 3.96 | 3.93 | 3.95 |
| | 2 | I | 99.50% | $4s^1$ | 4.08 | 4.52 | 4.33 | 4.33 | 4.16 | 4.21 | 4.18 | 4.17 |
| | 2 | G | 99.20% | $4s^1$ | 4.15 | 4.75 | 4.31 | 4.32 | 4.21 | 4.22 | 4.22 | 4.21 |
| | 2 | D | 98.40% | $4s^1$ | 4.49 | 5.11 | 4.61 | 4.61 | 4.54 | 4.54 | 4.51 | 4.53 |
| | 2 | S | 98.70% | $4s^1$ | 4.62 | 5.42 | 4.74 | 4.74 | 4.66 | 4.64 | 4.66 | 4.67 |
| | 2 | D | 98.50% | $4s^1$ | 4.73 | 5.39 | 4.84 | 4.85 | 4.77 | 4.80 | 4.73 | 4.74 |
| | 2 | F | 98.70% | $4s^1$ | 5.57 | 6.28 | 5.76 | 5.77 | 5.65 | 5.68 | 5.62 | 5.63 |
| | 4 | P | 97.70% | $4s^1$ | 6.17 | 6.34 | 6.38 | 6.39 | 6.28 | 6.29 | 6.24 | 6.27 |
| | 4 | F | 98.00% | $4s^1$ | 6.22 | 7.11 | 6.46 | 6.47 | 6.34 | 6.36 | 6.32 | 6.34 |
| | 4 | G | 96.40% | $4s^2$ | 6.73 | 5.65 | 6.78 | 6.76 | 6.88 | 6.84 | 6.90 | 6.84 |
| | 4 | P | 96.20% | $4s^2$ | 7.13 | 7.07 | 7.11 | 7.16 | 7.36 | 7.29 | 7.31 | 7.26 |
| | 4 | D | 96.10% | $4s^1$ | 7.49 | 6.51 | 7.49 | 7.50 | 7.65 | 7.62 | 7.62 | 7.59 |
| No Nist excIded | 4 | F | 96.20% | $4s^1$ | | 8.47 | 9.22 | 9.25 | 9.39 | 9.35 | 9.36 | 9.31 |

**Table 3.8.** *Shifted energies (in eV) of all methods for $Fe^{1+}$ $3d^6 4s^1$ configuration. The three rows in green have $3d^7 4s^0$ character and are not used in the $3d^6 4s^1$ statistical analysis. The bottom row is not used in the analysis because it cannot be matched with a proper J-averaged NIST value.*

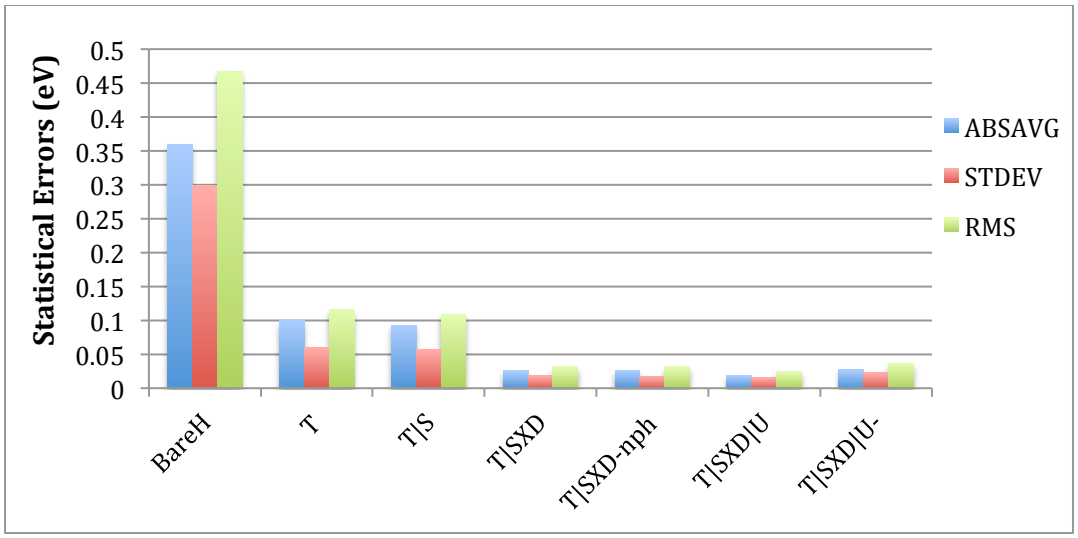


**Figure 3.2.** *Statistical errors of MR-EOM excitation energies (in eV) of valence states compared to J-averaged experimental results compiled by NIST for* $Fe^{1+}$ $3d^7 4s^0$ *states*

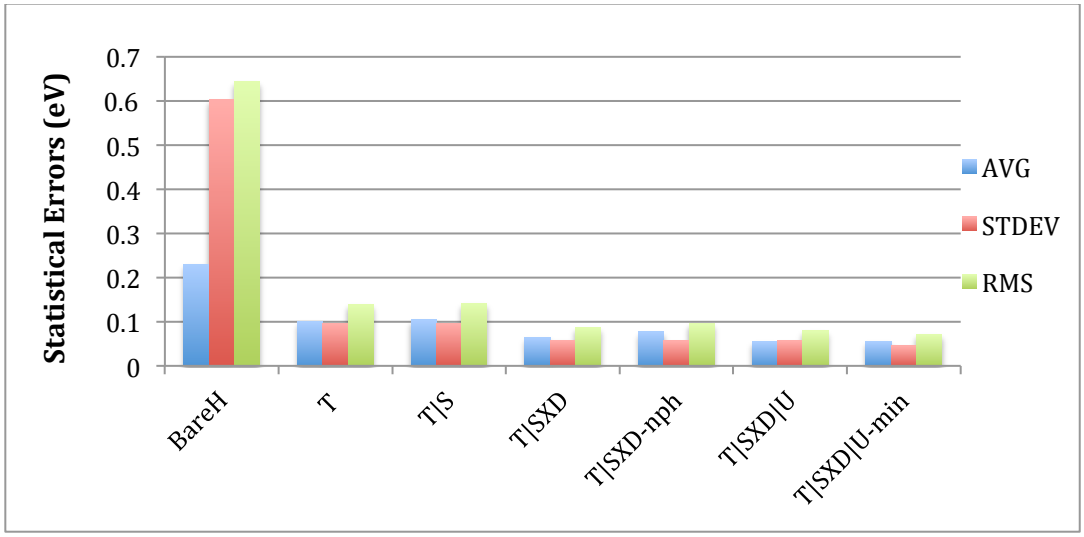


**Figure 3.3.** *Statistical errors of MR-EOM excitation energies (in eV) of valence states compared to J-averaged experimental results compiled by NIST for* $Fe^{1+}$ $3d^6 4s^1$ *states*

Let us next consider the case of neutral atoms. For the neutral atoms, we employed 3 different types of reference spaces.

(a). $4s^1 3d^{n-1}$ states only. Only states of this type are considered in final MR-EOM calculations.

(b). $4s^2 3d^{n-2}$ states only, again only these states are treated in final MR-EOM.

(c). Include both $4s^1 3d^{n-1}$ and $4s^2 3d^{n-2}$ states in a single calculation. All states are included in final MR-EOM and in statistics below.

Since in the separate calculations of type (a) and type (b) the orbitals are optimized to the particular configurations of interest one might anticipate that the RMS errors within each manifold are improved compared to the combined calculation. In addition the number of data in the calculation denoted as "total" (i.e. the combined calculation on $4s^1$ and $4s^2$ manifolds) equals the combined number of data points from the separate $4s^1$ and $4s^2$ calculations. The results are shown in figure 3.4. As seen the separate calculations are indeed more accurate for the Cr atom, but results are fairly equal for the other atoms.

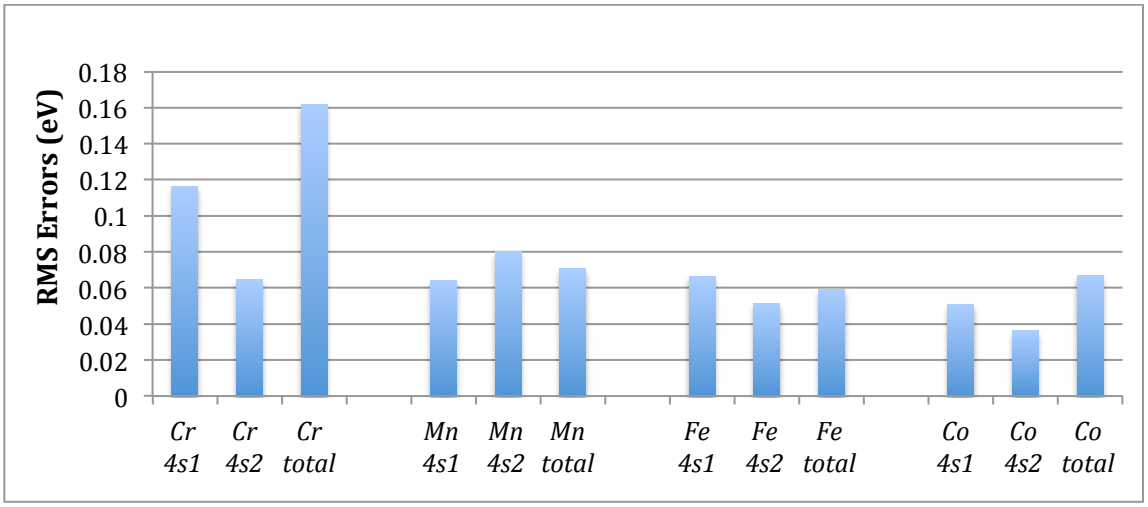


**Figure 3.4.** *Comparison of RMS errors (in eV) for $4s^1$+$4s^2$ (total) and separate calculations of $4s^1$ and $4s^2$ states for neutral atoms with the MR-EOM-T|SXD method*

However, there is also the consideration of the energy differences between the states of different characters. These excitation energies are obtained by subtracting total energies in the case of separate calculations on $4s^1$ and $4s^2$ manifolds. As before we define the excitation energies by aligning the weighted average excitation energy for states in the reference manifold exactly with the weighted average of the NIST experimental data. The results are depicted in Figure 3.5.

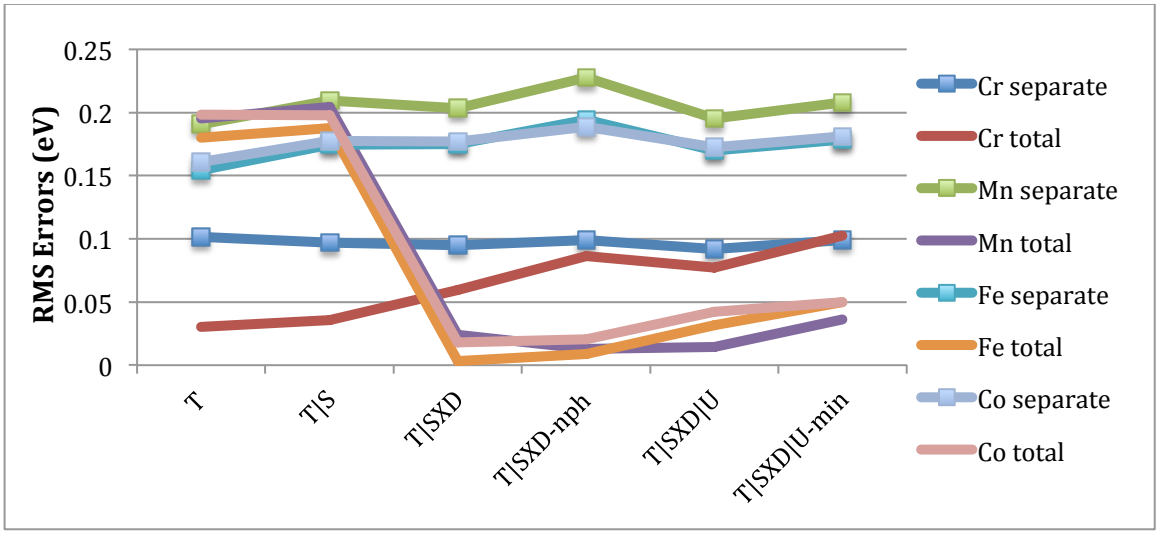


**Figure 3.5.** *Comparison of RMS errors (in eV) for $4s^1$+$4s^2$ (total) and separate calculations of $4s^1$ and $4s^2$ states for neutral atoms*

This figure shows convincingly that the MR-EOM results for a single calculation tend to be significantly more accurate. For Fe, Mn, and Co the results from the single calculation fall below 0.05 eV, while for the separate calculations errors are about 0.2 eV. This trend is followed as soon as $\widehat{X}$ and $\widehat{D}$ operators are included in the transformation. For the Cr atom, however, the separate calculations are a bit more accurate, but errors are larger than in the case of Mn, Fe and Co.

One more interesting observation can be made for the calculations of the $4s^2 3d^{n-2}$ states. In all cases (all atoms) we find a significant $\hat{X}$, $\hat{D}$ amplitude (~0.2) that indicates excitation from the 4s orbital. This does not seem to affect the accuracy of the results. On the other hand, for the Cr atom we find a fairly large $T_2$ amplitude and this compromises results, and lowers the active space character for many states.

To conclude this investigation of the reference state: It appears better to include all states of interest in a single MR-EOM calculation, even when the CASSCF orbitals are accurate in an average sense only. MR-EOM apparently benefits from a cancellation of errors. This balance is harder to achieve when subtracting total energies from separate calculations.

| Atoms | Excitations | NIST | BareH | MR-EOM | | | | | |
|---|---|---|---|---|---|---|---|---|---|
| | | | | T | T\|S | T\|SXD | T\|SXD-nph | T\|SXD\|U | T\|SXD\|U-min |
| $Cr^{1+}$ | $6S(4s^0)->6D(4s^1)$ | 1.522 | -0.099 | 1.563 | 1.554 | 1.499 | 1.481 | 1.508 | 1.483 |
| $Mn^{1+}$ | $7S(4s^1)->5D(4s^0)$ | 1.808 | 4.422 | 1.992 | 1.997 | 1.987 | 2.039 | 1.983 | 2.012 |
| $Fe^{1+}$ | $6D(4s^1)->4F(4s^0)$ | 0.248 | 2.919 | 0.454 | 0.468 | 0.458 | 0.498 | 0.452 | 0.471 |
| $Co^{1+}$ | $3F(4s^0)->5F(4s^1)$ | 0.429 | -2.460 | 0.221 | 0.209 | 0.215 | 0.195 | 0.225 | 0.209 |

**Table 3.9.** *Comparison of the lowest $4s^0$ to $4s^1$ excitation energies (in eV) from separate calculations and NIST values for $Cr^{1+}$, $Mn^{1+}$, $Fe^{1+}$ and $Co^{1+}$ atoms*

For the Cr, Mn, Fe and Co atoms of charge +1, we were unable to find a set of reference orbitals that describe both the $4s^0$ and $4s^1$ states. In Table 3.9 we report the excitation energies from separate calculations between the level $4s^0$ and $4s^1$ states. For $Mn^{1+}$ and $Fe^{1+}$ the $4s^1$ state is the ground state, while for $Cr^{1+}$ and $Co^{1+}$ the $4s^0$ state is the lowest state. Inspecting the results we see that consistently the $4s^1$ state is calculated to

be about 0.2 eV lower compared to the $4s^0$ state for the *$Mn^{1+}$, $Fe^{1+}$ and $Co^{1+}$ atoms*, and all MR-EOM methods. The results for the $Cr^{1+}$ atom on the other hand are quite accurate, although the Cr atom is a bit of an outlier as before.

Let us note that for the $4s^0$ states, only 3d orbitals are used to define the active space, while for the $4s^1$ states the active space comprises both 4s and 3d orbitals. The consistency of the errors for the charge +1 systems is also similar to the errors for the neutral atoms, shown in Figure 3.5 (with the exception of Cr). It is not totally clear what is missing. Remarkably, inclusion of ph excitations (which effectively includes a state specific relaxation of the 4s orbital) does not seem important, once $\widehat{\mathrm{X}}$ and $\widehat{\mathrm{D}}$ amplitudes are included.

We wish to discuss one more situation explicitly: The $Mn^{2+}$ and $Cr^{2+}$ atoms. We performed two sets of calculations: One with a small reference space, (A), and another with a larger reference space, (B). The statistical results are presented in Table 3.10. It is clear that the larger reference space yields the most accurate results. However, for the MR-EOM-T|SXD-nph and T|SXD|U-min approaches both reference spaces are quite satisfactory.

| | | MR-EOM | | | | | |
|---|---|---|---|---|---|---|---|
| **RMS** | **Bare H** | **T** | **T\|S** | **T\|SXD** | **T\|SXD-nph** | **T\|SXD\|U** | **T\|SXD\|U-min** |
| **$Cr^{2+}$/ A** | 0.609 | 0.187 | 0.195 | 0.111 | 0.074 | 0.149 | 0.085 |
| **$Cr^{2+}$/ B** | 0.380 | 0.089 | 0.095 | 0.075 | 0.094 | 0.049 | 0.061 |
| **$Mn^{2+}$/ A** | 0.512 | 0.207 | 0.209 | 0.081 | 0.114 | 0.202 | 0.066 |
| **$Mn^{2+}$/ B** | 0.521 | 0.125 | 0.132 | 0.075 | 0.094 | 0.056 | 0.066 |

**Table 3.10.** *Comparison of RMS errors (in eV) for $Cr^{2+}$ and $Mn^{2+}$ with small number of reference states (A) and large number of reference states (B)*

It is interesting that these approaches do not include ph excitations and are hence more nearly size-extensive. They also do not give flexibility to include orbital relaxation through ph excitations. The evidence up to now is anecdotal, but it may be that the more–extensive results are less sensitive to the choice of reference space. This would be very desirable of course. Finally, in Figure 3.6 and 3.7 we report the statistic for all atom species.

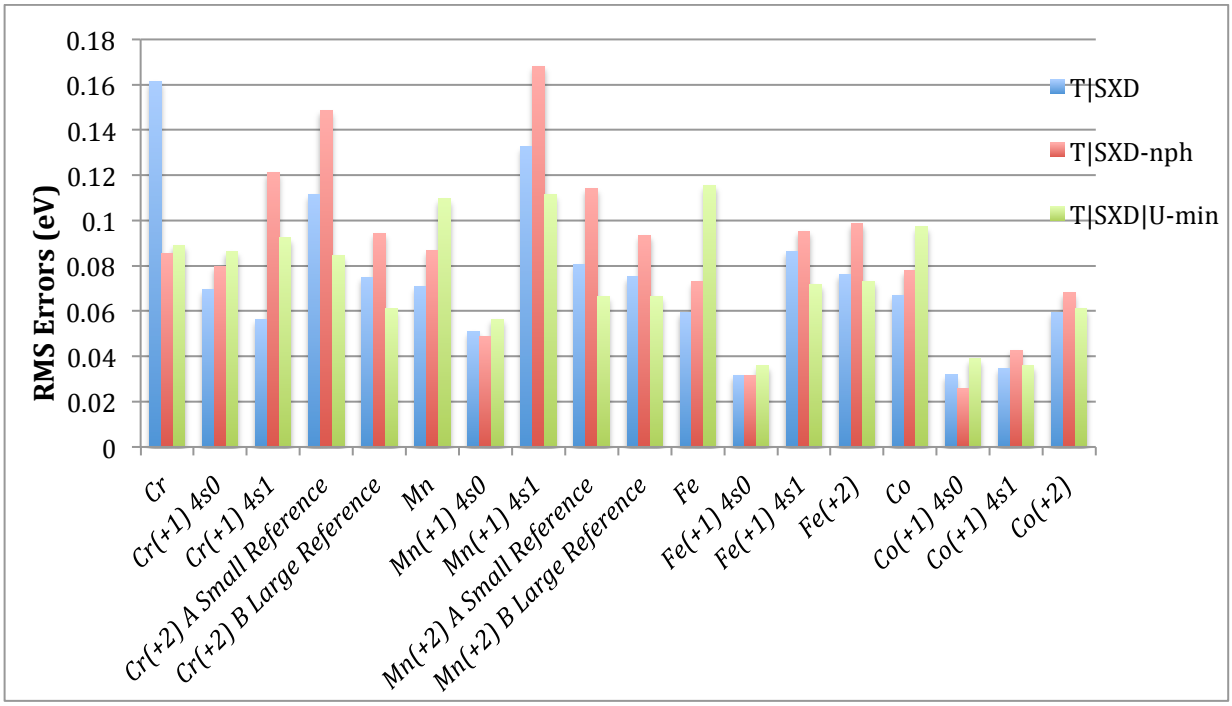


**Figure 3.6.** *RMS errors (in eV) in comparison to NIST for all atoms with MR-EOM methods T|SXD, T|SXD-nph and T|SXD|U-min*

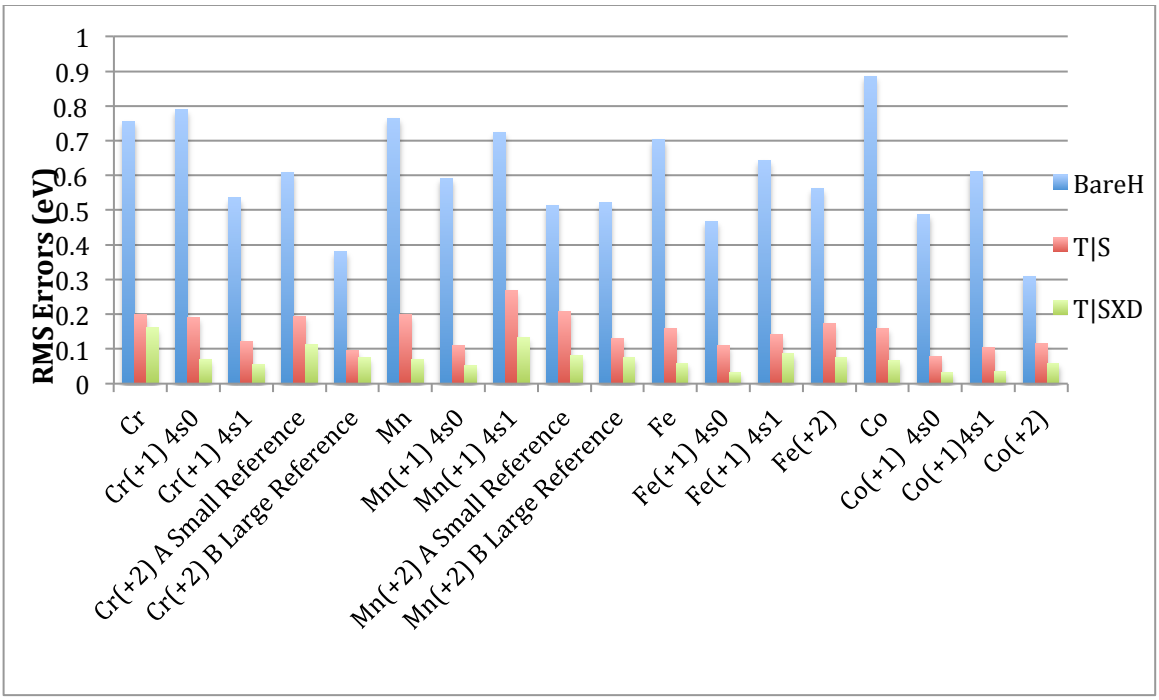


**Figure 3.7.** *RMS errors (in eV) in comparison to NIST for all atoms with methods Bare H, MR-EOM-T|S, and MR-EOM-T|SXD*

The statistics of the results for all atomic species are summarized in Figures 3.6 and 3.7. Figure 3.6 shows RMS errors for the T|SXD, T|SXD-nph and T|SXD|U-min MR-EOM approaches. The RMS errors for these approaches are typically smaller than 0.1 eV. Significantly larger RMS errors are found for the Cr neutral (0.16 eV for T|SXD) and for the $Mn^{1+}$ ($4s^1$) manifold of states (~ 0.16 eV for T|SXD and T|SXD-nph approaches). The Cr neutral atom has been considered before in reference (3), employing a larger set of reference states. The error for MR-EOM-T|SXD then drops to 0.043 eV. The Cr neutral shows a large sensitivity to the active space, and as for the $Mn^{2+}$ and $Cr^{2+}$ cases the effects are less pronounced for the –nph and –min approaches, which do not included ph excitations at the CI stage. Overall, the results from the MR-EOM approach that include at least the T|SXD transformations are highly satisfactory. The importance of

these operators is emphasized in Figure 3.7 in which we contrast the BareH against the T|S and T|SXD approaches. The errors in BareH which uses diagonalization over a sizable CI manifold including up to 2h1p configurations are typically 0.6 eV or larger. In the MR-EOM-T|S approach this is reduced to below 0.2 eV typically, and this is reduced further to about 0.1 eV in T|SXD. Every entry in Figure 3.6 and 3.7 is obtained using a single set of state-averaged CASSCF orbitals, and a single set of T|SXD|U amplitudes. Each L-S multiplet is fully spin- and symmetry-adapted.

### 3.5 Conclusions

In this paper results are presented for the valence excitation spectra of the transition metal atoms Cr, Mn, Fe and Co, having charges 0, +1 and +2. The MR-EOM approaches in which dynamical correlation effects are folded into a dressed Hamiltonian using a well defined sequence of many-body similarity transformations yield highly satisfactory results: 100's of electronic excited states are obtained from a compact diagonalization. The procedure does require the definition of an active space, and a selection of a weighted set of reference states. The results of MR-EOM calculations typically show only a modest sensitivity to details of the calculation. The MR-EOM approach is of course equally well applicable to molecular systems, but here we focused on atoms, which are exceedingly well characterized experimentally. The MR-EOM approaches show the nice feature that by increasing the number of types of cluster amplitudes included in the calculation, T|SXD|U, the resulting CI manifolds can be

accordingly more compact. Increasing the number of cluster operators reduces the CI manifold, this in turn decreases computation time; it also reduces issues with-size-extensivity, and overall increases the accuracy of results (with the exception of $\hat{U}$ perhaps which is less systematic). This triple benefit of the use of cluster expansions in multi-reference calculations is quite attractive.

In the case of the first-row transition metal atoms under consideration one can clearly distinguish configurations that differ in the occupation of the 4s orbital. For the atoms of charge +1, we were forced to do separate calculations on the $4s^0$ and $4s^1$ manifolds of states, as we could not obtain a suitable state-averaged CASSCF describing both manifolds. For the neutral atoms we explored two possibilities: Separate calculations on the $4s^1$ and $4s^2$ manifolds, or a single combined calculation of all states. Both approaches yield satisfactory results for the relative energies within each manifold. However, the excitation energies between manifolds are usually somewhat better reproduced in the combined calculation (reducing errors from about 0.2 eV in the separate to 0.1 eV in a combined calculation). Since the CASSCF solutions for the different manifolds are quite different, it is somewhat surprising perhaps that accurate results can be obtained at all from a single calculation. The results on the combined calculations convincingly demonstrate the power of the MR-EOM approach to get accurate results from a single compact calculation for electronic states that are quite different, even while using a single set of state-averaged orbitals and a single set of cluster amplitudes. This feature of the MR-EOM approach clearly enhances the ease of application of the approach also for molecular systems, for which a separation of

electronic states in different manifolds may be less clear-cut than for atoms. We anticipate the relative ease of use of the multireference EOM-CC approach to be an attractive feature in future applications.

# Chapter 4

**Application of Multireference Equation of Motion Coupled Cluster Method including spin-orbit coupling to atomic spectra of Cr, Mn, Fe and Co.**


**Abstract**

The recently introduced Multireference Equation of Motion (MR-EOM) approach is combined with a simple treatment of spin-orbit coupling, as implemented in the ORCA program. The resulting Multireference Equation of Motion Spin-Orbit Coupling (MR-EOM-SOC) approach is applied to the first-row transition metal atoms Cr, Mn, Fe and Co, for which experimental data are readily available. Using the MR-EOM-SOC approach the splitings in each L-S multiplet can be assessed accurately (RMS errors of about 70 $cm^{-1}$). The RMS errors for J-specific excitation energies range from 414 to 783 $cm^{-1}$ and are comparable to previously reported J-averaged MR-EOM results using the ACESII program. The MR-EOM approach is highly efficient. A typical MR-EOM calculation of a full spin-orbit spectrum takes about 2 hours, while the corresponding MR-AQCC calculation in ORCA can take weeks.

## 4.1 Introduction

In wave function based quantum chemistry there has been a sharp dividing line between systems that can be considered single reference and systems that benefit from a multi-reference treatment. Single reference methods are mature at present, and among these coupled cluster approaches[31] are considered most systematic. For ground state chemistry, CCSD(T)[10] has emerged as the method of choice.[3, 10] This method can be used in conjunction with domain based localized pair natural orbitals (DLPNOs)[42, 43, 44] to provide a highly efficient way to calculate ground state energies, that is applicable to large systems (~50 – 400 atoms).

Likewise, methods for the calculation of excited states are well established, provided a single reference parent state (not necessarily the ground state) is available. Versatile wave function based approaches would include SAC-CI[45, 46], CC-LRT[47, 48, 49] and EOM-CC[35, 50, 51]. Fock-space coupled cluster (FS-CC)[27, 52-57] is an interesting approach, as the origin of this method is clearly rooted in multireference theory. However, in its application, the solutions of the cluster equations are built on top of a single determinant. The final target states are multi-configurational, but this is also true in the other approaches to excited states. Similarity transformed EOM-CC (STEOM-CC)[18, 19] is operationally very close to FS-CC, although conceptually it is different. It is however, very closely related to the methods used in this paper. STEOM can be viewed as a transform and diagonalize approach. The zeroth order approximation is CI singles. In STEOM one defines a similarity transform of the Hamiltonian such that all second quantized operators that

excite out of the zeroth order CIS space are transformed to zero. The resulting equations are very close to FS-CC. All of these methods are most conveniently referred to as single reference.

In multireference problems, one cannot identity a single reference parent state. One necessarily has to approach the problem using a linear combination of determinants as a zeroth-order wave function. Much of the multireference coupled cluster literature today focuses on state-specific approaches (e.g. see Ref. 11 for a recent and extensive review of MR-CC approaches). The focus is on a single state at a time. The work on the MR-EOM approach[24, 25, 32] is different in this respect. In most physical problems that require a multireference description, both ground and excited states are of interest, as they are typically close in energy and "interesting". Hence we think it is natural to approach the problem in a multistate fashion.[53, 54] Early approaches (see Ref. 11 for discussion) suffer from the so-called intruder-state problem. In a way this can be attributed to the fact that in these earlier approaches, one tried to obtain an effective Hamiltonian that is no longer interacting with other states, or, it leads to a complete decoupling of the states of interest.

The philosophy underlying MR-EOM is different, and is analogous to the ideas underlying STEOM.[18, 19, 20] One first identifies states of interest. In the case of MR-EOM, they can always be described qualitatively by a compact CAS space.[21, 22] In the next step one introduces a set of transformations that aim to equate second quantized matrix elements of the transformed Hamiltonian which couple determinants in the CAS to other excited determinants to zero. In general, we do not achieve a full decoupling of

the CAS space to other excited determinants. In the currently employed MR-EOM approach, the transformed Hamiltonian contains matrix elements between CAS and 1-hole, 1-particle and 2-hole configurations. Here h (hole) indicates removal of an electron from a doubly occupied orbital in CAS determinants, while p (particle) refers to the population of a virtual or unoccupied orbital. We take a pragmatic approach and simply diagonalize the transformed Hamiltonian over the new first-order interacting space. Since we do not decouple the CAS from all other determinants, MR-EOM does not suffer from the intruder state problem. However, since we need to perform CI, the resulting energies are not completely extensive. A great virtue of the transform and diagonalize strategy is that the resulting transformed Hamiltonian commutes with $\hat{S}^2$ and $\hat{S}_Z$ and also has the proper point group symmetry. This allows us to include spin-orbit coupling in a very simple way. Using the procedure described in Ref. 33 and Ref. 58, Quasi-Degenerate Perturbation Theory (QDPT) is used to add spin-orbit coupling contributions to the MR-EOM state energies. Here, we make use of a bare (untransformed) spin-orbit mean-field (SOMF) operator $\widehat{H}_{SOMF}$ (see Ref. 33 and Ref. 58 and references therein), which is the most straightforward approach.

The paper is organized as follows. In section 4.2, we discuss the theory underlying MR-EOM, and briefly discuss some special features of the implementation of MR-EOM in the ORCA program. We also discuss the inclusion of spin-orbit coupling in MR-EOM-SOC. In section 4.3, we provide computational details and discuss results for the Cr, Mn, Fe and Co neutral atoms. Conclusions are presented in section 4.4.

## 4.2 Theory

The MR-EOM method provides efficient access to many electronic excited states (possibly hundreds) using a convenient transform and diagonalize strategy.[24, 25, 32] In an MR-EOM calculation, all of the accessible electronic states can be qualitatively described by linear combinations of electronic configurations that differ in the occupation of a relatively small number of orbitals. This defines the complete active space (CAS).[21, 22] The main feature of the MR-EOM approach is use of a sequence of similarity transformations of the bare second-quantized Hamiltonian. As a result of the transformation, most of the Hamiltonian matrix elements that couple determinants in the CAS to other determinants out of the CAS vanish. Details will be briefly discussed here.

The basic idea underlying MR-EOM is similar to single reference EOM-CC[2, 35] and similarity transformed EOM-CC,[18, 19] while the details are more complicated. In an MR-EOM calculation, the transformed Hamiltonian is diagonalized over a compact new first-order interacting subspace out of the CAS. The size of the subspace depends on the operator that is used in the similarity transformation. The transformed Hamiltonian is defined as follows:[24, 25, 32]

$$\begin{aligned} &G = \{e^Y\}^{-1} H \{e^Y\} \rightarrow \{e^Y\} G = H \{e^Y\} \rightarrow \\ &G = (H\{e^Y\})_{Connected} - (\{e^Y - 1\} G)_{Connected} = \cdots \\ &= g_0 + g_r^p \{p^+ r\} + \frac{1}{4} g_{rs}^{pq} \{p^+ r q^+ s\} + \cdots \end{aligned} \tag{4.1}$$

If the operators in the transformation do not commute, the transformations are expressed in terms of KM normal-ordered[29, 30, 31] exponentials of the excitation operators with respect to the CASSCF reference, as indicated by braces. In this work we will consider the use of operators $\hat{T}$, $\hat{S}$, $\hat{X}$and $\hat{D}$. The operator $\hat{\mathrm{T}}$ is defined as

$$\hat{\mathrm{T}} = \sum_{i,a} t_i^a \hat{E}_i^a + \frac{1}{2}\sum_{i,j,a,b} t_{ij}^{ab} \hat{E}_{ij}^{ab} \tag{4.2}$$

in which $t_i^a$ and $t_{ij}^{ab}$ are respectively, single and double excitation amplitudes. The operator $\hat{E}_i^a$ and $\hat{E}_{ij}^{ab}$ are spin-free, single and double excitation operators.

The transformed Hamiltonian $\overline{\mathrm{H}}$ used in this paper then takes the following form (see Refs. 24, 25 and 32):

$$\begin{aligned} \overline{\mathrm{H}} &= e^{-T} H e^{T} \\ &= \bar{h}_0 + \bar{h}_p^q \{E_q^p\} + \bar{h}_{pq}^{rs} \{E_{rs}^{pq}\} + \bar{h}_{pqr}^{stu} \{E_{stu}^{pqr}\} + \ldots \end{aligned} \tag{4.3}$$

The elements $\bar{h}_0$, $\bar{h}_q^p$, $\bar{h}_{rs}^{pq}$ and $\bar{h}_{stu}^{pqr}$ are determined in terms of the Fock matrix, two-electron integrals, the single and double excitation amplitudes and the reference state-averaged one- and two-electron reduced density matrices. All of these quantities can be obtained from the state-averaged CASSCF calculation, with the exception of the cluster amplitudes.

The t-amplitudes are determined as iterative solutions of a mixed set of amplitude equations. The singles residual equation is a projected residual equation[17]

$$\sum_k \omega_k \left\langle R_k \middle| E_a^{i/x} \overline{H} \middle| R_k \right\rangle = 0. \tag{4.4}$$

Here $\omega_k$ and $|R_k\rangle$ refer to the weights used and states obtained from the CAS CI (or CASSCF), while i and x denote an inactive or active orbital respectively. The doubles residual equation is obtained by setting the elements $\overline{h}_{ij}^{ab}$, $\overline{h}_{ix}^{ab}$, $\overline{h}_{xy}^{ab}$ of the similarity transformed Hamiltonian of Eq. (4.3) to zero,

$$\overline{h}_{ij}^{ab} = \overline{h}_{ix}^{ab} = \overline{h}_{xy}^{ab} = 0. \tag{4.5}$$

A subsequent transformation is given by

$$G = \{e^{S+X+D}\}^{-1} \overline{\mathrm{H}}_2 \{e^{S+X+D}\}. \tag{4.6}$$

Here $\overline{\mathrm{H}}_2$ denotes $\overline{\mathrm{H}}$ truncated to 2-body operators in KM normal-order. The S, X, D-amplitudes are solved from

$$\sum_k \omega_k \left\langle R_k \middle| E_a^{i/x} F \middle| R_k \right\rangle = 0 \tag{4.7}$$

$$g_{ax}^{ij} = g_{ay}^{ix} = g_{ya}^{ix} = 0 \tag{4.8}$$

In all equations, only terms up to quadratic in the transformation amplitudes are included, and the transformed Hamiltonian in KM normal-order only includes up to two-body terms. The preferred type of amplitude equation is the many-body type, in which elements of the transformed Hamiltonian are equated to zero.

In the MR-EOM-T|SXD-nph approach, the first order interacting space is reduced to the 1p, 1h and 2h configurations out of the CAS. All other matrix-elements coupling a CAS determinant to a determinant in the external space vanish. In the MR-EOM-T|SXD approach, we investigate potential couplings from the CAS + 1h + 1p + 2h space into the 1p1h space, and the latter is now included in the diagonalization space. This significantly increases the size of the diagonalization space, but it is not expected to change the results much. Many (hundreds of) excited states can be obtained accurately, while the transformed Hamiltonian is calculated only once and only a few states are included in the state-averaged CAS calculation, which determine the reference cumulants used in the amplitude equations. The final transformed Hamiltonian is not Hermitian, and is truncated to up to 2-body operators (in KM normal-order). This 2-body operator can be easily rewritten in bare vacuum form, and this is used as input in the Multireference Configuration Interaction (MR-CI) module of our local ACESII program.[27]

The above describes MR-EOM, as implemented in the ACESII program. However, the MR-EOM calculation in ORCA[28] proceeds in a slightly different way. The first transformation involves the operator $\hat{\mathrm{T}}$ which is the same as in ACESII, but the second transformation involves the $\hat{\mathrm{T}}^{+}$ operator which is defined as

$$\hat{T}^{+} = \sum_{i,a} t_a^i \, \hat{E}_a^i + \frac{1}{2} \sum_{i,a} t_{ab}^{ij} \, \hat{E}_{ab}^{ij} \, , \tag{4.9}$$

in which the de-excitation amplitudes are approximated as

$$t_a^i \approx t_i^a \, , \tag{4.10}$$

$$t_{ab}^{ij} \approx t_{ij}^{ab} \, .$$

The second transformation is therefore given by

$$\hat{F} = e^{\hat{T}^{+}} \hat{\bar{H}}_2 e^{-\hat{T}^{+}}$$

$$= f_0 + \sum_{p,q} f_q^p \{\hat{E}_q^p\} + \sum_{p,q,r,s} f_{rs}^{pq} \{\hat{E}_{rs}^{pq}\} + \sum_{p,q,r,s,t,u} f_{stu}^{pqr} \{\hat{E}_{stu}^{pqr}\} + \cdots \tag{4.11}$$

Then we follow the same scheme as in an ACESII calculation, which means the final similarity transformation $\hat{G}$ takes the following form:

$$\hat{G} = \{e^{S+X+D}\}^{-1} \hat{F} \{e^{S+X+D}\} \tag{4.12}$$

$$\hat{S} = S_{ax}^{ij} \hat{E}_{ij}^{ax} + S_a^i \hat{E}_i^a + S_a^x \hat{E}_x^a$$

$$\hat{D} = D_{ay}^{ix} \hat{E}_{ix}^{ay}$$

$$\hat{X} = X_{ya}^{ix} \hat{E}_{ix}^{ya}$$

The method is referred to as MR-EOM-T|T$^+$|SXD. The transformations with both $\hat{T}$ and $\hat{T}^+$ will make the transformed Hamiltonian more nearly Hermitian. However, the final transformed Hamiltonian $\hat{G}$ is not exactly Hermitian. A major difference between the ACESII and ORCA implementations is the MR-CI module. The MR-CI module in ACESII was designed to work for non-hermitian Hamiltonians, and is not all that efficient. The MR-CI module in ORCA was designed for MR-CI and MR-CEPA approaches and explicitly assumes the permutational symmetries of the one- and two- electron integrals of the bare Hamiltonian.

In particular,

$$\langle p|\hat{h}|q\rangle = \langle q|\hat{h}|p\rangle \tag{4.13}$$

$$\begin{aligned}\left\langle pq\left|\frac{1}{r_{12}}\right|rs\right\rangle &= \left\langle rq\left|\frac{1}{r_{12}}\right|ps\right\rangle \\ &= \left\langle ps\left|\tfrac{1}{r_{12}}\right|rq\right\rangle \\ &= \left\langle rs\left|\tfrac{1}{r_{12}}\right|pq\right\rangle\end{aligned} \tag{4.14}$$

These symmetries, however, *do not hold* for the transformed one- and two- electron integrals. However, until the MR-CI program in ORCA is adjusted we are forced to symmetrize the elements of $\hat{G}$ that enter the ORCA program.

We distinguish different types of permutational symmetries,

1. Hermitization:

$$g_q^p = g_p^q \tag{4.15}$$

$$g_{rs}^{pq} = g_{pq}^{rs} \tag{4.16}$$

2. Vertex symmetry:

$$g_{rs}^{pq} = g_{ps}^{rq} = g_{rq}^{ps} \tag{4.17}$$

The latter type of permutational symmetry has no justification, and is some reason for concern. We will address the issue in the results section.

Spin-orbit coupling effects are included in an a-posteriori fashion by employing Quasi-Degenerate Perturbation Theory (QDPT), as outlined in Refs. 33 and Ref. 58. Following the MR-CI diagonalization of the similarity transformed Hamiltonian G, we obtain I = 1, 2, . . . , $N_{states}$ electronic states $|\Psi_I^{SS}\rangle$, with spin S, M=S, and energy $E_I$ . For the inclusion of spin-orbit coupling effects, we must work in the basis of functions of the form $|\Psi_I^{SM}\rangle$, with spin projection quantum numbers M = −S, . . . , S. Evidently, the 2S functions $\{|\Psi_I^{S-S}\rangle, \ldots, |\Psi_I^{SS-1}\rangle\}$ can be generated by repeated action of the spin lowering operator $S_- = S_x - iS_y$ on the state $|\Psi_I^{SS}\rangle$, however these other functions are not explicitly required in the procedure discussed in Ref. 58. In the basis of functions $|\Psi_I^{SM}\rangle$, the QDPT expression for the state energies, with inclusion of spin-orbit coupling, takes the form

$$\left\langle \Psi_I^{SM} \middle| G \; + \; H_{SOMF} \middle| \Psi_J^{S'M'} \right\rangle = \delta_{IJ}\delta_{SS'}\delta_{MM'}E_I \; + \left\langle \Psi_I^{SM} \middle| H_{SOMF} \middle| \Psi_J^{S'M'} \right\rangle, \tag{4.18}$$

where the second-quantized form of the spin-orbit mean-field (SOMF) hamiltonian $H_{SOMF}$ and its matrix elements are given in Ref. 58. This small subspace Hamiltonian is diagonalized to obtain the final J-specific energy levels. Let us note that we add the bare $H_{SOMF}$ operator to the transformed scalar Hamiltonian, and hence picture change effects are not included in this procedure. Moreover, due to the incomplete set of states included in the diagonalization, not all $|J, M_J\rangle$, $M_J$= -J, …, J are exactly degenerate. In general the differences are small (a couple of $cm^{-1}$) and we use the averaged energy over all $M_J$ sublevels to define the J-specific energy.

**4.3. Results and discussion**

In a previous publication[59] we reported MR-EOM results for the neutral Cr, Mn, Fe and Co atoms, without including spin-orbit coupling (SOC). It was demonstrated that we can obtain good MR-EOM excitation energies from a single MR-EOM calculation, provided one makes a proper weighting of the states in the reference manifolds. Our preferred strategy for the reference space is to select a small number of low-lying reference states (complete multiplets) that have the 4s occupations of interest. If possible, we like to perform a *single* state-averaged CASSCF calculation to obtain a set of orbitals, in line with the general MR-EOM philosophy. In general, it is not very hard in MR-EOM to get a balanced description of various atomic states that all have the same 4s configuration in MR-EOM. However, it can be harder to achieve a proper balance of different types of states, e.g. the $4s^1 3d^{n-1}$ and $4s^2 3d^{n-2}$ states for neutral atoms. In order

not to bias the calculation towards one or the other type of 4s configuration we find it useful to define the weights of the CASSCF reference states such that the 4s occupation is the average of the two types of states. For example, in the above case for neutral atoms, this means we define the reference weights such that the average 4s occupation is 1.5. In addition, we choose the weights of each state of a particular 4s-type, included in the state-averaged CASSCF calculation, to be equal. Hence, this protocol yields a unique set of weights once the decision is made as to which multiplets are to be included in the reference manifold. In this paper we used the weights given in Table 4.1, which were also used in previous calculations.[59]

| Atom | Weighted CAS ensembles for calculations | Average 4s occupation |
|---|---|---|
| **Cr ($4s^1 3d^5 + 4s^2 3d^4$)** | 5x ($^7S + ^5S$) [$4s^1 3d^5$] + 2x ($^5D$) [$4s^2 3d^4$] | 1.5 |
| **Mn ($4s^1 3d^6 + 4s^2 3d^5$)** | 1x ($^6D$) [$4s^1 3d^6$] + 5x ($^6S$) [$4s^2 3d^5$] | 1.5 |
| **Fe ($4s^1 3d^7 + 4s^2 3d^6$)** | 5x ($^5F$) [$4s^1 3d^7$] + 7x ($^5D$) [$4s^2 3d^6$] | 1.5 |
| **Co ($4s^1 3d^8 + 4s^2 3d^7$)** | 1x ($^4F$) [$4s^1 3d^8$] + 1x ($^4F$) [$4s^2 3d^7$] | 1.5 |

**Table 4.1.** *Weighted CAS ensembles for all calculations on transition metal atoms*

In the previous paper, we compared the calculations that do not include SOC to J-averaged experimental data from the Moore atomic energy table[40], taken from the National Institute of Standards and Technology (NIST) website[41]. This is a comparison of J-averaged values. The formula for the J-averaged result is given as

$$E_{J-averaged} = \frac{\sum_{J \in LS} E_J \cdot (2J+1)}{\sum_{J \in LS} (2J+1)} \quad . \tag{4.19}$$

Using the current MR-EOM results, including SOC, we can investigate the adequacy of comparing results obtained without SOC to J-averaged experimental results. In Table 4.2, we report results for the neutral Co atom from an ORCA-MR-EOM calculation using the compact CAS + 1h + 1p + 2h diagonalization space (no-ph) and MR-EOM calculations which also include ph excitations (denoted ph). The results are obtained in two basis sets Def2-TZVPP[38] and Def2-QZVPP[38], using the corresponding relativistic basis for the core-electron in the ORCA program[60], which we abbreviate as TZV and QZV respectively. For Cr CC-PVTZ[60, 61] basis set will be discussed later. In the calculation the 1s, 2s and 2p orbitals are frozen, but the 3s and 3p orbitals are included in the correlation part of the calculations. Scalar relativistic effects are included using the Douglas-Kroll-Hess (DKH) scheme.[62, 63]

As can be seen in Table 4.2 the calculations that do include SOC and in which results are subsequently averaged over the J sublevels, compare very well to results obtained without SOC. The results can also be compared to J-averaged NIST values.

To compare the results of the calculations to the experimental data, we define a shift of the computational results such that the average of the MR-EOM results over states included in the reference manifold exactly equal the same average from NIST experimental values (see Eq. (4.20)). This procedure was also used in ref (59).

$$E_{J-specific} = E_J + \Delta E_{shift} \tag{4.20}$$

$$\Delta E_{shift} = E_{J-averaged(reference)}(NIST) - E_{J-averaged(reference)}$$

| 2S+1 | L | Char. of state | NIST | No SOC | | | | J-averaged SOC | | | |
|---|---|---|---|---|---|---|---|---|---|---|---|
| | | | | no-ph QZV | ph QZV | no-ph TZV | ph TZV | no-ph QZV | ph QZV | no-ph TZV | ph TZV |
| 4 | F | $4s^2$ | 793 | 1084 | 485 | 911 | 330 | 1088 | 488 | 914 | 332 |
| 4 | F | $4s^1$ | 4158 | 3867 | 4466 | 4040 | 4621 | 3863 | 4463 | 4037 | 4618 |
| 2 | F | $4s^1$ | 7879 | 7242 | 7856 | 7498 | 8097 | 7294 | 7910 | 7548 | 8148 |
| 4 | P | $4s^2$ | 13976 | 13707 | 13506 | 13721 | 13530 | 13645 | 13446 | 13662 | 13470 |
| 4 | P | $4s^1$ | 15549 | 14400 | 15311 | 14775 | 15671 | 14247 | 15121 | 14606 | 15463 |
| 2 | G | $4s^2$ | 16808 | 17968 | 17230 | 17942 | 17229 | 17967 | 17227 | 17941 | 17226 |
| 2 | D | $4s^1$ | 16655 | 15386 | 16093 | 15650 | 16333 | 15615 | 16365 | 15893 | 16623 |
| 2 | P | $4s^1$ | 18518 | 17148 | 17915 | 17441 | 18103 | 17367 | 18117 | 17656 | 18299 |
| 2 | P | $4s^2$ | 20739 | 20533 | 20329 | 20661 | 20549 | 20438 | 20248 | 20560 | 20470 |
| 2 | H | $4s^2$ | 22096 | 23823 | 22871 | 23890 | 22974 | 23909 | 22955 | 23974 | 23059 |
| 2 | D | $4s^2$ | 22413 | 22170 | 22018 | 22194 | 22038 | 22405 | 22260 | 22427 | 22279 |
| 2 | G | $4s^1$ | 23195 | 23037 | 23460 | 23496 | 23912 | 23080 | 23514 | 23537 | 23960 |

**Table 4.2.** *Shifted J-averaged energies (in $cm^{-1}$) of ORCA-MR-EOM methods for Co neutral atom. The states included in the reference manifold are indicated in yellow*

| Atom | Statistical Errors | Errors from NIST J-averaged SOC (ORCA) | | | | Deviations between SOC and No-SOC (ORCA) | | | |
|---|---|---|---|---|---|---|---|---|---|
| | | no-ph QZV | ph QZV | no-ph TZV | ph TZV | no-ph QZV | ph QZV | no-ph TZV | ph TZV |
| Cr | AVG | 696 | 595 | 950 | 845 | -11 | -11 | 10 | 11 |
| | RMS | 1230 | 917 | 1450 | 1142 | 26 | 38 | 26 | 41 |
| | MAX | 2631 | 1802 | 3086 | 2200 | 73 | 115 | 62 | 117 |
| Mn | AVG | 524 | 614 | 809 | 878 | -22 | -21 | -22 | -21 |
| | RMS | 1081 | 1009 | 1267 | 1241 | 75 | 62 | 77 | 60 |
| | MAX | 2874 | 2414 | 3085 | 2530 | 259 | 201 | 268 | 196 |
| Fe | AVG | 262 | 292 | 493 | 517 | -59 | -61 | -61 | -58 |
| | RMS | 999 | 605 | 1047 | 784 | 185 | 182 | 175 | 169 |
| | MAX | 2668 | 1415 | 2801 | 1600 | 802 | 792 | 750 | 730 |
| Co | AVG | -155 | -55 | -2 | 97 | -46 | -48 | -45 | -47 |
| | RMS | 888 | 426 | 786 | 464 | 131 | 139 | 133 | 143 |
| | MAX | 1812 | 858 | 1877 | 962 | 234 | 272 | 243 | 290 |

**Table 4.3.** *Statistical analysis of ORCA-MR-EOM data compared to NIST J-averaged values (in $cm^{-1}$) for the Cr, Mn, Fe and Co atoms*

Similar calculations have been performed for the other atoms, Cr, Mn, Fe , and the results are provided in the appendix. In Table 4.3 we have collected the statistical results (average, RMS and maximum deviations) for all four atoms. We used the MR-EOM-$T|T^{+}|SXD$ approach in ORCA in the spin-orbit calculations.

As noted before, two variants are considered including ph excitations and including only CAS + 1h + 1p + 2h (no-ph), which are denoted ph and no-ph. In the final four columns we compare the results of the J-averaged SOC calculation to results that do not include SOC. These No-SOC results are based on the MR-EOM result before the incorporation of SOC. The results imply that it is valid to compare J-averaged results to calculations without SOC. For all atoms the RMS errors range from 50 to 150 $cm^{-1}$, falling well below 0.02 eV. This suggests that the dominant contribution to SOC derives from the coupling within a single L-S multiplet, and intermultiplet coupling is (usually) small.

The J-averaged results are also compared with NIST J-averaged values in the first four columns of Table 4.3. Overall the results are fairly satisfactory, especially when ph excitations are included. We also note that the results are quite insensitive to the basis set. For Cr, using a Def2-TZVPP basis, the calculations yielded very large T-amplitudes (around 0.3). Surprisingly, the problem does not occur in the larger Def2-QZVPP basis set. It may be that the ORCA program converged to an erroneous, alternative solution of the non-linear cluster equations in the TZP basis set. The original results in the Def2-TZVPP basis set for Cr are quite poor (RMS errors of 2627 $cm^{-1}$ and 2810 $cm^{-1}$ for ph and noph respectively). In the results shown in the table we used a different CC-PVTZ basis set [61] of comparable size. In this basis set, no large amplitudes are observed, and results

are much better. This shows that T-amplitudes in MR-EOM should be small for results to be reliable. These results also indicate that the convergence of MR-EOM may be delicate. Further improvements of the algorithm may be needed.

While the results are satisfactory, it appears that the calculations are somewhat sensitive to the inclusion of the ph excitations. This was not observed in our earlier ACESII calculations (ref 59). It is of interest to make a more detailed comparison between the MR-EOM calculations as implemented in ACESII, and the current calculations in ORCA (without inclusion of SOC). In the ACESII version of MR-EOM-T|SXD the non-Hermitian transformed Hamiltonian is diagonalized over the desired MR-CI space. In ORCA the calculation proceeds a bit differently. We can summarize the ORCA calculation as MR-EOM-T|$T^+$|SXD-ph/noph. However, the CI program in ORCA at this point in time also assumes that the transformed Hamiltonian is Hermitian, and even that the transformed one- and two-electrons integrals have the same symmetries at the bare Hamiltonian integrals, in particular:

$$\bar{g}_q^p = \bar{g}_p^q \tag{4.21}$$

$$\bar{g}_{qs}^{pr} = \bar{g}_{ps}^{qr} = \bar{g}_{qr}^{ps} = \bar{g}_{pr}^{qs} \tag{4.22}$$

The middle two symmetry relations of Eq. (4.22) have no physical basis in the definition of the transformed Hamiltonian, and this may be a source of error. Below, we investigate the effect of the additional (ad hoc) symmetrization in ORCA. To this end, we

implemented exactly the same scheme in ACESII such that we can compare various symmetrization schemes on top of the MR-EOM-T|$T^+$|SXD calculation.

ORCA: Full ORCA symmetrization, Eq. (4.21) and Eq. (4.22) are applied.

ORCA_h: Only hermitization, $\bar{g}_{qs}^{pr} = \bar{g}_{pr}^{qs}$ and Eq. (4.21) are applied.

ORCA_noh: No symmetrization.

In addition, we compare to the original MR-EOM-T|SXD results. All calculations use a Def2-TZVPPD basis set[38, 39], and the scalar relativistic correction as implemented in ACESII is applied, which is slightly different from DKH (see ref. 59). The statistical errors are collected in Table 4.4.

| | | **ACESII (noph)** | | | | **ORCA** | |
|---|---|---|---|---|---|---|---|
| | | **T\|SXD** | **ORCA** | **ORCA_h** | **ORCA_noh** | **no-ph** | **ph** |
| **Cr** | **AVG** | 333 | 868 | 73 | 613 | 940 | 834 |
| | **RMS** | 693 | 1568 | 731 | 709 | 1439 | 1128 |
| | **MAX** | 1368 | 3038 | 1438 | 1334 | 3068 | 2190 |
| **Mn** | **AVG** | 268 | 738 | 200 | 692 | 787 | 857 |
| | **RMS** | 667 | 1398 | 675 | 854 | 1265 | 1213 |
| | **MAX** | 1606 | 3780 | 1666 | 1317 | 3094 | 2334 |
| **Fe** | **AVG** | 281 | 515 | 344 | 477 | 431 | 461 |
| | **RMS** | 621 | 905 | 863 | 640 | 1050 | 772 |
| | **MAX** | 1263 | 2399 | 1710 | 1844 | 2754 | 1548 |
| **Co** | **AVE** | 65 | -40 | 5 | 273 | 605 | 419 |
| | **RMS** | 628 | 1235 | 981 | 540 | 799 | 466 |
| | **MAX** | 1013 | 2491 | 1643 | 905 | 1794 | 878 |

**Table 4.4.** *Statistical analysis of ACESII-MR-EOM and ORCA-MR-EOM data compared to NIST J-averaged values (in $cm^{-1}$) for the Cr, Mn, Fe and Co atoms. The ACESII calculations use the Def2-TZVPPD basis (ref), and a slightly different scalar relativistic correction than in the ORCA calculation (with a Def2-TZVPP basis)*

It can be observed that the RMS errors from MR-EOM-T|SXD and MR-EOM-T|$T^+$|SXD are very similar (ORCA_noh). Hermitization (ORCA_h) may introduce somewhat larger errors, in particular for Fe and Co. However, the errors are always more significant when the ORCA-symmetrized transformed Hamiltonian is used (ORCA). The ACESII version of ORCA-MR-EOM yields similar results as the true ORCA calculations (using slightly different basis / relativistic effects). It appears that the additional symmetrization in ORCA does lead to a slight deterioration of the accuracy of results. This is completely a (current) technical limitation of the ORCA program. It would require a straightforward but tedious modification of the CI implementation in ORCA to overcome this error. We also note that the inclusion of ph excitations can improve results in ORCA significantly, as seen in the last two columns of table 4.4 (again, in particular for Fe and Co atoms). This effect is not observed in previous ACESII calculations (ref. 59), and it may be a consequence of the additional symmetrization in ORCA.

| Co Neutral | Term | Char. of State | J-specific SOC Energies | | | | |
|---|---|---|---|---|---|---|---|
| | | | NIST | no-ph QZV | ph QZV | no-ph TZV | ph TZV |
| | **$4F_{9/2}$** | $4s^2$ | 0 | 310 | -310 | 144 | -459 |
| | **$4F_{7/2}$** | | 816 | 1108 | 509 | 933 | 353 |
| | **$4F_{5/2}$** | | 1407 | 1691 | 1107 | 1511 | 945 |
| | **$4F_{3/2}$** | | 1809 | 2089 | 1513 | 1905 | 1349 |
| | **$4F_{9/2}$** | $4s^1$ | 3483 | 3200 | 3795 | 3380 | 3957 |
| | **$4F_{7/2}$** | | 4143 | 3845 | 4445 | 4020 | 4602 |
| | **$4F_{5/2}$** | | 4690 | 4387 | 4990 | 4555 | 5141 |
| | **$4F_{3/2}$** | | 5076 | 4770 | 5376 | 4934 | 5522 |
| | **$2F_{7/2}$** | $4s^1$ | 7442 | 6864 | 7477 | 7122 | 7719 |
| | **$2F_{5/2}$** | | 8461 | 7869 | 8487 | 8117 | 8720 |
| | **$4P_{5/2}$** | $4s^2$ | 13796 | 13454 | 13264 | 13480 | 13290 |
| | **$4P_{3/2}$** | | 14036 | 13714 | 13503 | 13723 | 13525 |
| | **$4P_{1/2}$** | | 14399 | 14078 | 13880 | 14085 | 13900 |
| | **$4P_{5/2}$** | $4s^1$ | 15184 | 13911 | 14763 | 14263 | 15104 |
| | **$4P_{3/2}$** | | 15774 | 14455 | 15341 | 14818 | 15677 |
| | **$4P_{1/2}$** | | 16196 | 14837 | 15755 | 15209 | 16111 |
| | **$2G_{9/2}$** | $4s^2$ | 16468 | 17630 | 16876 | 17608 | 16879 |
| | **$2G_{7/2}$** | | 17234 | 18389 | 17666 | 18357 | 17659 |
| | **$2D_{3/2}$** | $4s^1$ | 16471 | 15399 | 16151 | 15685 | 16418 |
| | **$2D_{5/2}$** | | 16778 | 15760 | 16507 | 16032 | 16760 |
| | **$2P_{3/2}$** | $4s^1$ | 18390 | 17277 | 18008 | 17561 | 18182 |
| | **$2P_{1/2}$** | | 18775 | 17548 | 18335 | 17844 | 18533 |
| | **$2P_{3/2}$** | $4s^2$ | 20501 | 20172 | 19990 | 20297 | 20221 |
| | **$2P_{1/2}$** | | 21216 | 20972 | 20765 | 21087 | 20968 |
| | **$2H_{11/2}$** | $4s^2$ | 21780 | 23607 | 22650 | 23676 | 22754 |
| | **$2H_{9/2}$** | | 22475 | 24270 | 23320 | 24331 | 23424 |
| | **$2D_{5/2}$** | $4s^2$ | 21920 | 21898 | 21753 | 21925 | 21776 |
| | **$2D_{3/2}$** | | 23153 | 23166 | 23021 | 23180 | 23035 |
| | **$2G_{9/2}$** | $4s^1$ | 23184 | 23067 | 23510 | 23523 | 23952 |
| | **$2G_{7/2}$** | | 23208 | 23095 | 23519 | 23554 | 23970 |

**Table 4.5.** *Shifted J-specific SOC energies (in $cm^{-1}$) of all MR-EOM methods for Co neutral atom. The states included in the reference manifold are indicated in yellow*

Let us again first consider the detailed results for the neutral Co atom. For Co, we have four sets of results that include SOC: MR-EOM-no-ph and MR-EOM-ph in both the TZV and QZV basis sets. All of these results are obtained using the ORCA program. The results are listed in Table 4.5. If one compares the NIST and MR-EOM data, one finds satisfactory results for most states up to about 23,000 $cm^{-1}$ (2.85 eV). Similar calculations are performed for the other atoms, and the statistical errors compared to NIST are reported in Table 4.7. The results are consistent with the J-averaged results reported above. It is seen that basis set effects are very minor. Results seem converged at the TZV level. There is a clear increase in the accuracy when the ph excitations are included in the diagonalization manifold, however. This is in contrast to calculations done using the ACESII program (see ref. 59). As discussed before, it appears that with the additional symmetrization in ORCA the ph excitations gain importance. Results for the ORCA-ph calculations are quite satisfactory (errors below 0.05 eV). There is very little difference between the results in the TZP and QZP basis sets, however, results improve drastically for Fe and Co when ph excitations are included. Overall results are quite satisfactory.

We can also investigate the splittings due to spin orbital coupling in each L-S multiplet. If we set the lowest J-level in each L-S multiplet to zero, we can look at the excitation energies per multiplet. The results for the Co atom are collected in Table 4.6. In general, the results from MR-EOM-ph and MR-EOM-no-ph are very similar, indicating that the similarity transform works well.

| Co | Term | Splitting in multiplets | | | | |
|---|---|---|---|---|---|---|
| | | NIST | no-ph QZV | ph QZV | no-ph TZV | ph TZV |
| **a $^4$F** | **$^4F_{9/2}$** | 0 | 0 | 0 | 0 | 0 |
| | **$^4F_{7/2}$** | 816 | 797 | 819 | 789 | 812 |
| | **$^4F_{5/2}$** | 1407 | 1381 | 1417 | 1366 | 1404 |
| | **$^4F_{3/2}$** | 1809 | 1778 | 1823 | 1760 | 1807 |
| b $^4$F | **$^4F_{9/2}$** | 0 | 0 | 0 | 0 | 0 |
| | **$^4F_{7/2}$** | 660 | 645 | 649 | 640 | 645 |
| | **$^4F_{5/2}$** | 1207 | 1187 | 1195 | 1176 | 1185 |
| | **$^4F_{3/2}$** | 1593 | 1570 | 1580 | 1554 | 1566 |
| **a $^2$F** | **$^2F_{7/2}$** | 0 | 0 | 0 | 0 | 0 |
| | **$^2F_{5/2}$** | 1018 | 1005 | 1010 | 995 | 1001 |
| a $^4$P | **$^4P_{5/2}$** | 0 | 0 | 0 | 0 | 0 |
| | **$^4P_{3/2}$** | 241 | 259 | 239 | 244 | 234 |
| b $^4$P | **$^4P_{1/2}$** | 604 | 624 | 616 | 605 | 610 |
| | **$^4P_{5/2}$** | 0 | 0 | 0 | 0 | 0 |
| | **$^4P_{3/2}$** | 590 | 544 | 578 | 555 | 573 |
| | **$^4P_{1/2}$** | 1012 | 926 | 993 | 945 | 1007 |
| a $^2$G | **$^2G_{9/2}$** | 0 | 0 | 0 | 0 | 0 |
| | **$^2G_{7/2}$** | 766 | 758 | 790 | 749 | 781 |
| a $^2$D | **$^2D_{3/2}$** | 0 | 0 | 0 | 0 | 0 |
| | **$^2D_{5/2}$** | 308 | 361 | 356 | 347 | 342 |
| a $^2$P | **$^2P_{3/2}$** | 0 | 0 | 0 | 0 | 0 |
| | **$^2P_{1/2}$** | 385 | 271 | 327 | 283 | 351 |
| b $^2$P | **$^2P_{3/2}$** | 0 | 0 | 0 | 0 | 0 |
| | **$^2P_{1/2}$** | 715 | 800 | 774 | 790 | 748 |
| a $^2$H | **$^2H_{11/2}$** | 0 | 0 | 0 | 0 | 0 |
| | **$^2H_{9/2}$** | 695 | 663 | 670 | 655 | 669 |
| b $^2$D | **$^2D_{5/2}$** | 0 | 0 | 0 | 0 | 0 |
| | **$^2D_{3/2}$** | 1232 | 1268 | 1267 | 1254 | 1260 |
| b $^2$G | **$^2G_{9/2}$** | 0 | 0 | 0 | 0 | 0 |
| | **$^2G_{7/2}$** | 24 | 28 | 9 | 31 | 18 |

**Table 4.6.** *Splitting in multiplets (in $cm^{-1}$) of all MR-EOM methods for Co neutral atom. The states included in the reference manifold are indicated in yellow*

| Atom | Statistical Errors | J-specific SOC Energies Errors | | | |
|---|---|---|---|---|---|
| | | no-ph QZV | ph QZV | no-ph TZV | ph TZV |
| **Cr** | AVG | 710 | 666 | 667 | 695 |
| | RMS | 910 | 783 | 911 | 848 |
| | MAX | 2631 | 1705 | 1945 | 1577 |
| **Mn** | AVG | 325 | 493 | 602 | 755 |
| | RMS | 719 | 799 | 878 | 1014 |
| | MAX | 1433 | 2492 | 1590 | 2602 |
| **Fe** | AVG | 117 | 188 | 308 | 377 |
| | RMS | 789 | 527 | 811 | 692 |
| | MAX | 1808 | 1178 | 1838 | 1623 |
| **Co** | AVG | -181 | -77 | -47 | 57 |
| | RMS | 842 | 416 | 730 | 457 |
| | MAX | 1827 | 870 | 1895 | 974 |

**Table 4.7.** *Statistical analysis of MR-EOM data compared to NIST J-specific values (in $cm^{-1}$) for the Cr, Mn, Fe and Co atoms*

It is observed in Table 4.7 that the deviations between the ph and no-ph calculations for Cr, Fe and Co are large; the ph calculations provide better results for the excitation energy in each multiplet, while, the difference between ph calculation and no-ph calculation is not obvious for Mn atom. It also can be seen that the QZV calculations yield slightly better results compared to the TZV calculations, but there are no large deviations between QZV and TZV basis sets based calculations.

Table 4.8 shows the errors of splitting in multiplets. Here, we present % RMS error, which is a more straightforward look at the statistical errors. Since contributions to the % RMS would be large for very small splittings, we remove all small splittings that are under 50 $cm^{-1}$ to get reasonable % RMS errors. For Mn, Fe and Co the % RMS errors are

small but Cr atom has a relatively large % RMS. We note that the spin-orbit splittings for Cr atom are fairly small, and this tends to increase the % RMS. The absolute RMS errors for Cr are satisfactory. The differences between QZV and TZV basis sets based calculations are negligible.

| Atom | Statistical Errors | Splitting in multiplets Errors | | | |
|---|---|---|---|---|---|
| | | no-ph QZV | ph QZV | no-ph TZV | ph TZV |
| **Cr** | **AVG** | 2 | 1 | -6 | -3 |
| | **RMS** | 61 | 55 | 61 | 58 |
| | **MAX** | 203 | 178 | 180 | 183 |
| | **%RMS** | 11% | 14% | 10% | 14% |
| **Mn** | **AVG** | -31 | -41 | -36 | -22 |
| | **RMS** | 74 | 102 | 79 | 58 |
| | **MAX** | 261 | 373 | 280 | 183 |
| | **%RMS** | 3% | 2% | 3% | 4% |
| **Fe** | **AVG** | -15 | -28 | -24 | -44 |
| | **RMS** | 53 | 73 | 56 | 84 |
| | **MAX** | 231 | 248 | 197 | 268 |
| | **%RMS** | 4% | 5% | 5% | 6% |
| **Co** | **AVG** | -7 | 1 | -12 | -2 |
| | **RMS** | 37 | 21 | 34 | 16 |
| | **MAX** | 115 | 59 | 103 | 35 |
| | **%RMS** | 6% | 5% | 5% | 4% |

**Table 4.8.** *Statistical analysis of splitting in multiplets (in $cm^{-1}$) for the Cr, Mn, Fe and Co atoms*

The results for the Co atom are shown in detail in Figure 4.1 for all four calculations and are compared to NIST. On the left side of the figure we show the splittings in each L-S multiplet, where we indicate the ground state J-level at -50 $cm^{-1}$ for visibility. On the

right side of the figure, the total excitation energies are indicated. MR-EOM-no-ph and MR-EOM-ph both in QZV and TZV basis sets approaches are compared to the NIST experimental values. Overall, the results are satisfactory.

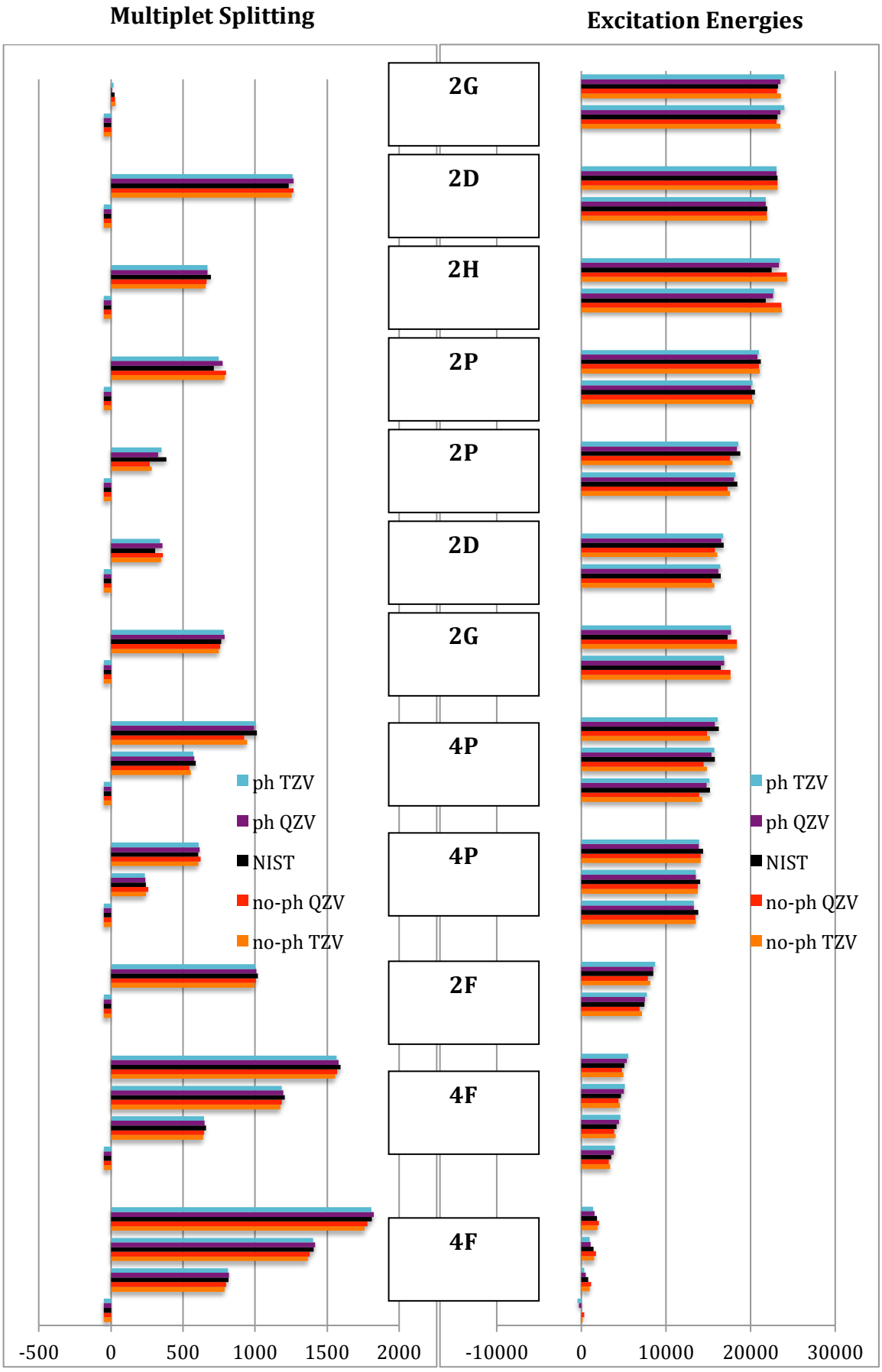


**Figure 4.1.** *MR-EOM-SOC results for Co atom* 80

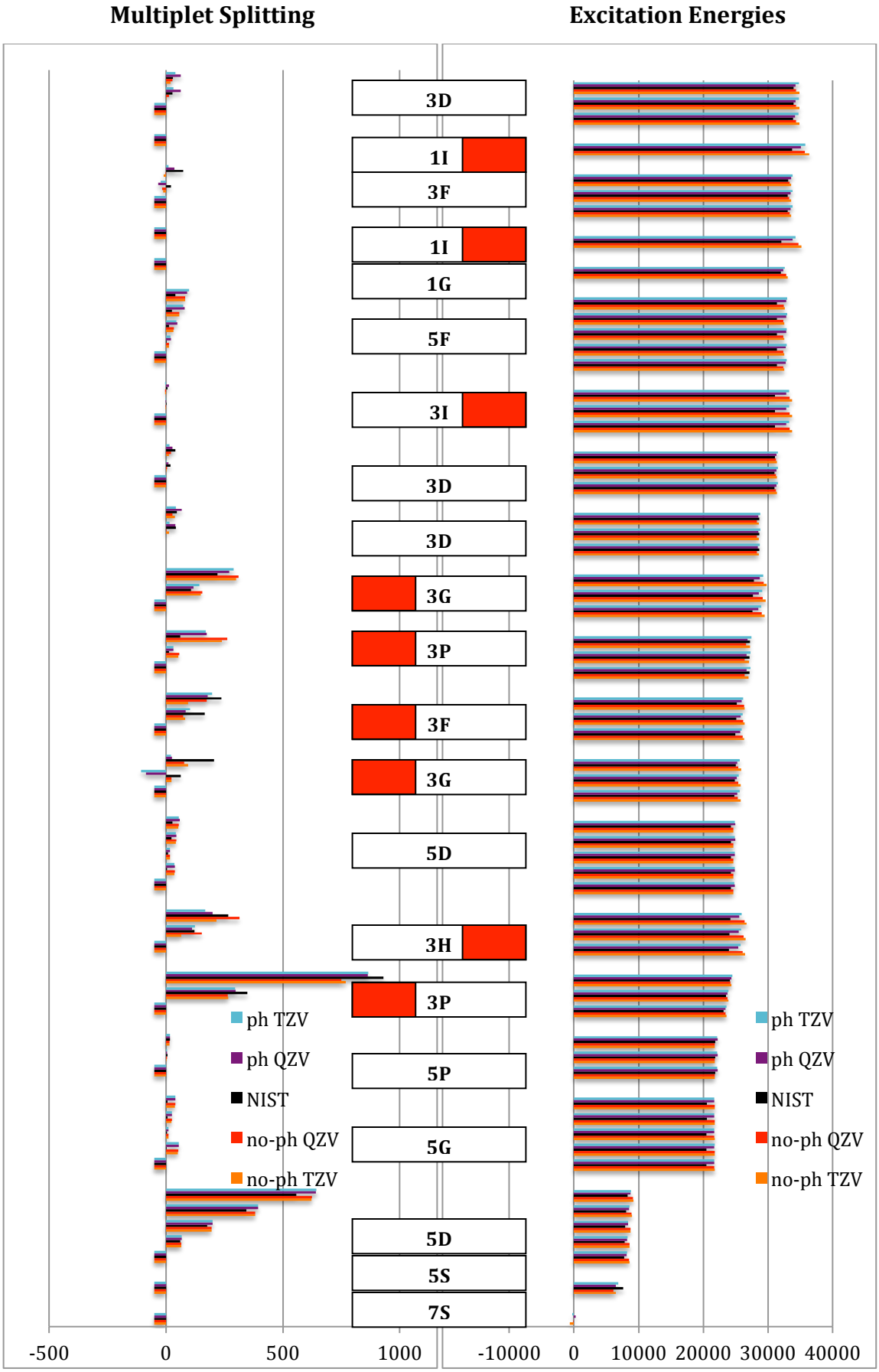


**Figure 4.2.** *MR-EOM-SOC results for Cr atom* 81

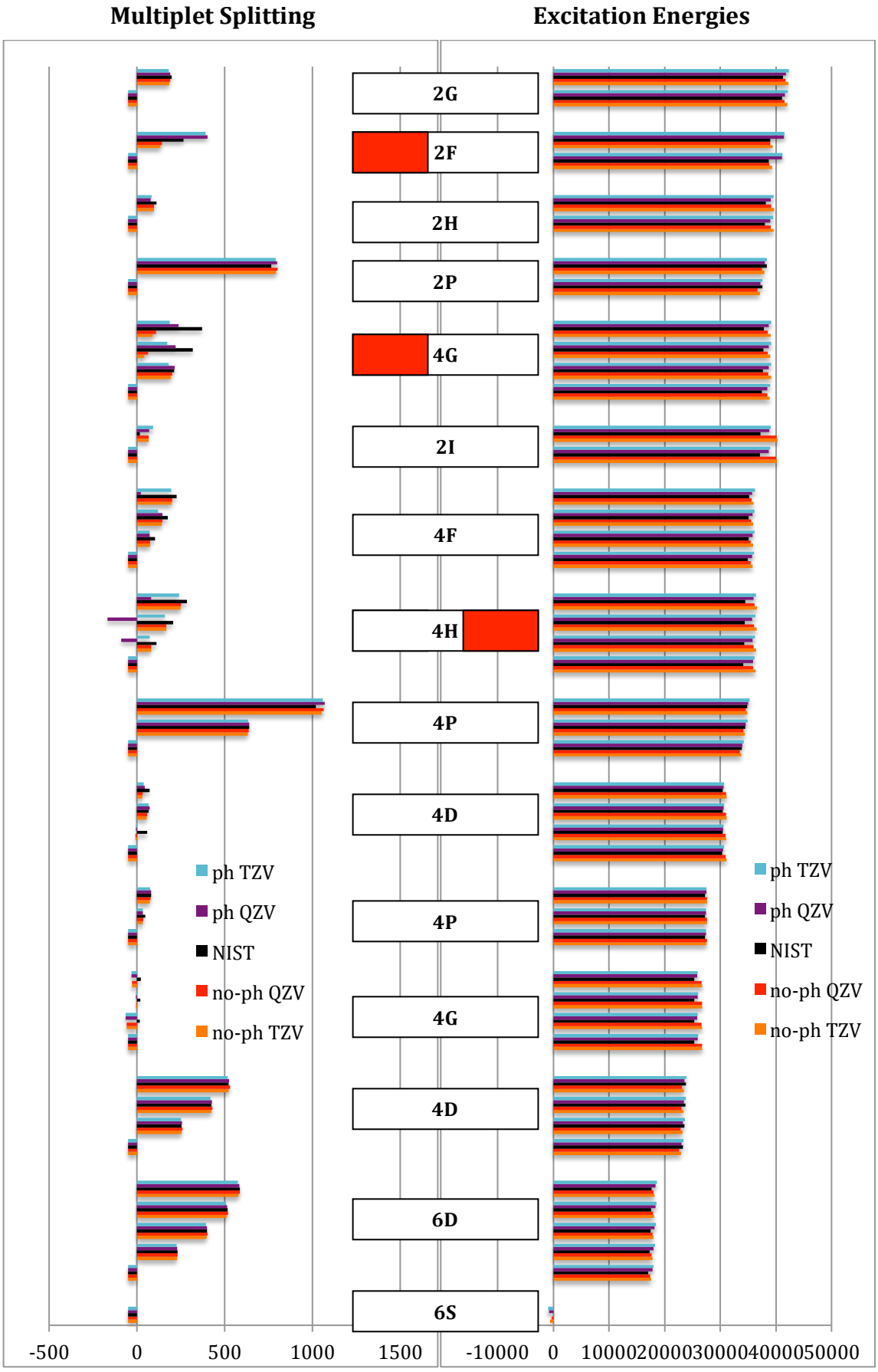


**Figure 4.3.** *MR-EOM-SOC results for Mn atom*

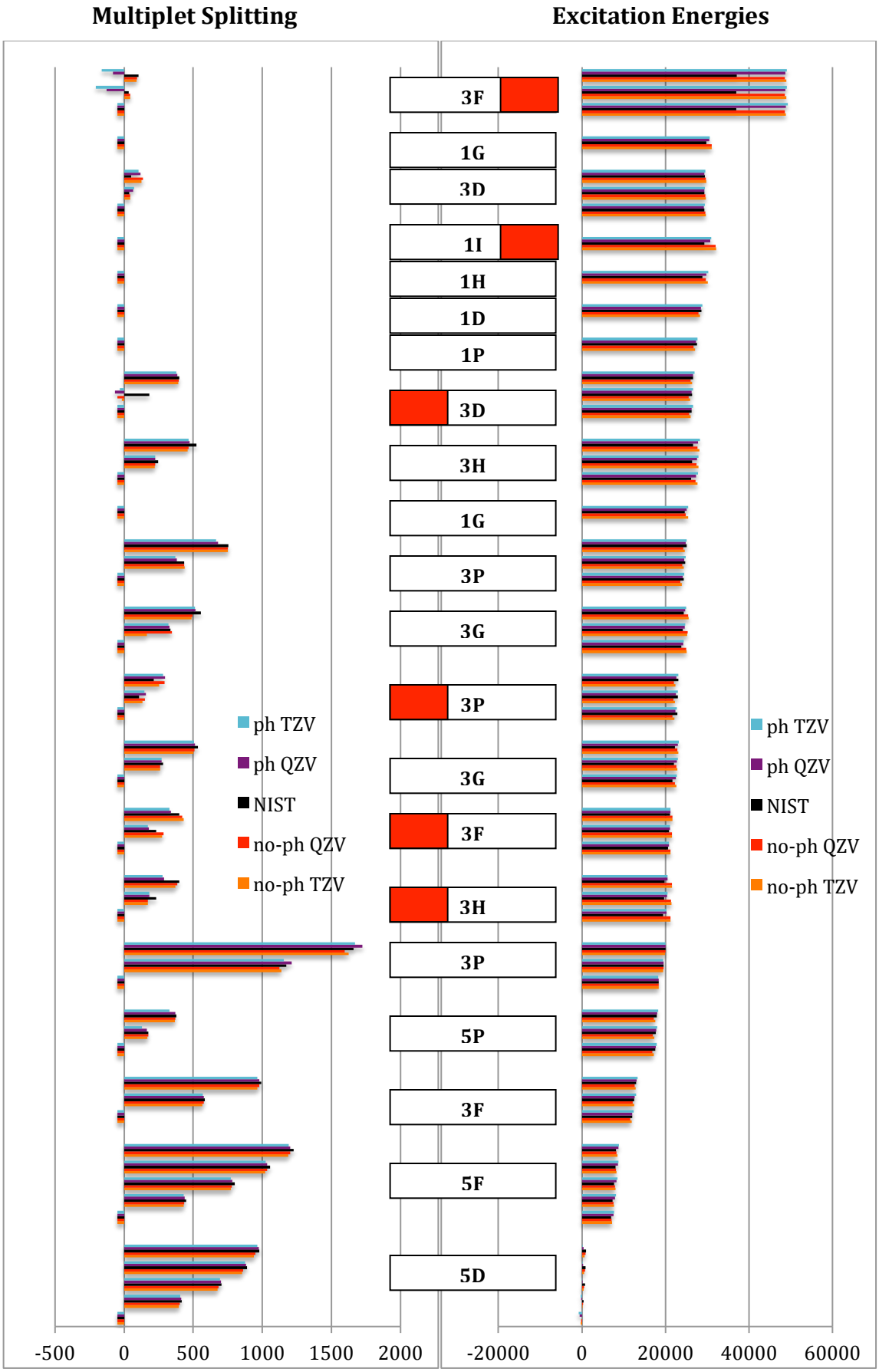


**Figure 4.4.** *MR-EOM-SOC results for Fe atom*

In Figure 4.2, Figure 4.3 and Figure 4.4, we graphically illustrate MR-EOM-SOC results for the Cr, Mn and Fe atoms. On the left side of the figure, the spin-orbit splittings within each L-S multiplet are shown, where we set the lowest energy in each L-S multiplet to zero (and picture them at – 50 $cm^{-1}$ for visibility).

With some exceptions, indicated in red, in the center boxes, the multiplet splittings are calculated in a satisfactory fashion. There is little difference between MR-EOM-ph-SOC and MR-EOM-noph-SOC and this demonstrates the robustness of the MR-EOM calculations and the effectiveness of the similarity transformation that decouples the ph excitations from the CAS reference states. If we compare the excitation spectra to the J-specific levels there are some large errors, but the majority of calculated levels are adequate. The large errors are indicated in red (such as both $^3P$ energies in Figure 4.2 and $^2F$ in Figure 4.3). The full set of data for all atoms are included in the appendix.

**4.4. Conclusions**

The MR-EOM-T|$T^+$|SXD approach in ORCA is combined with the same atomic mean field approach to spin-orbit coupling as used in the MR-CI implementation in the ORCA program. We obtain satisfactory results for the spin-orbit splittings in each L-S multiplet for the first row transition metal atoms. The RMS errors (< 100 $cm^{-1}$) for the spin-orbit splittings are quite satisfactory at the MR-EOM-ph/QZV level. For the Mn, Fe, and Co atoms the RMS errors is only about 5 %, while it is large for Cr (14 %) but here the splittings tend to be smaller. Also the absolute excitation energies are obtained

satisfactorily. Including the ph excitations in the ORCA based MR-EOM-T|$T^+$|SXD calculation yields womewhat higher accuracy. For all calculations, the results also depend little on the basis set. This is not true for the Cr atom, however. For Cr, results at the QZV level are significantly more accurate than with the TZV basis set. Clearly, the treatment of spin-orbit coupling, using MR-EOM, is quite satisfactory. This is somewhat surprising, as we evaluated the spin-orbit coupling energies based on the matrix elements of the bare AMFI spin-orbit operator, using the eigenstates of the transformed Hamiltonian. The "picture" change effects from the many-body transformation are therefore, not included. This issue will need to be addressed in due time, but for now this simplest inclusion of spin-orbit coupling in MR-EOM yields satisfactory results. The results in Table 4.4 clearly show that the extra unphysical symmetrization in ORCA deteriorates results somewhat. Therefore, we think the most important future improvement will be to generalize the MR-CI module in the ORCA program, lifting the constraint on the symmetry of the integrals.

# Chapter 5

# Concluding remarks

The MR-EOM approaches are benchmarked and applied to the atomic excitation spectra of the first-row transition metal atoms Cr, Mn, Fe and Co in my research project. The calculation without spin-orbit coupling is processed in ACESII program. To include the effects of spin-orbit coupling, the MR-EOM is combined with a simple treatment of spin-orbit coupling to calculate the splitings in each L-S multiplet using the ORCA program.

The MR-EOM approaches show that by introducing more cluster amplitudes included in the calculation, the resulting final CI manifolds can be more compact compared to the methods without any operators. This feature of the MR-EOM method yields three important advantages. First, when increasing the number of types of cluster operators included in the calculation, the resulting CI manifold is reduced and the computation

time of the calculation is decreased. Second, when increasing the number of types of cluster operators, the overall accuracy of results increases. Third, as the resulting CI manifold is reduced, the extensivity errors become smaller. This has been demonstrated for the case of $O_2$ dimer in ref 32.

The MR-EOM-T|$T^+$|SXD approach in ORCA generates satisfactory results for the spin-orbit splittings in each L-S multiplet for the first row transition metal atoms. The RMS errors are relatively small and the overall results are quite satisfactory. The excitation energies obtained in ORCA program with spin-orbit coupling in calculations are also reasonable. Hence the treatment of spin-orbit coupling, using MR-EOM, is quite satisfactory. However, compared to ACESII MR-EOM calculations the MR-EOM calculations in ORCA are somewhat less accurate. This is attributed to the use of further symmetrization operations on the transformed Hamiltonian, in ORCA, which are imposed on the algorithm, but do not reflect the correct physics.

It is worthwhile to relate an experience to me here, to warn future users of some peculiarities of the ORCA program. In the process of exploring the effects of spin-obit coupling, a wrong basis set Def2-TZVPPD was used in previous calculation. The Def2-TZVPPD basis set does not exist in ORCA program. When looking at the output files, there were no error messages or any warning messages that said anything was wrong with the basis set. Even though the results obtained were not as good as the calculations done in the ACESII program, the final statistical results could still be explained anyway. We thought the puzzling problems about the results were related to the ORCA program. By searching the code of ORCA program, we finally found that the

Def2-TZVPPD basis set did not exist. Therefore, new calculations with correct basis sets Def2-TZVPP and Def2-QZVPP were performed. In this way, we got quite satisfactory results for the calculations with spin-orbit coupling, reported in this thesis.

This thesis focuses on benchmarking the MR-EOM method. For this purpose, atoms are very suitable as accurate experimental data are readily available, and there are no uncertainties regarding ro-vibrational effects or solution effects which lead to common complications for molecules. For atoms there is nowhere to hide and the comparison between theory and experiment is unambiguous. The MR-EOM approach has passed this test with flying colors.

Of course, there is no real interest in the calculation of atomic excitation spectra, except for benchmarking purposes. The future of MR-EOM will be the calculation of molecular excitation spectra, in particular for molecules containing transition metal atoms. Many molecules of this type require a multireference treatment, and spin-orbit coupling is of interest. Such calculations are in the pioneering stage. Graduate student Lee M. J. Huntington in the Nooijen group is the author of the MR-EOM module in ORCA, and has pursued (benchmark) applications for molecules like ferrocene, CpNiNO, and $Cr(CO)_6$. Results of this study have recently been published (L. M. J. Huntington and M. Nooijen, J. Chem. Phys. **142**, 194111 (2015)).

The future is wide open for many applications of Multireference Equation of Motion Coupled Cluster Theory. I am proud to have been a member of the team that developed this promising new method in quantum chemistry.

**Safety considerations**

Because this is a theoretical chemistry project, using only calculations, this laboratory does not contain hazardous chemicals; no special safety precautions are required.

**References**


1. Rodney J. Bartlett, John F. Stanton Applications of Post-Hartree—Fock Methods: A Tutorial ISBN: 9780470125823. In book: Reviews in Computational Chemistry, Volume **5**, 65-169 (1994).
2. R. J. Bartlett and M. Musial, Rev. Mod. Phys. **79**, 291 (2007).
3. R. J. Bartlett, Mol. Phys. **108**, 2905-2920 (2010).
4. I. Shavitt and R. J. Bartlett. Many-Body Methods in Chemistry and Physics: MBPT and Coupled-Cluster Theory. Cambridge University Press. ISBN 978-0-521-81832-2 (2009).
5. R. G. Parr, W. Yang. Density-Functional Theory of Atoms and Molecules. Oxford University Press. IBSN: 978-0195092769 (1992).
6. J.M. Seminario, P. Politzer. Modern Density Functional Theory: A Tool For Chemistry. ISBN: 978-0444821713 (1995).
7. J. M. Seminario. Recent Developments and Applications of Modern Density Functional Theory. IBSN: 978-0444824042 (1996).
8. A. Szabo and N. S. Ostlund. Modern Quantum Chemistry: Introduction to Advanced Electronic Structure Theory. Dover. ISBN 0-486-69186-1 (1996).
9. J. $\check{C}$ížek, J. Chem. Phys. **45**, 4256 (1966); Adv. Chem. Phys. **14**, 35 (1969); J. $\check{C}$ížek and J. Paldus, Int. J. Quantum Chem. **5**, 359 (1971).
10. K. Raghavachari, G. W. Trucks, J. A. Pople, and M. Head-Gordon, Chem. Phys. Lett. **157**, 479 (1989).

11. D. I. Lyakh, M. Musia l, V. F. Lotrich, and R. J. Bartlett, Chem. Rev. 112, 182 (2012).
12. H.-J. Werner and P. J. Knowles, J. Chem. Phys. 89, 5803 (1988).
13. P. J. Knowles and H.-J. Werner, Chem. Phys. Lett. 145, 514 (1988).
14. S. R. Langhoff and E. R. Davidson, Int. J. Quantum Chem. 8, 61 (1974).
15. P. G. Szalay and R. J. Bartlett, Chem. Phys. Lett. 214, 481 (1993).
16. R. Gdanitz and R. Ahlrichs, Chem. Phys. Lett. 143, 413 (1988).
17. D. Datta, L. Kong and M. Nooijen, J. Chem. Phys. 134, 214116 (2011).
18. M. Nooijen and R. J. Bartlett, J. Chem. Phys. 106, 6441-6448 (1997).
19. M. Nooijen and R. J. Bartlett, J. Chem. Phys. 107, 6812-6830 (1997).
20. J. Sous, P. Goel, and M. Nooijen, Mol. Phys. (2013).
21. B. O. Roos, P. R. Taylor, and P. Siegbahn. J. Chem. Phys. **48**, 157–173 (1980).
22. B. O. Roos. Lecture Notes in Quantum Chemistry I. ISBN: 0387553711 (1992).
23. M. Nooijen, K. R. Shamasundar, and D. Mukherjee, Mol. Phys. **103**, 2277 (2005).
24. D. Datta, and M. Nooijen, J. Chem. Phys. **137**, 204107 (2012).
25. O. Demel, D. Datta, and M. Nooijen, J. Chem. Phys. **138**, 134108 (2013).
26. L. Kong, K. R. Shamasundar, O. Demel, and M. Nooijen, J. Chem. Phys. **130**, 114101 (2009).
27. K. Jankowski, J. Paldus, I. Grabowski, and K. Kowalski, J. Chem. Phys. **97**, 7600 (1992).
28. F. Neese, WIREs Comput. Mol. Sci. **2**, 73 (2012). ORCA program. Available: http://cec.mpg.de/forum/

29. D. Mukherjee, Chem. Phys. Lett. **274**, 561 (1997).

30. W. Kutzelnigg and D. Mukherjee, J. Chem. Phys. **107**, 432 (1997).

31. L. Kong, M. Nooijen, and D. Mukherjee, J. Chem. Phys. **132**, 234107(2010).

32. M. Nooijen, O. Demel, D. Datta, L. Kong, K. R. Shamasundar, V. Lotrich, L. M. Huntington, and F. Neese, J. Chem. Phys. **140**, 081102 (2014).

33. F. Neese, T. Petrenko, D. Ganyushin, and G. Olbrich, Coord. Chem. Rev. **251**, 288 (2007).

34. F. Neese, Coord. Chem. Rev. **253**, 526 (2009).

35. J. F. Stanton and R. J. Bartlett, J. Chem. Phys. **98**, 7029 (1993).

36. M. Nooijen, J. Chem. Phys. **104**, 2638-2651 (1996).

37. G. D. Purvis and R. J. Bartlett, J. Chem. Phys. **76**, 1910 (1982).

38. F. Weigend and R. Ahlrichs, Phys. Chem. Chem. Phys. **7**, 3297 (2005).

39. D. Rappoport and F. Furche, J. Chem. Phys. **133**, 134105 (2010).

40. C. E. Moore, Atomic Energy Levels, Vol. II (Chromium through Niobium), Circular of the National Bureau of Standards 467, U.S. Government Printing Office, Washington, DC (1952).

41. National Institute of Standards and Technology (NIST) Atomic Spectra Database. Available: http://physics.nist.gov/asd

42. F. Neese, F. Wennmohs, and A. Hansen, J. Chem. Phys. **130**, 114108 (2009).

43. F. Neese, A. Hansen, and D. G. Liakos, J. Chem. Phys. **131**, 064103 (2009).

44. C. Riplinger, B. Sandh¨ofer, A. Hansen, and F. Neese, J. Chem. Phys. **139**, 134101 (2013).

45. H. Nakatsuji and K. Hirao, J. Chem. Phys. **68**, 2053 (1978).

46. H. Nakatsuji, Chem. Phys. Lett. **67**, 329 (1979).

47. H. J. Monkhorst, Int. J. Quant. Chem. Symp. **11**, 421 (1977).

48. D. Mukherjee and P. K. Mukherjee, Chem. Phys. **39**, 325 (1979).

49. H. Koch, H. J. Jensen, P. Jørgensen, and T. Helgaker, J. Chem. Phys. **93**, 3345 (1990).

50. J. Geertsen, M. Rittby, and R. J. Bartlett, Chem. Phys. Lett. **164**, 57 (1989).

51. D. C. Comeau and R. J. Bartlett, Chem. Phys. Lett. **207**, 414 (1993).

52. I. Lindgren, Int. J. Quantum Chem. Symp. **12**, 33 (1978).

53. I. Lindgren and D. Mukherjee, Phys. Rep. **1**, 93 (1987).

54. D. Mukherjee and S. Pal, Adv. Quantum Chem. **20**, 291 (1989).

55. B. Jeziorski and J. Paldus, J. Chem. Phys. **90**, 2714 (1989).

56. U. Kaldor, Theor. Chim. Acta **80**, 427 (1991).

57. K. Jankowski and P. Malinowski, J. Phys. B **27**, 829 (1994).

58. D. Ganyushin and F. Neese, J. Chem. Phys. **125**, 024103 (2006).

59. Z. Liu, O. Demel and M. Nooijen, J. Mol. Spectro. **311**, 54-63 (2015).

60. D. A. Pantazis, X. Y. Chen, C. R. Landis and F. Neese, J. Chem. Theory Comput. **4**, 908 (2008).

61. D.E. Woon and T.H. Dunning, Jr. J. Chem. Phys. **98**, 1358 (1993).

62. Douglas M, Kroll NM (1974) Ann Phys. **82**: 89.

63. Hess BA (1986) Phys. Rev A **33**: 3742.

## Appendix

In this appendix, shifted J-averaged and J-specific SOC energies, statistical errors compared to NIST values, and splitting in multiplets of all MR-EOM methods for Cr, Mn and Fe are shown.

| Cr | Term | NIST | Shifted Energies | | | | | | | |
|---|---|---|---|---|---|---|---|---|---|---|
| Character | | | No SOC | | | | J-averaged SOC | | | |
| | | | no-ph QZV | ph QZV | no-ph TZV | ph TZV | no-ph QZV | ph QZV | no-ph TZV | ph TZV |
| 4 | 7S | 0 | -122 | 250 | -609 | -262 | -121 | 252 | -607 | -261 |
| 4 | 5S | 7593 | 6094 | 6476 | 6510 | 6874 | 6094 | 6476 | 6510 | 6875 |
| 4 | 5D | 8090 | 8901 | 8524 | 8936 | 8581 | 8900 | 8523 | 8936 | 8580 |
| 4 | 5G | 20521 | 21742 | 21701 | 21768 | 21713 | 21746 | 21705 | 21771 | 21716 |
| 4 | 5P | 21846 | 21761 | 22238 | 21763 | 22200 | 21738 | 22214 | 21741 | 22176 |
| 4 | 3P | 23796 | 23965 | 24051 | 24110 | 24178 | 23956 | 24048 | 24103 | 24177 |
| 4 | 3H | 24080 | 26275 | 25444 | 26589 | 25801 | 26265 | 25493 | 26608 | 25873 |
| 4 | 5D | 24292 | 24649 | 24899 | 24641 | 24858 | 24663 | 24914 | 24656 | 24873 |
| 4 | 3G | 24938 | 25394 | 25321 | 25816 | 25716 | 25388 | 25241 | 25801 | 25599 |
| 4 | 3F | 25097 | 26210 | 25834 | 26418 | 26059 | 26205 | 25833 | 26383 | 26073 |
| 4 | 3P | 27201 | 26510 | 26790 | 27137 | 27399 | 26519 | 26792 | 27138 | 27393 |
| 4 | 3G | 27722 | 29168 | 28594 | 29596 | 29075 | 29208 | 28645 | 29633 | 29112 |
| 4 | 3D | 28661 | 28243 | 28481 | 28564 | 28753 | 28266 | 28488 | 28588 | 28779 |
| 4 | 3D | 31023 | 31222 | 31333 | 31405 | 31521 | 31209 | 31331 | 31397 | 31520 |
| 4 | 3I | 31050 | 33345 | 32838 | 33743 | 33241 | 33355 | 32852 | 33753 | 33251 |
| 4 | 5F | 31375 | 32376 | 32808 | 32517 | 32917 | 32394 | 32817 | 32535 | 32932 |
| 4 | 1G | 31987 | 32785 | 32278 | 32988 | 32502 | 32848 | 32344 | 33050 | 32568 |
| 4 | 1I | 32097 | 34711 | 33782 | 35165 | 34258 | 34728 | 33802 | 35183 | 34278 |
| 4 | 3F | 33078 | 33297 | 33538 | 33584 | 33792 | 33316 | 33526 | 33608 | 33797 |
| 4 | 1I | 33763 | 35717 | 35065 | 36396 | 35784 | 35730 | 35077 | 36409 | 35795 |
| 4 | 3D | 33929 | 34270 | 34145 | 34833 | 34687 | 34343 | 34260 | 34894 | 34773 |

**Table 7.1.** *Shifted J-averaged energies (in $cm^{-1}$) for Cr neutral atom*

| Cr Character of state | Term | Errors from NIST | | | | | | | | Deviations between SOC and No-SOC | | | |
|---|---|---|---|---|---|---|---|---|---|---|---|---|---|
| | | No SOC | | | | J-averaged SOC | | | | | | | |
| | | no-ph QZV | ph QZV | no-ph TZV | ph TZV | no-ph QZV | ph QZV | no-ph TZV | ph TZV | no-ph QZV | ph QZV | no-ph TZV | ph TZV |
| 4s1 | 7S | -122 | 250 | -609 | -262 | -121 | 252 | -607 | -261 | -1 | -1 | 1 | 1 |
| 4s1 | 5S | -1499 | -1117 | -1083 | -719 | -1499 | -1117 | -1083 | -719 | 0 | 0 | 0 | 0 |
| 4s2 | 5D | 811 | 433 | 846 | 490 | 810 | 433 | 845 | 490 | 0 | 1 | 0 | -1 |
| 4s1 | 5G | 1221 | 1180 | 1246 | 1191 | 1224 | 1184 | 1250 | 1195 | -3 | -4 | 3 | 4 |
| 4s1 | 5P | -85 | 392 | -83 | 354 | -108 | 367 | -106 | 330 | 23 | 25 | -23 | -24 |
| 4s2 | 3P | 169 | 255 | 314 | 382 | 160 | 252 | 307 | 381 | 10 | 3 | -7 | -2 |
| 4s2 | 3H | 2195 | 1364 | 2509 | 1721 | 2185 | 1414 | 2529 | 1793 | 10 | -50 | 19 | 72 |
| 4s1 | 5D | 357 | 607 | 349 | 566 | 371 | 622 | 363 | 581 | -14 | -15 | 15 | 15 |
| 4s1 | 3G | 455 | 383 | 878 | 778 | 450 | 302 | 862 | 661 | 5 | 81 | -15 | -117 |
| 4s2 | 3F | 1112 | 737 | 1321 | 962 | 1108 | 735 | 1286 | 976 | 5 | 2 | -35 | 14 |
| 4s1 | 3P | -691 | -410 | -63 | 198 | -682 | -408 | -63 | 193 | -9 | -2 | 1 | -6 |
| 4s2 | 3G | 1445 | 872 | 1874 | 1352 | 1486 | 922 | 1911 | 1389 | -40 | -50 | 37 | 37 |
| 4s1 | 3D | -417 | -180 | -96 | 92 | -394 | -173 | -72 | 118 | -23 | -7 | 24 | 26 |
| 4s1 | 3D | 199 | 310 | 382 | 498 | 185 | 307 | 373 | 497 | 14 | 3 | -9 | -1 |
| 4s1 | 3I | 2294 | 1787 | 2692 | 2190 | 2304 | 1802 | 2702 | 2200 | -10 | -15 | 10 | 10 |
| 4s1 | 5F | 1001 | 1434 | 1142 | 1542 | 1020 | 1442 | 1161 | 1557 | -19 | -9 | 19 | 15 |
| 4s2 | 1G | 799 | 291 | 1001 | 515 | 861 | 357 | 1063 | 581 | -62 | -66 | 62 | 66 |
| 4s2 | 1I | 2614 | 1685 | 3068 | 2161 | 2631 | 1705 | 3086 | 2180 | -17 | -20 | 18 | 20 |
| 4s1 | 3F | 219 | 460 | 506 | 714 | 238 | 448 | 530 | 719 | -19 | 12 | 24 | 5 |
| 4s1 | 1I | 1954 | 1303 | 2634 | 2021 | 1968 | 1314 | 2646 | 2033 | -13 | -12 | 13 | 12 |
| 4s2 | 3D | 340 | 215 | 904 | 758 | 414 | 330 | 965 | 844 | -73 | -115 | 61 | 86 |

**Table 7.2.** *Statistical analysis of ORCA-MR-EOM data compared to NIST J-averaged values (in $cm^{-1}$) for Cr neutral atom*

| Character of state | Term | NIST | J-specific SOC Energies | | | | J-specific SOC Energies Errors | | | |
|---|---|---|---|---|---|---|---|---|---|---|
| | | | no-ph QZV | ph QZV | no-ph TZV | ph TZV | no-ph QZV | ph QZV | no-ph TZV | ph TZV |
| 4s1 | $^7S_3$ | 0 | -121 | 252 | -607 | -261 | -121 | 252 | -607 | -261 |
| 4s1 | $^5S_2$ | 7593 | 6094 | 6476 | 6510 | 6875 | -1499 | -1117 | -1083 | -719 |
| 4s2 | $^5D_0$ | 7751 | 8522 | 8134 | 8558 | 8190 | 771 | 383 | 807 | 440 |
| | $^5D_1$ | 7811 | 8588 | 8201 | 8624 | 8258 | 777 | 391 | 813 | 447 |
| | $^5D_2$ | 7927 | 8716 | 8334 | 8752 | 8390 | 789 | 406 | 825 | 463 |
| | $^5D_3$ | 8095 | 8904 | 8527 | 8939 | 8584 | 809 | 432 | 844 | 489 |
| | $^5D_4$ | 8308 | 9146 | 8776 | 9181 | 8833 | 838 | 468 | 873 | 525 |
| 4s1 | $^5G_2$ | 20517 | 21714 | 21673 | 21741 | 21684 | 1197 | 1155 | 1224 | 1167 |
| | $^5G_6$ | 20520 | 21767 | 21727 | 21792 | 21738 | 1247 | 1208 | 1272 | 1219 |
| | $^5G_3$ | 20521 | 21725 | 21684 | 21752 | 21696 | 1204 | 1163 | 1231 | 1175 |
| | $^5G_4$ | 20524 | 21739 | 21698 | 21765 | 21709 | 1215 | 1174 | 1241 | 1186 |
| | $^5G_5$ | 20524 | 21753 | 21713 | 21779 | 21724 | 1229 | 1189 | 1255 | 1200 |
| 4s1 | $^5P_3$ | 21841 | 21734 | 22209 | 21736 | 22171 | -107 | 368 | -104 | 331 |
| | $^5P_2$ | 21848 | 21738 | 22213 | 21740 | 22175 | -110 | 365 | -108 | 327 |
| | $^5P_1$ | 21857 | 21750 | 22225 | 21752 | 22188 | -107 | 368 | -105 | 331 |
| 4s2 | $^3P_0$ | 23163 | 23451 | 23470 | 23587 | 23597 | 288 | 307 | 424 | 434 |
| | $^3P_1$ | 23512 | 23715 | 23767 | 23854 | 23893 | 203 | 255 | 342 | 381 |
| | $^3P_2$ | 24093 | 24201 | 24333 | 24356 | 24462 | 108 | 240 | 263 | 369 |
| 4s2 | $^3H_4$ | 23934 | 26090 | 25377 | 26502 | 25765 | 2156 | 1444 | 2568 | 1831 |
| | $^3H_5$ | 24056 | 26244 | 25489 | 26566 | 25889 | 2188 | 1433 | 2510 | 1833 |
| | $^3H_6$ | 24200 | 26404 | 25577 | 26718 | 25934 | 2204 | 1376 | 2518 | 1733 |
| 4s1 | $^5D_0$ | 24277 | 24623 | 24873 | 24618 | 24835 | 346 | 596 | 341 | 558 |
| | $^5D_4$ | 24282 | 24661 | 24911 | 24653 | 24871 | 378 | 629 | 371 | 588 |
| | $^5D_1$ | 24287 | 24640 | 24890 | 24634 | 24851 | 354 | 604 | 348 | 565 |
| | $^5D_2$ | 24300 | 24666 | 24917 | 24659 | 24876 | 367 | 617 | 359 | 576 |
| | $^5D_3$ | 24304 | 24678 | 24931 | 24671 | 24890 | 374 | 627 | 367 | 586 |
| 4s1 | $^3G_3$ | 24834 | 25350 | 25259 | 25755 | 25625 | 516 | 425 | 921 | 792 |
| | $^3G_4$ | 24897 | 25372 | 25172 | 25777 | 25519 | 474 | 275 | 880 | 622 |
| | $^3G_5$ | 25038 | 25426 | 25285 | 25849 | 25648 | 388 | 246 | 810 | 609 |
| 4s2 | $^3F_2$ | 24941 | 26106 | 25729 | 26315 | 25954 | 1165 | 789 | 1375 | 1014 |
| | $^3F_3$ | 25106 | 26179 | 25812 | 26398 | 26058 | 1073 | 706 | 1292 | 951 |
| | $^3F_4$ | 25177 | 26280 | 25906 | 26410 | 26151 | 1103 | 729 | 1233 | 974 |
| 4s1 | $^3P_0$ | 27163 | 26354 | 26685 | 26988 | 27289 | -809 | -478 | -176 | 126 |
| | $^3P_1$ | 27176 | 26411 | 26717 | 27040 | 27320 | -765 | -459 | -136 | 144 |
| | $^3P_2$ | 27223 | 26616 | 26859 | 27227 | 27458 | -607 | -364 | 4 | 236 |
| 4s2 | $^3G_3$ | 27597 | 29030 | 28495 | 29462 | 28946 | 1433 | 898 | 1865 | 1349 |
| | $^3G_4$ | 27704 | 29185 | 28612 | 29610 | 29088 | 1481 | 909 | 1906 | 1385 |
| | $^3G_5$ | 27817 | 29340 | 28766 | 29761 | 29236 | 1523 | 949 | 1945 | 1419 |

| | | | | | | | | | | |
|---|---|---|---|---|---|---|---|---|---|---|
| 4s1 | 3D3 | 28637 | 28257 | 28458 | 28573 | 28762 | -380 | -179 | -64 | 125 |
| | 3D1 | 28679 | 28258 | 28497 | 28585 | 28777 | -421 | -182 | -94 | 97 |
| | 3D2 | 28682 | 28284 | 28524 | 28611 | 28803 | -398 | -158 | -71 | 121 |
| 4s1 | 3D3 | 31009 | 31203 | 31322 | 31393 | 31516 | 194 | 313 | 384 | 507 |
| | 3D2 | 31028 | 31207 | 31332 | 31395 | 31519 | 178 | 303 | 367 | 490 |
| | 3D1 | 31049 | 31225 | 31349 | 31407 | 31532 | 176 | 300 | 358 | 483 |
| 4s1 | 3I7 | 31048 | 33357 | 32850 | 33754 | 33252 | 2309 | 1802 | 2568 | 1831 |
| | 3I6 | 31049 | 33355 | 32848 | 33753 | 33250 | 2305 | 1798 | 2510 | 1833 |
| | 3I5 | 31055 | 33353 | 32862 | 33751 | 33249 | 2298 | 1807 | 2518 | 1733 |
| 4s1 | 5F1 | 31352 | 32345 | 32755 | 32487 | 32870 | 993 | 1403 | 1135 | 1518 |
| | 5F2 | 31355 | 32358 | 32776 | 32500 | 32889 | 1003 | 1421 | 1145 | 1534 |
| | 5F3 | 31364 | 32378 | 32804 | 32519 | 32914 | 1014 | 1440 | 1155 | 1550 |
| | 5F4 | 31378 | 32402 | 32835 | 32543 | 32943 | 1025 | 1457 | 1165 | 1565 |
| | 5F5 | 31393 | 32427 | 32846 | 32568 | 32970 | 1034 | 1453 | 1175 | 1577 |
| 4s2 | 1G4 | 31987 | 32848 | 32344 | 33050 | 32568 | 861 | 357 | 1063 | 581 |
| 4s2 | 1I6 | 32097 | 34728 | 33802 | 35183 | 34278 | 2631 | 1705 | 2646 | 2033 |
| 4s1 | 3F2 | 33040 | 33322 | 33522 | 33617 | 33801 | 282 | 482 | 577 | 761 |
| | 3F3 | 33061 | 33306 | 33488 | 33604 | 33777 | 246 | 428 | 544 | 716 |
| | 3F4 | 33113 | 33320 | 33558 | 33606 | 33811 | 207 | 445 | 492 | 698 |
| 4s1 | 1I6 | 33763 | 35730 | 35077 | 36409 | 35795 | 1968 | 1314 | 3086 | 2180 |
| 4s2 | 3D1 | 33907 | 34327 | 34209 | 34887 | 34745 | 421 | 303 | 980 | 839 |
| | 3D3 | 33935 | 34341 | 34272 | 34889 | 34776 | 406 | 337 | 954 | 842 |
| | 3D2 | 33936 | 34355 | 34273 | 34907 | 34785 | 420 | 337 | 971 | 849 |

**Table 7.3.** *Shifted J-specific SOC energies of all MR-EOM methods and statistical analysis of MR-EOM data compared to NIST J-specific values (in $cm^{-1}$) for Cr neutral atom*

| Character of state | Term | Splitting in multiplets | | | | | Splitting in multiplets errors | | | |
|---|---|---|---|---|---|---|---|---|---|---|
| | | NIST | no-ph QZV | ph QZV | no-ph TZV | ph TZV | no-ph QZV | ph QZV | no-ph TZV | ph TZV |
| 4s1 | $^7S_3$ | 0 | 0 | 0 | 0 | 0 | 0 | 0 | 0 | 0 |
| 4s1 | $^5S_2$ | 0 | 0 | 0 | 0 | 0 | 0 | 0 | 0 | 0 |
| 4s2 | $^5D_0$ | 0 | 0 | 0 | 0 | 0 | 0 | 0 | 0 | 0 |
| | $^5D_1$ | 60 | 66 | 67 | 66 | 68 | 6 | 7 | 5 | 8 |
| | $^5D_2$ | 177 | 194 | 200 | 194 | 200 | 18 | 23 | 17 | 23 |
| | $^5D_3$ | 344 | 382 | 393 | 381 | 393 | 38 | 49 | 37 | 49 |
| | $^5D_4$ | 557 | 624 | 642 | 623 | 643 | 67 | 85 | 66 | 86 |
| 4s1 | $^5G_2$ | 0 | 0 | 0 | 0 | 0 | 0 | 0 | 0 | 0 |
| | $^5G_6$ | 2 | 53 | 55 | 51 | 54 | 50 | 53 | 49 | 52 |
| | $^5G_3$ | 3 | 11 | 11 | 11 | 11 | 7 | 8 | 7 | 8 |
| | $^5G_4$ | 6 | 25 | 25 | 23 | 25 | 18 | 19 | 17 | 19 |
| | $^5G_5$ | 6 | 39 | 40 | 38 | 40 | 32 | 34 | 31 | 33 |
| 4s1 | $^5P_3$ | 0 | 0 | 0 | 0 | 0 | 0 | 0 | 0 | 0 |
| | $^5P_2$ | 7 | 3 | 3 | 3 | 4 | -4 | -4 | -4 | -3 |
| | $^5P_1$ | 16 | 15 | 16 | 16 | 16 | -1 | 0 | -1 | 0 |
| 4s2 | $^3P_0$ | 0 | 0 | 0 | 0 | 0 | 0 | 0 | 0 | 0 |
| | $^3P_1$ | 349 | 264 | 297 | 267 | 296 | -85 | -52 | -82 | -53 |
| | $^3P_2$ | 930 | 750 | 863 | 768 | 865 | -180 | -67 | -161 | -65 |
| 4s2 | $^3H_4$ | 0 | 0 | 0 | 0 | 0 | 0 | 0 | 0 | 0 |
| | $^3H_5$ | 122 | 154 | 112 | 64 | 124 | 32 | -10 | -58 | 2 |
| | $^3H_6$ | 266 | 314 | 199 | 216 | 169 | 47 | -67 | -50 | -98 |
| 4s1 | $^5D_0$ | 0 | 0 | 0 | 0 | 0 | 0 | 0 | 0 | 0 |
| | $^5D_4$ | 5 | 38 | 38 | 35 | 36 | 32 | 33 | 30 | 31 |
| | $^5D_1$ | 9 | 17 | 18 | 16 | 17 | 8 | 8 | 7 | 7 |
| | $^5D_2$ | 23 | 44 | 44 | 41 | 42 | 21 | 21 | 18 | 19 |
| | $^5D_3$ | 27 | 55 | 58 | 53 | 55 | 29 | 31 | 26 | 29 |
| 4s1 | $^3G_3$ | 0 | 0 | 0 | 0 | 0 | 0 | 0 | 0 | 0 |
| | $^3G_4$ | 64 | 22 | -86 | 22 | -106 | -41 | -150 | -41 | -170 |
| | $^3G_5$ | 205 | 77 | 26 | 94 | 22 | -128 | -178 | -111 | -183 |
| 4s2 | $^3F_2$ | 0 | 0 | 0 | 0 | 0 | 0 | 0 | 0 | 0 |
| | $^3F_3$ | 166 | 73 | 83 | 83 | 103 | -93 | -83 | -83 | -63 |
| | $^3F_4$ | 237 | 175 | 177 | 95 | 197 | -62 | -59 | -142 | -40 |
| 4s1 | $^3P_0$ | 0 | 0 | 0 | 0 | 0 | 0 | 0 | 0 | 0 |
| | $^3P_1$ | 13 | 57 | 32 | 52 | 31 | 44 | 18 | 39 | 18 |
| | $^3P_2$ | 60 | 263 | 174 | 240 | 169 | 203 | 114 | 180 | 110 |
| 4s2 | $^3G_3$ | 0 | 0 | 0 | 0 | 0 | 0 | 0 | 0 | 0 |
| | $^3G_4$ | 10 | 15 | 11 | 14 | 14 | 48 | 11 | 41 | 36 |
| | $^3G_5$ | 220 | 310 | 270 | 300 | 289 | 90 | 51 | 80 | 70 |

| | | | | | | | | | | |
|---|---|---|---|---|---|---|---|---|---|---|
| 4s1 | $^3D_3$ | 0 | 0 | 0 | 0 | 0 | 0 | 0 | 0 | 0 |
| | $^3D_1$ | 42 | 1 | 39 | 12 | 15 | -41 | -3 | -31 | -28 |
| | $^3D_2$ | 45 | 27 | 66 | 38 | 42 | -18 | 21 | -8 | -4 |
| 4s1 | $^3D_3$ | 0 | 0 | 0 | 0 | 0 | 0 | 0 | 0 | 0 |
| | $^3D_2$ | 19 | 3 | 10 | 2 | 2 | -16 | -10 | -18 | -17 |
| | $^3D_1$ | 40 | 21 | 27 | 13 | 16 | -19 | -12 | -26 | -24 |
| 4s1 | $^3I_7$ | 0 | 0 | 0 | 0 | 0 | 0 | 0 | 0 | 0 |
| | $^3I_6$ | 1 | -2 | -2 | -2 | -2 | -3 | -4 | -3 | -3 |
| | $^3I_5$ | 7 | -4 | 12 | -3 | -3 | -11 | 5 | -11 | -11 |
| 4s1 | $^5F_1$ | -50 | 0 | 0 | 0 | 0 | 0 | 0 | 0 | 0 |
| | $^5F_2$ | 3 | 13 | 21 | 13 | 19 | 10 | 18 | 10 | 16 |
| | $^5F_3$ | 12 | 33 | 49 | 32 | 44 | 21 | 37 | 20 | 32 |
| | $^5F_4$ | 25 | 57 | 79 | 56 | 73 | 32 | 54 | 31 | 47 |
| | $^5F_5$ | 41 | 82 | 90 | 81 | 99 | 41 | 50 | 40 | 59 |
| 4s2 | $^1G_4$ | 0 | 0 | 0 | 0 | 0 | 0 | 0 | 0 | 0 |
| 4s2 | $^1I_6$ | 0 | 0 | 0 | 0 | 0 | 0 | 0 | 0 | 0 |
| 4s1 | $^3F_2$ | 0 | 0 | 0 | 0 | 0 | 0 | 0 | 0 | 0 |
| | $^3F_3$ | 21 | -16 | -34 | -12 | -24 | -36 | -54 | -33 | -44 |
| | $^3F_4$ | 73 | -2 | 36 | -11 | 10 | -75 | -37 | -84 | -63 |
| 4s1 | $^1I_6$ | 0 | 0 | 0 | 0 | 0 | 0 | 0 | 0 | 0 |
| 4s2 | $^3D_1$ | 0 | 0 | 0 | 0 | 0 | 0 | 0 | 0 | 0 |
| | $^3D_3$ | 28 | 13 | 62 | 2 | 31 | -15 | 34 | -26 | 3 |
| | $^3D_2$ | 29 | 28 | 63 | 20 | 40 | -1 | 34 | -9 | 11 |

**Table 7.4.** *Splitting in multiplets of all MR-EOM methods and statistical analysis of splitting in multiplets (in $cm^{-1}$) for Cr atoms*

| Mn Character of state | Term | NIST | Shifted Energies | | | | | | | |
|---|---|---|---|---|---|---|---|---|---|---|
| | | | No SOC | | | | J-averaged SOC | | | |
| | | | no-ph QZV | ph QZV | no-ph TZV | ph TZV | no-ph QZV | ph QZV | no-ph TZV | ph TZV |
| 4s2 | 6S | 0 | -328 | -756 | -542 | -953 | -330 | -759 | -545 | -956 |
| 4s1 | 6D | 17301 | 17629 | 18058 | 17843 | 18254 | 17632 | 18060 | 17846 | 18257 |
| 4s1 | 4D | 23509 | 22792 | 23246 | 23177 | 23621 | 22793 | 23247 | 23178 | 23621 |
| 4s2 | 4G | 25279 | 26682 | 25879 | 26740 | 25972 | 26681 | 25878 | 26739 | 25971 |
| 4s2 | 4P | 27230 | 27637 | 27512 | 27599 | 27479 | 27583 | 27448 | 27548 | 27420 |
| 4s2 | 4D | 30394 | 30964 | 30510 | 31058 | 30622 | 31006 | 30558 | 31097 | 30667 |
| 4s1 | 4P | 34208 | 33838 | 34327 | 34138 | 34600 | 33855 | 34343 | 34154 | 34617 |
| 4s1 | 4H | 34268 | 35964 | 35823 | 36407 | 36268 | 35957 | 35835 | 36400 | 36266 |
| 4s1 | 4F | 35038 | 35483 | 35768 | 35845 | 36114 | 35481 | 35738 | 35844 | 36107 |
| 4s2 | 2I | 37157 | 40041 | 38754 | 40251 | 39023 | 40031 | 38745 | 40242 | 39003 |
| 4s1 | 4G | 37611 | 38567 | 38640 | 39057 | 39124 | 38503 | 38614 | 38988 | 39103 |
| 4s1 | 2P | 37841 | 36888 | 37408 | 37291 | 37786 | 36947 | 37466 | 37347 | 37843 |
| 4s1 | 2H | 38059 | 39078 | 38950 | 39618 | 39497 | 39106 | 38997 | 39643 | 39537 |
| 4s1 | 2F | 38783 | 38600 | 40996 | 39068 | 41117 | 38859 | 41198 | 39336 | 41313 |
| 4s1 | 2G | 41120 | 41492 | 41580 | 42052 | 42136 | 41552 | 41639 | 42109 | 42192 |

**Table 7.5.** *Shifted J-averaged energies (in $cm^{-1}$) for Mn neutral atom*

| Mn Character Of state | Term | Errors from NIST | | | | | | | | Deviations between SOC and No-SOC | | | |
|---|---|---|---|---|---|---|---|---|---|---|---|---|---|
| | | No SOC | | | | J-averaged SOC | | | | | | | |
| | | no-ph QZV | ph QZV | no-ph TZV | ph TZV | no-ph QZV | ph QZV | no-ph TZV | ph TZV | no-ph QZV | ph QZV | no-ph TZV | ph TZV |
| 4s2 | 6S | -328 | -756 | -542 | -953 | -330 | -759 | -545 | -956 | 2 | 3 | 2 | 3 |
| 4s1 | 6D | 328 | 756 | 542 | 953 | 330 | 759 | 545 | 956 | -2 | -3 | -2 | -3 |
| 4s1 | 4D | -717 | -263 | -332 | 111 | -716 | -262 | -332 | 112 | -1 | -1 | -1 | -1 |
| 4s2 | 4G | 1404 | 600 | 1462 | 693 | 1403 | 599 | 1461 | 692 | 1 | 1 | 1 | 1 |
| 4s2 | 4P | 406 | 282 | 368 | 249 | 353 | 218 | 318 | 190 | 53 | 64 | 50 | 59 |
| 4s2 | 4D | 570 | 116 | 664 | 228 | 612 | 164 | 704 | 273 | -42 | -48 | -39 | -45 |
| 4s1 | 4P | -370 | 119 | -70 | 392 | -353 | 135 | -54 | 409 | -17 | -16 | -16 | -16 |
| 4s1 | 4H | 1697 | 1555 | 2139 | 2000 | 1690 | 1567 | 2133 | 1999 | 7 | -12 | 6 | 1 |
| 4s1 | 4F | 445 | 730 | 807 | 1076 | 443 | 700 | 806 | 1069 | 2 | 30 | 1 | 7 |
| 4s2 | 2I | 2884 | 1597 | 3094 | 1866 | 2874 | 1588 | 3085 | 1846 | 9 | 10 | 9 | 20 |
| 4s1 | 4G | 957 | 1029 | 1446 | 1514 | 892 | 1003 | 1377 | 1493 | 64 | 26 | 69 | 21 |
| 4s1 | 2P | -954 | -434 | -551 | -55 | -894 | -375 | -494 | 2 | -59 | -59 | -57 | -56 |
| 4s1 | 2H | 1018 | 890 | 1559 | 1438 | 1047 | 938 | 1584 | 1477 | -29 | -47 | -25 | -40 |
| 4s1 | 2F | -183 | 2213 | 285 | 2334 | 75 | 2414 | 553 | 2530 | -259 | -201 | -268 | -196 |
| 4s1 | 2G | 372 | 460 | 932 | 1016 | 432 | 519 | 989 | 1072 | -60 | -59 | -57 | -56 |

**Table 7.6.** *Statistical analysis of ORCA-MR-EOM data compared to NIST J-averaged values (in $cm^{-1}$) for Mn neutral atom*

| Character of state | Term | NIST | J-specific SOC Energies | | | | J-specific SOC Energies Errors | | | |
|---|---|---|---|---|---|---|---|---|---|---|
| | | | no-ph QZV | ph QZV | no-ph TZV | ph TZV | no-ph QZV | ph QZV | no-ph TZV | ph TZV |
| 4s2 | $^6S_{5/2}$ | 0 | -330 | -759 | -545 | -956 | -330 | -759 | -545 | -956 |
| 4s1 | $^6D_{9/2}$ | 17052 | 17382 | 17812 | 17599 | 18012 | 330 | 760 | 547 | 960 |
| | $^6D_{7/2}$ | 17282 | 17612 | 18041 | 17827 | 18238 | 330 | 759 | 545 | 956 |
| | $^6D_{5/2}$ | 17452 | 17783 | 18210 | 17995 | 18405 | 331 | 759 | 543 | 954 |
| | $^6D_{3/2}$ | 17568 | 17900 | 18327 | 18110 | 18520 | 331 | 758 | 542 | 952 |
| | $^6D_{1/2}$ | 17637 | 17968 | 18395 | 18178 | 18587 | 331 | 758 | 541 | 950 |
| 4s1 | $^4D_{7/2}$ | 23297 | 22576 | 23033 | 22965 | 23411 | -720 | -264 | -332 | 115 |
| | $^4D_{5/2}$ | 23549 | 22835 | 23288 | 23218 | 23662 | -715 | -261 | -331 | 112 |
| | $^4D_{3/2}$ | 23720 | 23007 | 23459 | 23388 | 23829 | -712 | -261 | -332 | 110 |
| | $^4D_{1/2}$ | 23819 | 23107 | 23557 | 23486 | 23926 | -712 | -262 | -333 | 107 |
| 4s2 | $^4G_{11/}$ | 25266 | 26699 | 25897 | 26757 | 25991 | 1433 | 631 | 1492 | 725 |
| | $^4G_{5/2}$ | 25281 | 26639 | 25833 | 26697 | 25926 | 1358 | 552 | 1416 | 645 |
| | $^4G_{9/2}$ | 25285 | 26694 | 25891 | 26752 | 25984 | 1409 | 606 | 1467 | 699 |
| | $^4G_{7/2}$ | 25288 | 26671 | 25866 | 26728 | 25959 | 1383 | 578 | 1440 | 671 |
| 4s2 | $^4P_{5/2}$ | 27202 | 27559 | 27424 | 27526 | 27397 | 357 | 222 | 324 | 195 |
| | $^4P_{3/2}$ | 27248 | 27593 | 27458 | 27558 | 27429 | 345 | 210 | 310 | 181 |
| | $^4P_{1/2}$ | 27282 | 27636 | 27504 | 27598 | 27472 | 354 | 222 | 316 | 190 |
| 4s2 | $^4D_{7/2}$ | 30354 | 30982 | 30528 | 31076 | 30640 | 628 | 174 | 722 | 286 |
| | $^4D_{1/2}$ | 30412 | 30973 | 30522 | 31066 | 30633 | 561 | 110 | 654 | 221 |
| | $^4D_{5/2}$ | 30420 | 31040 | 30599 | 31130 | 30706 | 621 | 179 | 711 | 287 |
| | $^4D_{3/2}$ | 30426 | 31016 | 30572 | 31107 | 30680 | 590 | 146 | 681 | 254 |
| 4s1 | $^4P_{5/2}$ | 33825 | 33465 | 33952 | 33769 | 34229 | -360 | 127 | -57 | 404 |
| | $^4P_{3/2}$ | 34463 | 34101 | 34591 | 34399 | 34863 | -362 | 128 | -64 | 400 |
| | $^4P_{1/2}$ | 34845 | 34530 | 35020 | 34822 | 35286 | -315 | 175 | -23 | 441 |
| 4s1 | $^4H_{13/}$ | 34139 | 35852 | 35883 | 36296 | 36167 | 1713 | 1744 | 2157 | 2028 |
| | $^4H_{11/}$ | 34251 | 35932 | 35793 | 36375 | 36239 | 1681 | 1543 | 2125 | 1988 |
| | $^4H_{9/2}$ | 34344 | 36020 | 35715 | 36462 | 36326 | 1676 | 1371 | 2118 | 1982 |
| | $^4H_{7/2}$ | 34423 | 36103 | 35964 | 36544 | 36407 | 1680 | 1541 | 2121 | 1984 |
| 4s1 | $^4F_{9/2}$ | 34939 | 35400 | 35683 | 35764 | 36033 | 462 | 745 | 825 | 1094 |
| | $^4F_{7/2}$ | 35041 | 35475 | 35756 | 35838 | 36105 | 433 | 715 | 797 | 1064 |
| | $^4F_{5/2}$ | 35115 | 35545 | 35827 | 35907 | 36153 | 430 | 712 | 792 | 1038 |
| | $^4F_{3/2}$ | 35165 | 35602 | 35706 | 35962 | 36228 | 436 | 541 | 797 | 1063 |
| 4s2 | $^2I_{11/}$ | 37149 | 39995 | 38707 | 40207 | 38953 | 2847 | 1558 | 3058 | 1805 |
| | $^2I_{13/}$ | 37164 | 40062 | 38777 | 40272 | 39045 | 2898 | 1613 | 3108 | 1881 |
| 4s1 | $^4G_{11/}$ | 37420 | 38416 | 38466 | 38910 | 38984 | 996 | 1046 | 1490 | 1563 |
| | $^4G_{9/2}$ | 37631 | 38615 | 38680 | 39103 | 39165 | 984 | 1050 | 1472 | 1535 |
| | $^4G_{7/2}$ | 37737 | 38478 | 38686 | 38952 | 39156 | 741 | 949 | 1215 | 1419 |
| | $^4G_{5/2}$ | 37790 | 38525 | 38704 | 39000 | 39170 | 735 | 914 | 1210 | 1380 |

| | | | | | | | | | | |
|---|---|---|---|---|---|---|---|---|---|---|
| 4s1 | $^2P_{3/2}$ | 37586 | 36680 | 37200 | 37083 | 37579 | -906 | -386 | -503 | -7 |
| | $^2P_{1/2}$ | 38352 | 37481 | 37998 | 37876 | 38370 | -871 | -353 | -476 | 18 |
| 4s1 | $^2H_{11/}$ | 38009 | 39062 | 38961 | 39599 | 39499 | 1054 | 953 | 1590 | 1490 |
| | $^2H_{9/2}$ | 38120 | 39159 | 39040 | 39697 | 39582 | 1039 | 920 | 1576 | 1462 |
| 4s1 | $^2F_{7/2}$ | 38670 | 38798 | 41025 | 39278 | 41146 | 128 | 2356 | 609 | 2476 |
| | $^2F_{5/2}$ | 38935 | 38940 | 41427 | 39413 | 41537 | 5 | 2492 | 478 | 2602 |
| 4s1 | $^2G_{9/2}$ | 41031 | 41468 | 41555 | 42028 | 42112 | 436 | 524 | 997 | 1080 |
| | $^2G_{7/2}$ | 41230 | 41658 | 41743 | 42211 | 42292 | 427 | 513 | 980 | 1062 |

**Table 7.7.** *Shifted J-specific SOC energies of all MR-EOM methods and statistical analysis of MR-EOM data compared to NIST J-specific values (in $cm^{-1}$) for Mn neutral atom*

| Character of state | Term | Splitting in multiplets | | | | | Splitting in multiplets errors | | | |
|---|---|---|---|---|---|---|---|---|---|---|
| | | NIST | no-ph QZV | ph QZV | no-ph TZV | ph TZV | no-ph QZV | ph QZV | no-ph TZV | ph TZV |
| 4s | $^6S_{5/2}$ | 0 | 0 | 0 | 0 | 0 | 0 | 0 | 0 | 0 |
| 4s | $^6D_{9/2}$ | 0 | 0 | 0 | 0 | 0 | 0 | 0 | 0 | 0 |
| | $^6D_{7/2}$ | 230 | 230 | 229 | 227 | 226 | 1 | -1 | -2 | -4 |
| | $^6D_{5/2}$ | 399 | 401 | 398 | 395 | 393 | 1 | -1 | -4 | -6 |
| | $^6D_{3/2}$ | 516 | 518 | 515 | 511 | 508 | 1 | -2 | -5 | -8 |
| | $^6D_{1/2}$ | 585 | 586 | 583 | 578 | 575 | 1 | -2 | -7 | -9 |
| 4s | $^4D_{7/2}$ | 0 | 0 | 0 | 0 | 0 | 0 | 0 | 0 | 0 |
| | $^4D_{5/2}$ | 253 | 258 | 255 | 253 | 250 | 6 | 2 | 1 | -2 |
| | $^4D_{3/2}$ | 423 | 431 | 426 | 423 | 418 | 8 | 3 | 0 | -5 |
| | $^4D_{1/2}$ | 522 | 530 | 524 | 521 | 515 | 8 | 2 | -1 | -7 |
| 4s | $^4G_{11/2}$ | 0 | 0 | 0 | 0 | 0 | 0 | 0 | 0 | 0 |
| | $^4G_{5/2}$ | 15 | -60 | -64 | -60 | -65 | -75 | -80 | -75 | -80 |
| | $^4G_{9/2}$ | 20 | -5 | -6 | -5 | -7 | -24 | -26 | -25 | -26 |
| | $^4G_{7/2}$ | 22 | -29 | -31 | -29 | -32 | -51 | -53 | -51 | -54 |
| 4s | $^4P_{5/2}$ | 0 | 0 | 0 | 0 | 0 | 0 | 0 | 0 | 0 |
| | $^4P_{3/2}$ | 46 | 34 | 34 | 32 | 32 | -12 | -13 | -14 | -14 |
| | $^4P_{1/2}$ | 80 | 77 | 80 | 72 | 75 | -4 | 0 | -8 | -5 |
| 4s | $^4D_{7/2}$ | 0 | 0 | 0 | 0 | 0 | 0 | 0 | 0 | 0 |
| | $^4D_{1/2}$ | 58 | -9 | -6 | -10 | -7 | -67 | -64 | -68 | -65 |
| | $^4D_{5/2}$ | 65 | 58 | 71 | 54 | 66 | -7 | 5 | -11 | 0 |
| | $^4D_{3/2}$ | 72 | 34 | 43 | 31 | 39 | -38 | -28 | -41 | -32 |
| 4s | $^4P_{5/2}$ | 0 | 0 | 0 | 0 | 0 | 0 | 0 | 0 | 0 |
| | $^4P_{3/2}$ | 638 | 636 | 639 | 631 | 634 | -2 | 1 | -7 | -4 |
| | $^4P_{1/2}$ | 1020 | 1065 | 1068 | 1053 | 1057 | 45 | 48 | 33 | 37 |
| 4s | $^4H_{13/2}$ | 0 | 0 | 0 | 0 | 0 | 0 | 0 | 0 | 0 |
| | $^4H_{11/2}$ | 112 | 80 | -90 | 80 | 72 | -32 | -201 | -32 | -39 |
| | $^4H_{9/2}$ | 205 | 168 | -168 | 166 | 160 | -37 | -373 | -39 | -45 |
| | $^4H_{7/2}$ | 284 | 251 | 81 | 249 | 240 | -33 | -203 | -36 | -44 |
| 4s | $^4F_{9/2}$ | 0 | 0 | 0 | 0 | 0 | 0 | 0 | 0 | 0 |
| | $^4F_{7/2}$ | 103 | 74 | 73 | 74 | 72 | -28 | -30 | -29 | -30 |
| | $^4F_{5/2}$ | 176 | 144 | 143 | 143 | 121 | -32 | -33 | -34 | -56 |
| | $^4F_{3/2}$ | 226 | 201 | 23 | 198 | 195 | -25 | -204 | -28 | -31 |
| 4s | $^2I_{11/2}$ | 0 | 0 | 0 | 0 | 0 | 0 | 0 | 0 | 0 |
| | $^2I_{13/2}$ | 16 | 67 | 70 | 65 | 92 | 51 | 55 | 50 | 77 |
| 4s | $^4G_{11/2}$ | 0 | 0 | 0 | 0 | 0 | 0 | 0 | 0 | 0 |
| | $^4G_{9/2}$ | 210 | 199 | 214 | 192 | 181 | -11 | 4 | -18 | -29 |
| | $^4G_{7/2}$ | 317 | 62 | 220 | 41 | 172 | -255 | -97 | -276 | -145 |

| | | | | | | | | | | |
|---|---|---|---|---|---|---|---|---|---|---|
| | $^4G_{5/2}$ | 370 | 109 | 238 | 90 | 187 | -261 | -132 | -280 | -183 |
| 4s1 | $^2P_{3/2}$ | 0 | 0 | 0 | 0 | 0 | 0 | 0 | 0 | 0 |
| | $^2P_{1/2}$ | 766 | 801 | 798 | 793 | 791 | 35 | 32 | 27 | 25 |
| 4s1 | $^2H_{11/}$ | 0 | 0 | 0 | 0 | 0 | 0 | 0 | 0 | 0 |
| | $^2H_{9/2}$ | 111 | 96 | 78 | 98 | 83 | -15 | -33 | -14 | -29 |
| 4s1 | $^2F_{7/2}$ | 0 | 0 | 0 | 0 | 0 | 0 | 0 | 0 | 0 |
| | $^2F_{5/2}$ | 265 | 142 | 402 | 135 | 391 | -123 | 136 | -131 | 125 |
| 4s1 | $^2G_{9/2}$ | 0 | 0 | 0 | 0 | 0 | 0 | 0 | 0 | 0 |
| | $^2G_{7/2}$ | 199 | 190 | 188 | 182 | 181 | -9 | -10 | -16 | -18 |

**Table 7.8.** *Splitting in multiplets of all MR-EOM methods and statistical analysis of splitting in multiplets (in $cm^{-1}$) for Mn atoms*

| Fe Character of state | Term | NIST | Shifted Energies | | | | | | | |
|---|---|---|---|---|---|---|---|---|---|---|
| | | | No SOC | | | | J-averaged SOC | | | |
| | | | no-ph QZV | ph QZV | no-ph TZV | ph TZV | no-ph QZV | ph QZV | no-ph TZV | ph TZV |
| 4s2 | 5D | 403 | 263 | -192 | 82 | -356 | 260 | -196 | 79 | -360 |
| 4s1 | 5F | 7460 | 7599 | 8055 | 7780 | 8219 | 7602 | 8058 | 7783 | 8223 |
| 4s1 | 3F | 12407 | 12023 | 12503 | 12328 | 12796 | 12034 | 12515 | 12338 | 12807 |
| 4s1 | 5P | 17685 | 16986 | 17771 | 17328 | 18094 | 16972 | 17754 | 17313 | 18057 |
| 4s2 | 3P | 18954 | 18941 | 18920 | 18868 | 18817 | 18950 | 18941 | 18884 | 18873 |
| 4s2 | 3H | 19576 | 21385 | 20394 | 21412 | 20459 | 21360 | 20343 | 21386 | 20406 |
| 4s2 | 3F | 20814 | 21533 | 21047 | 21511 | 21041 | 21449 | 21010 | 21440 | 21010 |
| 4s1 | 3G | 21949 | 22494 | 22663 | 22806 | 22941 | 22508 | 22683 | 22823 | 22968 |
| 4s1 | 3P | 22898 | 21807 | 22464 | 22236 | 22910 | 21780 | 22415 | 22192 | 22856 |
| 4s2 | 3G | 24039 | 25054 | 24388 | 25176 | 24563 | 25159 | 24479 | 25216 | 24645 |
| 4s1 | 3P | 24565 | 23802 | 24344 | 24125 | 24639 | 23782 | 24331 | 24108 | 24631 |
| 4s1 | 1G | 24575 | 24829 | 25064 | 25239 | 25466 | 24821 | 25081 | 25405 | 25478 |
| 4s1 | 3H | 26330 | 27385 | 27431 | 27830 | 27875 | 27439 | 27489 | 27883 | 27930 |
| 4s1 | 3D | 26394 | 25789 | 26430 | 26124 | 26736 | 25746 | 26387 | 26088 | 26701 |
| 4s1 | 1P | 27543 | 25935 | 26558 | 26333 | 26929 | 26737 | 27350 | 27082 | 27659 |
| 4s1 | 1D | 28605 | 27738 | 28386 | 28091 | 28716 | 27879 | 28487 | 28219 | 28783 |
| 4s1 | 1H | 28820 | 29613 | 29678 | 30121 | 30186 | 29677 | 29744 | 30182 | 30248 |
| 4s2 | 1I | 29313 | 31933 | 30678 | 32067 | 30861 | 31981 | 30728 | 32114 | 30910 |
| 4s2 | 3D | 29356 | 29544 | 29226 | 29696 | 29400 | 29574 | 29273 | 29728 | 29458 |
| 4s2 | 1G | 29799 | 30875 | 30309 | 30944 | 30405 | 31009 | 30448 | 31075 | 30540 |

**Table 7.9.** *Shifted J-averaged energies (in $cm^{-1}$) for Fe neutral atom*

| Fe Character of state | Term | Errors from NIST | | | | | | | | Deviations between SOC and No SOC | | | |
|---|---|---|---|---|---|---|---|---|---|---|---|---|---|
| | | No SOC | | | | J-averaged SOC | | | | | | | |
| | | no-ph QZV | ph QZV | no-ph TZV | ph TZV | no-ph QZV | ph QZV | no-ph TZV | ph TZV | no-ph QZV | ph QZV | no-ph TZV | ph TZV |
| 4s2 | 5D | -140 | -595 | -321 | -759 | -143 | -599 | -324 | -763 | 3 | 4 | 3 | 4 |
| 4s1 | 5F | 140 | 595 | 321 | 759 | 143 | 599 | 324 | 763 | -3 | -4 | -3 | -4 |
| 4s1 | 3F | -384 | 96 | -80 | 389 | -373 | 107 | -69 | 399 | -11 | -11 | -11 | -11 |
| 4s1 | 5P | -698 | 87 | -356 | 409 | -713 | 70 | -372 | 373 | 14 | 17 | 16 | 37 |
| 4s2 | 3P | -13 | -34 | -86 | -137 | -4 | -13 | -70 | -81 | -9 | -21 | -16 | -55 |
| 4s2 | 3H | 1809 | 819 | 1836 | 883 | 1785 | 767 | 1811 | 830 | 24 | 52 | 26 | 53 |
| 4s2 | 3F | 719 | 233 | 698 | 228 | 636 | 197 | 626 | 197 | 84 | 37 | 72 | 31 |
| 4s1 | 3G | 545 | 715 | 857 | 993 | 559 | 734 | 874 | 1019 | -14 | -20 | -17 | -26 |
| 4s1 | 3P | -1092 | -435 | -662 | 12 | -1118 | -483 | -706 | -42 | 26 | 49 | 44 | 54 |
| 4s2 | 3G | 1015 | 349 | 1137 | 524 | 1120 | 440 | 1177 | 606 | -105 | -91 | -39 | -82 |
| 4s1 | 3P | -763 | -221 | -441 | 74 | -783 | -234 | -457 | 66 | 19 | 13 | 16 | 8 |
| 4s1 | 1G | 255 | 490 | 664 | 891 | 246 | 506 | 830 | 903 | 9 | -16 | -166 | -13 |
| 4s1 | 3H | 1055 | 1101 | 1500 | 1545 | 1110 | 1159 | 1553 | 1600 | -54 | -57 | -53 | -56 |
| 4s1 | 3D | -605 | 36 | -270 | 342 | -648 | -7 | -306 | 307 | 43 | 43 | 36 | 35 |
| 4s1 | 1P | -1608 | -985 | -1210 | -614 | -806 | -193 | -461 | 116 | -802 | -792 | -750 | -730 |
| 4s1 | 1D | -867 | -218 | -513 | 111 | -726 | -117 | -386 | 179 | -141 | -101 | -127 | -67 |
| 4s1 | 1H | 793 | 859 | 1301 | 1366 | 857 | 924 | 1362 | 1428 | -64 | -65 | -61 | -62 |
| 4s2 | 1I | 2620 | 1365 | 2754 | 1548 | 2668 | 1415 | 2801 | 1597 | -48 | -50 | -46 | -49 |
| 4s2 | 3D | 188 | -130 | 339 | 44 | 217 | -83 | 372 | 102 | -30 | -47 | -33 | -58 |
| 4s2 | 1G | 1076 | 510 | 1145 | 606 | 1210 | 649 | 1276 | 741 | -134 | -138 | -131 | -136 |

**Table 7.10.** *Statistical analysis of ORCA-MR-EOM data compared to NIST J-averaged values (in $cm^{-1}$) for Fe neutral atom*

| Character of state | Term | NIST | J-specific SOC Energies | | | | J-specific SOC Energies Errors | | | |
|---|---|---|---|---|---|---|---|---|---|---|
| | | | no-ph QZV | ph QZV | no-ph TZV | ph TZV | no-ph QZV | ph QZV | no-ph TZV | ph TZV |
| 4s2 | $^5D_4$ | 0 | -130 | -596 | -306 | -756 | -130 | -596 | -306 | -756 |
| | $^5D_3$ | 416 | 272 | -184 | 90 | -349 | -144 | -600 | -326 | -765 |
| | $^5D_2$ | 704 | 552 | 104 | 368 | -64 | -152 | -601 | -336 | -768 |
| | $^5D_1$ | 888 | 732 | 288 | 546 | 119 | -156 | -600 | -342 | -769 |
| | $^5D_0$ | 978 | 820 | 378 | 633 | 208 | -158 | -600 | -345 | -770 |
| 4s1 | $^5F_5$ | 6928 | 7083 | 7539 | 7270 | 7708 | 155 | 610 | 342 | 780 |
| | $^5F_4$ | 7377 | 7520 | 7976 | 7702 | 8141 | 143 | 599 | 325 | 764 |
| | $^5F_3$ | 7728 | 7864 | 8320 | 8042 | 8482 | 136 | 592 | 314 | 754 |
| | $^5F_2$ | 7986 | 8117 | 8575 | 8292 | 8733 | 132 | 589 | 307 | 748 |
| | $^5F_1$ | 8155 | 8284 | 8741 | 8457 | 8899 | 129 | 587 | 302 | 744 |
| 4s1 | $^3F_4$ | 11976 | 11609 | 12090 | 11919 | 12388 | -367 | 114 | -57 | 412 |
| | $^3F_3$ | 12561 | 12185 | 12666 | 12487 | 12956 | -376 | 105 | -74 | 395 |
| | $^3F_2$ | 12969 | 12587 | 13068 | 12884 | 13353 | -381 | 99 | -85 | 384 |
| 4s1 | $^5P_3$ | 17550 | 16840 | 17626 | 17183 | 17949 | -710 | 75 | -367 | 399 |
| | $^5P_2$ | 17727 | 17013 | 17790 | 17352 | 18077 | -714 | 63 | -375 | 350 |
| | $^5P_1$ | 17927 | 17211 | 17996 | 17550 | 18277 | -716 | 68 | -377 | 350 |
| 4s2 | $^3P_2$ | 18378 | 18399 | 18346 | 18324 | 18302 | 20 | -32 | -55 | -76 |
| | $^3P_1$ | 19552 | 19521 | 19557 | 19463 | 19457 | -31 | 5 | -90 | -95 |
| | $^3P_0$ | 20038 | 19996 | 20071 | 19949 | 19972 | -42 | 33 | -89 | -66 |
| 4s2 | $^3H_6$ | 19390 | 21199 | 20203 | 21228 | 20270 | 1808 | 813 | 1838 | 880 |
| | $^3H_5$ | 19621 | 21369 | 20386 | 21399 | 20451 | 1748 | 765 | 1778 | 830 |
| | $^3H_4$ | 19788 | 21583 | 20492 | 21600 | 20548 | 1795 | 703 | 1812 | 760 |
| 4s2 | $^3F_4$ | 20641 | 21253 | 20869 | 21246 | 20875 | 612 | 228 | 605 | 234 |
| | $^3F_3$ | 20874 | 21539 | 21049 | 21520 | 21046 | 665 | 175 | 645 | 171 |
| | $^3F_2$ | 21039 | 21675 | 21209 | 21676 | 21204 | 636 | 170 | 637 | 165 |
| 4s1 | $^3G_5$ | 21716 | 22288 | 22460 | 22606 | 22746 | 573 | 744 | 890 | 1030 |
| | $^3G_4$ | 21999 | 22550 | 22730 | 22868 | 23019 | 551 | 731 | 869 | 1019 |
| | $^3G_3$ | 22249 | 22798 | 22973 | 23107 | 23251 | 548 | 724 | 858 | 1001 |
| 4s1 | $^3P_2$ | 22838 | 21698 | 22330 | 22120 | 22775 | -1140 | -509 | -718 | -63 |
| | $^3P_1$ | 22947 | 21847 | 22486 | 22252 | 22924 | -1100 | -461 | -695 | -23 |
| | $^3P_0$ | 23052 | 21991 | 22625 | 22375 | 23056 | -1061 | -426 | -677 | 4 |
| 4s2 | $^3G_5$ | 23784 | 24915 | 24236 | 25034 | 24406 | 1132 | 453 | 1251 | 622 |
| | $^3G_4$ | 24119 | 25262 | 24564 | 25198 | 24727 | 1143 | 445 | 1079 | 608 |
| | $^3G_3$ | 24339 | 25409 | 24752 | 25524 | 24917 | 1070 | 413 | 1185 | 579 |
| 4s1 | $^3P_2$ | 24336 | 23554 | 24128 | 23879 | 24433 | -782 | -207 | -457 | 98 |
| | $^3P_1$ | 24772 | 23989 | 24509 | 24316 | 24805 | -783 | -263 | -456 | 33 |
| | $^3P_0$ | 25092 | 24306 | 24807 | 24631 | 25100 | -786 | -284 | -460 | 8 |
| 4s1 | $^1G_4$ | 24575 | 24821 | 25081 | 25405 | 25478 | 246 | 506 | 830 | 903 |
| 4s1 | $^3H_6$ | 26106 | 27237 | 27284 | 27684 | 27728 | 1131 | 1178 | 1578 | 1623 |

| | | | | | | | | | | |
|---|---|---|---|---|---|---|---|---|---|---|
| | $^3H_5$ | 26351 | 27461 | 27510 | 27905 | 27953 | 1110 | 1159 | 1554 | 1602 |
| | $^3H_4$ | 26628 | 27704 | 27758 | 28143 | 28195 | 1077 | 1130 | 1516 | 1567 |
| 4s1 | $^3D_3$ | 26225 | 25624 | 26272 | 25961 | 26582 | -601 | 47 | -264 | 357 |
| | $^3D_1$ | 26406 | 25574 | 26206 | 25945 | 26551 | -832 | -201 | -461 | 144 |
| | $^3D_2$ | 26624 | 26020 | 26658 | 26351 | 26959 | -603 | 34 | -273 | 335 |
| 4s1 | $^1P_1$ | 27543 | 26737 | 27350 | 27082 | 27659 | -806 | -193 | -461 | 116 |
| 4s1 | $^1D_2$ | 28605 | 27879 | 28487 | 28219 | 28783 | -726 | -117 | -386 | 179 |
| 4s1 | $^1H_5$ | 28820 | 29677 | 29744 | 30182 | 30248 | 857 | 924 | 1362 | 1428 |
| 4s2 | $^1I_6$ | 29313 | 31981 | 30728 | 32114 | 30910 | 2668 | 1415 | 2801 | 1597 |
| 4s2 | $^3D_1$ | 29320 | 29495 | 29195 | 29654 | 29385 | 175 | -125 | 334 | 65 |
| | $^3D_2$ | 29357 | 29538 | 29262 | 29699 | 29459 | 181 | -95 | 342 | 102 |
| | $^3D_3$ | 29372 | 29633 | 29315 | 29781 | 29489 | 261 | -57 | 409 | 117 |
| 4s2 | $^1G_4$ | 29799 | 31009 | 30448 | 31075 | 30540 | 1210 | 649 | 1276 | 741 |

**Table 7.11.** *Shifted J-specific SOC energies of all MR-EOM methods and statistical analysis of MR-EOM data compared to NIST J-specific values (in $cm^{-1}$) for Fe neutral atom*

| Character of state | Term | Splitting in multiplets | | | | | Splitting in multiplets errors | | | |
|---|---|---|---|---|---|---|---|---|---|---|
| | | NIST | no-ph QZV | ph QZV | no-ph TZV | ph TZV | no-ph QZV | ph QZV | no-ph TZV | ph TZV |
| 4s2 | $^5D_4$ | 0 | 0 | 0 | 0 | 0 | 0 | 0 | 0 | 0 |
| | $^5D_3$ | 416 | 401 | 412 | 397 | 408 | -14 | -4 | -19 | -8 |
| | $^5D_2$ | 704 | 682 | 699 | 675 | 692 | -22 | -5 | -30 | -12 |
| | $^5D_1$ | 888 | 862 | 884 | 853 | 875 | -26 | -4 | -36 | -13 |
| | $^5D_0$ | 978 | 950 | 974 | 940 | 964 | -28 | -4 | -38 | -14 |
| 4s1 | $^5F_5$ | 0 | 0 | 0 | 0 | 0 | 0 | 0 | 0 | 0 |
| | $^5F_4$ | 448 | 436 | 437 | 431 | 433 | -12 | -11 | -17 | -16 |
| | $^5F_3$ | 800 | 780 | 782 | 771 | 774 | -19 | -18 | -28 | -26 |
| | $^5F_2$ | 1058 | 1034 | 1036 | 1022 | 1025 | -24 | -22 | -36 | -32 |
| | $^5F_1$ | 1226 | 1201 | 1203 | 1187 | 1190 | -26 | -24 | -40 | -36 |
| 4s1 | $^3F_4$ | 0 | 0 | 0 | 0 | 0 | 0 | 0 | 0 | 0 |
| | $^3F_3$ | 585 | 576 | 575 | 568 | 568 | -9 | -9 | -17 | -17 |
| | $^3F_2$ | 992 | 978 | 977 | 965 | 965 | -14 | -15 | -28 | -27 |
| 4s1 | $^5P_3$ | 0 | 0 | 0 | 0 | 0 | 0 | 0 | 0 | 0 |
| | $^5P_2$ | 177 | 174 | 165 | 169 | 128 | -3 | -12 | -8 | -49 |
| | $^5P_1$ | 377 | 372 | 370 | 367 | 328 | -6 | -7 | -10 | -49 |
| 4s2 | $^3P_2$ | 0 | 0 | 0 | 0 | 0 | 0 | 0 | 0 | 0 |
| | $^3P_1$ | 1174 | 1122 | 1211 | 1139 | 1155 | -52 | 37 | -35 | -19 |
| | $^3P_0$ | 1660 | 1597 | 1724 | 1626 | 1670 | -62 | 65 | -34 | 10 |
| 4s2 | $^3H_6$ | 0 | 0 | 0 | 0 | 0 | 0 | 0 | 0 | 0 |
| | $^3H_5$ | 231 | 171 | 183 | 171 | 181 | -60 | -48 | -60 | -49 |
| | $^3H_4$ | 398 | 385 | 289 | 372 | 278 | -14 | -109 | -26 | -120 |
| 4s2 | $^3F_4$ | 0 | 0 | 0 | 0 | 0 | 0 | 0 | 0 | 0 |
| | $^3F_3$ | 233 | 286 | 180 | 274 | 171 | 52 | -54 | 40 | -63 |
| | $^3F_2$ | 398 | 422 | 340 | 429 | 329 | 24 | -58 | 32 | -69 |
| 4s1 | $^3G_5$ | 0 | 0 | 0 | 0 | 0 | 0 | 0 | 0 | 0 |
| | $^3G_4$ | 283 | 262 | 271 | 262 | 273 | -21 | -13 | -21 | -10 |
| | $^3G_3$ | 534 | 509 | 513 | 501 | 505 | -24 | -20 | -32 | -29 |
| 4s1 | $^3P_2$ | 0 | 0 | 0 | 0 | 0 | 0 | 0 | 0 | 0 |
| | $^3P_1$ | 108 | 149 | 156 | 132 | 149 | 40 | 48 | 23 | 40 |
| | $^3P_0$ | 213 | 293 | 296 | 255 | 280 | 79 | 82 | 42 | 67 |
| 4s2 | $^3G_5$ | 0 | 0 | 0 | 0 | 0 | 0 | 0 | 0 | 0 |
| | $^3G_4$ | 335 | 347 | 328 | 164 | 321 | 12 | -8 | -171 | -15 |
| | $^3G_3$ | 555 | 494 | 516 | 489 | 511 | -61 | -39 | -66 | -44 |
| 4s1 | $^3P_2$ | 0 | 0 | 0 | 0 | 0 | 0 | 0 | 0 | 0 |
| | $^3P_1$ | 436 | 435 | 381 | 437 | 371 | -1 | -55 | 1 | -65 |
| | $^3P_0$ | 756 | 752 | 679 | 752 | 666 | -4 | -77 | -4 | -89 |
| 4s1 | $^1G_4$ | 0 | 0 | 0 | 0 | 0 | 0 | 0 | 0 | 0 |
| 4s1 | $^3H_6$ | 0 | 0 | 0 | 0 | 0 | 0 | 0 | 0 | 0 |

| | | | | | | | | | | |
|---|---|---|---|---|---|---|---|---|---|---|
| | $^3H_5$ | 245 | 224 | 226 | 222 | 224 | -21 | -19 | -23 | -21 |
| | $^3H_4$ | 522 | 467 | 474 | 460 | 467 | -55 | -48 | -62 | -55 |
| 4s1 | $^3D_3$ | 0 | 0 | 0 | 0 | 0 | 0 | 0 | 0 | 0 |
| | $^3D_1$ | 181 | -50 | -67 | -15 | -31 | -231 | -248 | -197 | -212 |
| | $^3D_2$ | 399 | 396 | 386 | 390 | 377 | -2 | -13 | -8 | -22 |
| 4s1 | $^1P_1$ | 0 | 0 | 0 | 0 | 0 | 0 | 0 | 0 | 0 |
| 4s1 | $^1D_2$ | 0 | 0 | 0 | 0 | 0 | 0 | 0 | 0 | 0 |
| 4s1 | $^1H_5$ | 0 | 0 | 0 | 0 | 0 | 0 | 0 | 0 | 0 |
| 4s2 | $^1I_6$ | 0 | 0 | 0 | 0 | 0 | 0 | 0 | 0 | 0 |
| | $^5F_2$ | 0 | 0 | 0 | 0 | 0 | 0 | 0 | 0 | 0 |
| | $^5F_3$ | 37 | 43 | 66 | 45 | 74 | 6 | 30 | 8 | 37 |
| | $^5F_4$ | 52 | 138 | 120 | 127 | 103 | 86 | 68 | 75 | 52 |

**Table 7.12.** *Splitting in multiplets of all MR-EOM methods and statistical analysis of splitting in multiplets (in $cm^{-1}$) for Fe atoms*